UNIVERSITÀ POLITECNICA DELLE MARCHE

DEPARTMENT OF ENGINEERING

Master's Degree in Biomedical Engineering

Dynamic Finite element analysis of malposition in mobile and fixed bearing UKA prosthesis during gait

Supervisor:

Prof. Marco Mandolini

Candidate:

Anita Broshka

Co-supervisor:

Prof. Bernardo Innocenti

Academic Year 2021-2022

I. Contents

II. List of figures

III. List of Tables

IV. Acronyms

UKA= Unicompartmental Knee Arthroplasty

OA= Osteoarthritis

TKA= Total Knee Arthroplasty

FEA= Finite Element Analysis

ROI= Region Of Interest

BW= Body Weight

ACL= Anterior Cruciate Ligament

aACL= anterior ACL

pACL= posterior ACL

PCL = Posterior Cruciate Ligament

aPCL= anterior PCL

pPCL= posterior PCL

MCL= Medial Collateral Ligament

aMCL= anterior MCL

pMCL= posterior MCL

LCL= Lateral Collateral Ligament

MPFL= Medial Patella-Femoral Ligament

AMB = Antero-Medial Bundle

PLB= Postero-Lateral Bundle

ALB= Antero-Lateral Bundle

PMB= Postero-Medial Bundle

sMCL= superficial MCL

dMCL= deep MCL

GC= Gait Cycle

FB= Fixed-Bearing

MB= Mobile-Bearing

UHMWPE= Ultra High Molecular Weight Polyethylene

AP= Antero-Posterior

ML= Medio-Lateral

IE= Internal-External

OPK= Oxford Partial Knee

CAGR= Compounded Average Growth Rate

bi-UKA= Bi-unicompartmental UKA

EEA= European Economic Area

Co-Cr-Mo= Cobalt Chromium Molybdenum

3D= Three-Dimensional

CAE= Computer-Aided Engineering

ULB= Université Libre De Bruxelles

Abstract

Over the past two decades, the Unicompartmental knee arthroplasty (UKA) for the treatment of isolated compartment osteoarthritis (OA) of the knee has risen a lot if compared to the surgical rate of the early 80s. Nowadays UKA prosthesis is performed on 10% of all knee arthroplasties worldwide. The principal reason for this increasing trend is due to the bone and ligament spearing, especially of the preserved compartment, when compared to total knee arthroplasty (TKA). Thus, UKA was found more suitable to restore knee kinematics that is very similar to the physiological knee. Moreover, the UKA allows a less invasive surgery and an earlier return to normal daily activity with an overall reduction of costs. The only negative aspect highlighted by several studies results is a higher revision rate in UKA if compared to TKA.

However, although great improvements have been made over the years, since the earlier 1970 when the UKA was first performed, the results obtained in real clinical practice underline the need to define more optimal design systems, instrumentation, and surgical techniques. Indeed, UKA represents a technically challenging surgical procedure, which requires a lot of attention to the correct sizing of the components, bone cuts, and postoperative alignment as overstuffing or understuffing. Indeed, an implant loosening or an osteoarthritis progression can be noticed in the preserved compartment if a UKA is not performed correctly.

Thus, a better comprehension of knee joint biomechanics is necessary to achieve optimal performance after a UKA implant. Numerical methods such as the finite element analysis (FEA) are currently used in the knee prosthesis field due to their effective costs and the possibility to simulate a different range of loadings and configurations to evaluate which could be the best outcomes to apply in UKAs surgery.

FEA was applied to the present study to analyze the difference in knee biomechanics performances after a UKA implant with different configurations by analyzing a mobile-bearing and a fixed-bearing UKA during the dynamic daily tasks of gait. Then different parameters were changed in both the designs to assess which of them apported significant changes in the simulated behaviors. Finally, different outputs were evaluated, and among these, the von Mises stress and collateral-cruciate length. Results found highlighted different factors. One of them is the average von Mises stress on the polyethylene bearing insert and on the tibia bone which was found lower in the fixed bearing configurations for most of the regions of interest (ROI) analyzed. Moreover, the overstuffed configurations seem to be very challenging for both cruciate and collateral ligaments that tend to increase their length, often in a rapid way. This can overstretch them leading to serious consequences arriving in a probable rupture of them.

The present study represents one first approach but a very promising study for the analyses and comparisons, during gait, of the mobile and fixed bearing. Thus future development will focus also on the simulations of other dynamic movements such as squat to have a more in deep knowledge of the behavior of these two types of prostheses and improve biomechanical performance to extend the life expectancy of a UKA.

Riassunto

Negli ultimi due decenni, l'artroplastica del ginocchio mono-compartimentale (UKA) per il trattamento dell'osteoartrite compartimentale (OA), ha visto un maggior uso rispetto ai primi anni '80. Al giorno d'oggi la protesi UKA corrisponde al 10% di tutte le artroplastiche del ginocchio eseguite mondialmente. La ragione principale di questa tendenza crescente è dovuta alla conservazione ossea e legamentosa, specialmente del compartimento non affetto da osteoartriti , delle protesi UKA rispetto all'artroplastica totale del ginocchio (TKA). Inoltre, è stato provato che le UKA ripristinano la cinematica del ginocchio in un modo molto similare a quella del ginocchio fisiologico. L'UKA consente la performance di una chirurgia meno invasiva con conseguente ritorno anticipato alla normale attività quotidiana con una riduzione complessiva dei costi. L'unico aspetto negativo evidenziato da diversi studi è un più alto tasso di revisione delle UKA rispetto alle TKA.

Tuttavia, anche se grandi miglioramenti sono stati fatti nel corso degli anni a partire dal 1970, quando l'UKA è stato eseguito per la prima volta, i risultati nella pratica clinica, ottenuti successivamente, sottolineano la necessità di definire sistemi di progettazione, strumentazione e tecniche chirurgiche più ottimali. Infatti, UKA rappresenta una procedura chirurgica tecnicamente impegnativa, che richiede molta attenzione al corretto dimensionamento dei componenti, al sezionamento osseo e all'allineamento post-operatorio come sovra-posizionamento (overstuffing) o sotto-posizionamento (understuffing). Infatti, un dislocamento dell'impianto o una progressione di osteoartrite può essere notato nel compartimento sano se un UKA non viene eseguito correttamente.

Pertanto, una migliore comprensione della biomeccanica articolare del ginocchio è necessaria per ottenere prestazioni ottimali dopo un impianto UKA.

Metodi numerici come l'analisi degli elementi finiti (FEA) sono attualmente utilizzati nel campo della protesi al ginocchio, grazie al loro basso costo e alla possibilità di simulare una diversa gamma di carichi e configurazioni per valutare

quali potrebbero essere i fattori da migliorare ed applicare successivamente al design ed alla tecnica chirurgia usata nelle UKA.

La FEA è stata applicata al presente studio per analizzare la differenza nelle prestazioni biomeccaniche del ginocchio dopo un impianto UKA con diverse configurazioni analizzando un inserto in polietilene mobile e uno fisso durante il passo. In seguito diversi parametri sono stati cambiati in entrambi i modelli per valutare quale di loro apporti cambiamenti significativi nei comportamenti simulati. Infine, sono stati valutati diversi risultati e, tra questi, lo stress di von Mises e la lunghezza dei legamenti crociati e collaterali.

I risultati hanno evidenziato diversi output. Uno di questi è lo stress medio di von Mises sull'inserto in polietilene e sull'osso tibiale. Lo stress è risultato più basso nelle configurazioni aventi gli inserti fissi nella maggioranza delle regioni di interesse (ROI) analizzate. Inoltre, le configurazioni in cui si ha una sovra-poszionamento sembrano essere negative sia per i legamenti crociati che per i collaterali che tendono ad aumentare la loro lunghezza, spesso in modo repentino. Questo può sovraccaricarli portando a gravi conseguenze che possono arrivare ad una loro probabile rottura.

Il presente studio rappresenta un primo approccio ma uno studio molto promettente per le analisi e i confronti, durante il passo , con protesi monocmpartimentali aventi inserto mobile e fisso. Per cui sviluppi futuro si dovrebbero concentrare anche sulle simulazioni di altri movimenti dinamici come il piegamento, per avere una conoscenza più approfondita del comportamento di questi due tipi di protesi e migliorare le prestazioni biomeccaniche per estendere l'aspettativa di vita di una UKA.

1 Introduction

1.1 Physiological joint anatomy

The human knee (**Figure 1.1**) is an intermediate hinge-type synovial joint of the lower limb and the most complex articulation of the human body [1]. Its main responsibility is to allow motion between the femur, tibia, and patella providing, in the meanwhile, stability during static and dynamic daily life tasks of sitting, walking, stair ascent, stair descent, jumping, running, squatting [1],[2],[3]. The basic movement performed by the knee joint is the flexion and extension of the lower limb, but it allows also internal/external rotation, medial/lateral translation, and varus/valgus angulation.

Hence, the normal functioning of the knee joint necessitates a proper balance between mobility and stability that rely on the active constraints generated by the interactions between bone structures and the soft tissues (muscles, tendons, ligaments, and menisci) [2], [4].

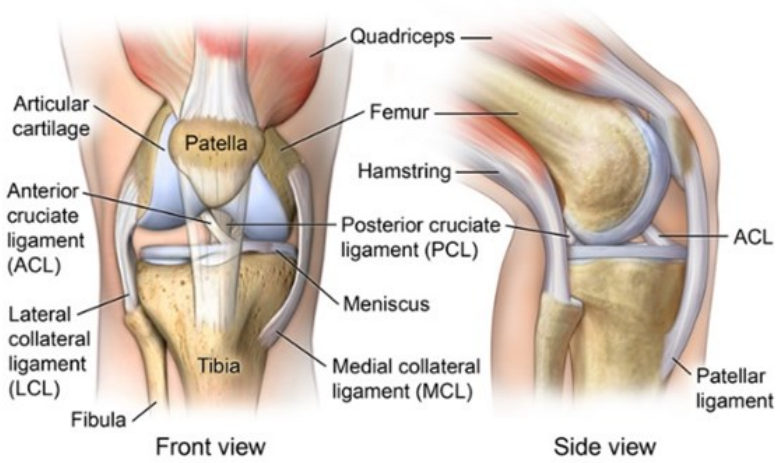

Figure 1.1 Anatomy of the knee joint [5]

The knee joint is composed of two joints:

- Tibio-femoral joint articulates the femur and tibial bone. This joint, which sustains a major part of the body weight (BW), can be subdivided into medial

and lateral part permitting a more detailed analysis of the femoral condyle with the corresponding portion of the underlying tibial plateau [6], [7].

- Patella-femoral joint articulates the femoral trochlear groove and the patella giving rise to forces transfer due to the contraction of the quadriceps femoris muscle [6].

1.1.1 Bones and Cartilage

The bones involved in the knee joint are the femur (thigh bone), tibia (shin bone), patella (kneecap), and fibula (calf bone).

The femur, which extends from the hip to the knee, is the longest, heaviest, and strongest bone in the human body [8] (**Figure 1.2**). The proximal epiphysis of the femur is a hemispherical head that articulates with the acetabulum of the pelvic bone forming the hip joint. While the distal epiphysis is constituted by the medial and lateral condyles to which the collateral ligaments are attached [9]. In particular, the medial condyle presents a large posterior offset and an elliptical shape [10], providing so a bigger articular area[11]; the lateral one presents a smaller posterior offset and a spherical shape [12] positioned more sagittal respect to the medial one. Femoral condyles are connected anteriorly by a smooth shallow articular depression called femoral trochlear groove, where the patella is located. While posteriorly they are separated by a deep notch named intercondylar fossa [13].

The femur condyles interact with the tibial surfaces, called tibial plateaus, which are asymmetric and divided in medial and lateral separated by an intercondylar eminence [14] (**Figure 1.3**). The medial tibial plateau presents a larger and more oval shape with respect to the lateral tibial plateau that instead is smaller and more rounded [15].
Moreover, in the medio-lateral direction both the tibial plateaus present a concave shape whereas in the antero-posterior direction the concavity shape is present only in the medial one, while the lateral one has a convex shape. This asymmetry is important since it leads to increased lateral mobility of the knee joint.

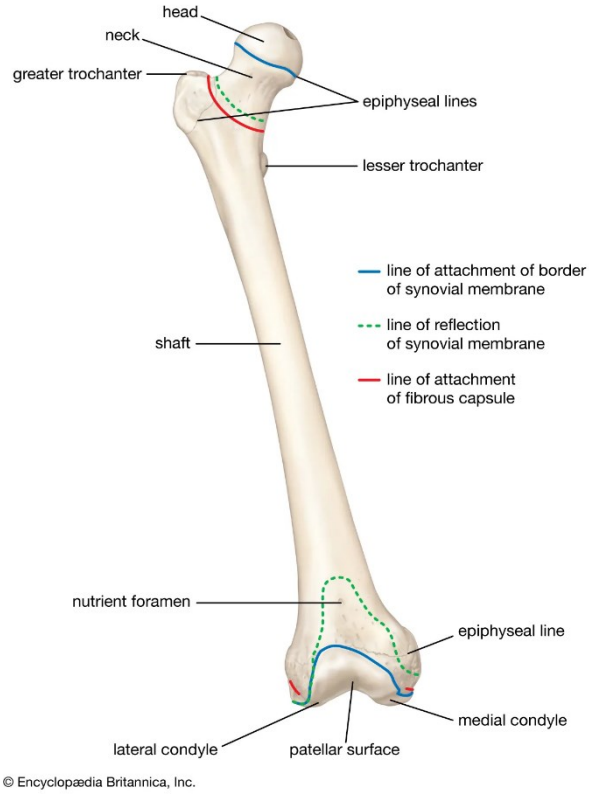

Figure 1.2 Anatomy an human knee [16]

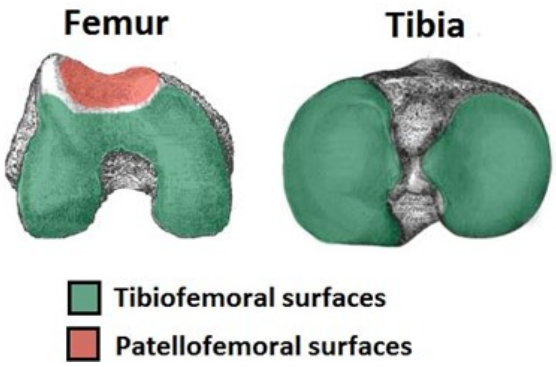

Figure 1.3 Articulation areas in femur and tibia [17]

Another important aspect of the tibia is its posterior slope, presenting an anterior elevation with respect to the posterior part. This factor is important especially when is applied a large compressive joint reaction force that may have an anteriorly directed shear component that acts to produce a corresponding anteriorly directed translation of the tibia [18].

On the lateral side of the tibia there is the fibula (**Figure 1.4**) which articulates with the tibial head, by means of the interosseous membrane, and the ankle joint. This bone is smaller and much thinner with respect to the tibia, representing an important attachment site for muscles. So, the tibia and fibula cooperate to stabilize the ankle joint and provide support to the muscles of the lower leg, even if it is not directly involved in weight transmission [19].

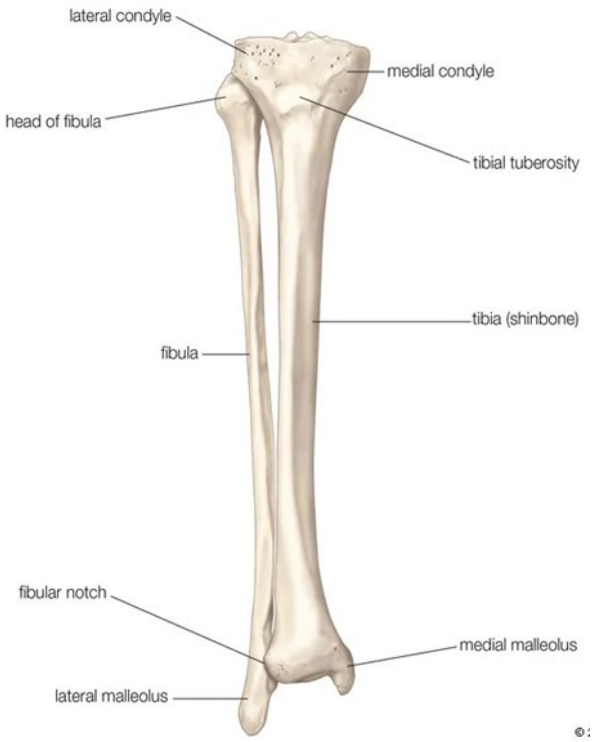

Figure 1.4 Anatomy of an huma Tibia and Fibula [20]

The patellar bone presents a triangular shape located in the intercondylar notch, anteriorly with respect to the distal part of the femur and placed between the quadriceps femoris muscle tendon and the patellar tendon [10]. This tendon connects respectively to the quadriceps muscles and to the frontal part of the tibia. Since the posterior surface of the patella articulates with the distal part of the femur, it is divided into a medial and lateral to better fit the medial and lateral femoral condyles; this shape enables the sliding up and down of the patella in the patellar groove during the knee flexion and extension [21].

Therefore, due to all these characteristics, the patellar bone increases the efficiency of the muscle during the knee extension by as much as 50%, by increasing the leverage exerted by the quadriceps tendon on the femur [21], [22]. Moreover, the patella protects the anterior part of the knee joint (trochlea and femoral condyles) against impact trauma when the knee is flexed [21]. As all the synovial joints of the body, also the knee joint articular bones surfaces are covered by articular cartilage as seen in **Figure 1.1.** It covers the femoral condyles, the tibial plateaus, the posterior surface of the patella, and the patellar groove.

The articular cartilage is a thin and elastic layer of hyaline cartilage that absolves several important roles; it allows a smooth motion at the joint, thanks to the extremely low coefficient of friction, provide shock absorption, increases the contact area between the articular surfaces to grant a more homogeneous distribution of the forces [23]. Moreover, the articular cartilage does not present any innervation or vascularization, so the eventual damage that occurs on it is noticeable just when the bones rub one against the other. Indeed, the articular cartilage undergoes, over the years, wear presenting also a restricted capacity for self-restoration [23].

1.1.2 Menisci

The knee joint presents two menisci, lateral and medial, having a wedge-shaped semi-lunar fibrocartilaginous structure subdivided into the anterior horn, posterior horn, and body segment (**Figure 1.5**). They are situated respectively between the corresponding femoral condyle and tibial plateau. The menisci have a very important role in shock absorption, and load transmission by increasing the contact area, improvement of joint stability and synovial fluid diffusion, and the proprioception of the knee joint [24], [25]. Moreover, they provide a great improvement in terms of joint congruence between the spherical-shaped femoral condyles and the flat tibial plateaus [26], [27].

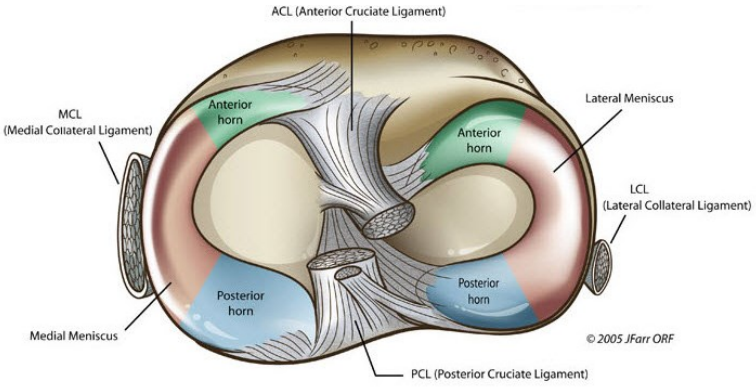

Figure 1.5 Top-down view of knee joint without the femur. Left and right meniscus can be seen [28]

This is possible since in the menisci can be notice a concave upper surface in contact with the femoral condyles and a flat lower surface in contact with the tibial plateaus.

Consequently, the contact stress during motion is reduced preventing the onsets of various complications [13]. In particular, the lateral meniscus is more mobile than the medial ones with a circular shape covering a larger portion of the lateral tibial plateau; the medial meniscus instead shows a semi-circular shape that is larger and thicker respect the lateral one.

1.1.3 Ligaments and Tendons

In the prevention of undesired motions and stability of the knee joint, the pivotal role played by the knee ligaments (**Figure 1.6**) also prevents undesired motions [13], [10]. They are composed of collagen fiber bundles closely packed together [22] and divided into:

- Cruciate ligaments: anterior cruciate ligament (ACL) and posterior cruciate ligament (PCL);
- Collateral ligaments: medial collateral ligament (MCL) and lateral collateral ligament (LCL);
- Patello-femoral ligament or tendon: medial patella-femoral ligament (MPFL) and the lateral retinaculum.

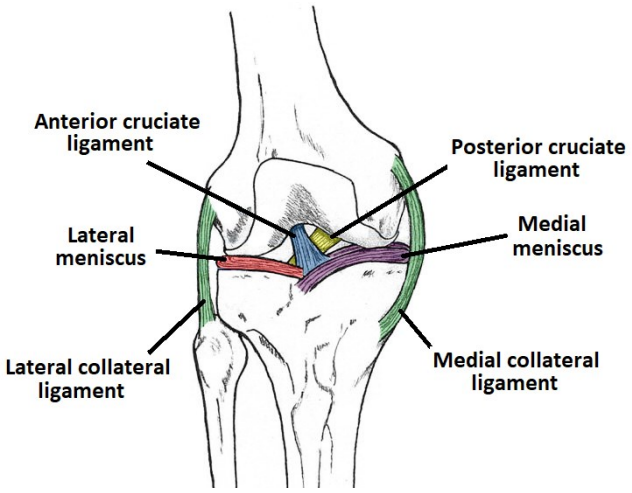

Figure 1.6 Anterior point of some of the major ligaments of the knee joint [17]

The ACL originates from the anterior part of the tibia intercondylar eminence extending then to the posteromedial portion of the lateral femoral condyle [1]. Its main function is to prevent the tibia translation on the femur in the anterior direction during the knee flexion, ensuring up to 85% of stability [25]. Moreover, the ACL opposes to internal rotation of the tibia until 30° of flexion, and varus-valgus deviations [25]. The ACL is composed of the antero-medial bundle (AMB) that limits the anterior-posterior translation of the knee and the postero-lateral bundle (PLB) that limit the knee rotational moment. Both are non-isometric bundles. The ACL will always have a part that is in tension since the AMB is taut in flexion and the PLB is taut in extension.

The PCL, which has a higher average thickness and tensile strength with respect to the ACL [29], originates from the lateral part of the medial femoral condyle extending distally to the postero-lateral tibial plateau [1]. Its primary function is to prevent the sliding backward i.e., posterior translation of the tibia on the femur [25]. Its secondary function instead is to prevent an excessive external rotation of the tibia and varus-valgus angulation at the knee [1]. Indeed, it stretches when faced with high degrees of flexion and internal rotation of the tibia [25]. Also the PCL is composed of two non-isometric bundles [29] known as anterolateral bundle (ALB) that is taut at 90° of flexion and posteromedial bundle (PMB) that is taut in full extension [30], [31], [25].

The MCL which originates from the femur medial epicondyle inserts then into the postero-medial surface of the proximal part of the tibia. It is composed of two different fiber bundles: the superficial MCL (sMCL) and the deep MCL (dMCL). In particular, the sMCL counteracts the valgus forces in all the degrees of knee flexion and stabilizes the knee external rotation at 30° flexion. While the dMCL supports the stability of the knee during internal rotation [25]. A secondary function carried out by the MCL is the limitation to the anterior translation of the tibia on the femur when the ACL is injured [32]. The sMCL bundle results in taut, whereas the dMCL one is unstretched during the knee flexion [25].

The LCL originates as a single bundle on the postero-lateral femoral epicondyle and attaches anteriorly to the fibula head [25]. Its function is to ensure stability to the lateral side of the knee resisting the varus forces and excessive internal rotation of the tibia

with respect to the femur[1], [33]; this is done jointly with the PCL. The LCL results in taut during the knee joint full extension increasing the varus laxity when the knee flex. Moreover, the LCL is less prone to injuries since it's shorter than the MCL [25].

The patella-femoral ligament works as a stabilizer of the patella keeping it in the patellar groove and since it's a very strong collagenous structure, it's capable to transmit a high tensile load [13]. It is in the anterior part of the knee joint and is composed of the distal part of the quadriceps tendon and originates from the patella apex and attaches to the tibial tuberosity [34].

1.1.4 Muscles

Along with the ligaments, also the muscles work as a stabilizer of the knee joint interacting with the neuromuscular system to control its motion [13]. They are divided into two main groups based on their function. The quadriceps femoris muscle and the hamstring muscles.

The quadriceps (**Figure 1.7**) is the strongest muscle in the human body, composed of four different single muscles (vastus medialis, vastus lateralis, vastus intermedius, and rectus femoris) that work together as extensors of the leg at the knee joint and as flexors

of the thigh at the hip joint thanks to the rectus femoris. Hence, the quadriceps femoris has a central role in walking, running, squatting, and jumping [10]. Moreover, in cooperation with the patellar tendon, it guarantees that the patella stays in the trochlear groove of the femur during motions [35]. The quadriceps femoris extends along the anterior part of the femur and all four single muscles join above the patella generating the quadriceps femoris tendon that so connects the quadriceps muscle to the patella [36].

The hamstring muscles (**Figure 1.7**) are composed of three individual muscles (biceps femoris, semimembranosus, and semitendinosus muscle) that work together as flexors of the knee and extensors of the thigh at the hip joint. Moreover, the hamstring muscles participate in the internal rotation of the knee and help the standing position. The hamstring muscles extend to the rear part of the femur and attach to the tibia and fibula [37].

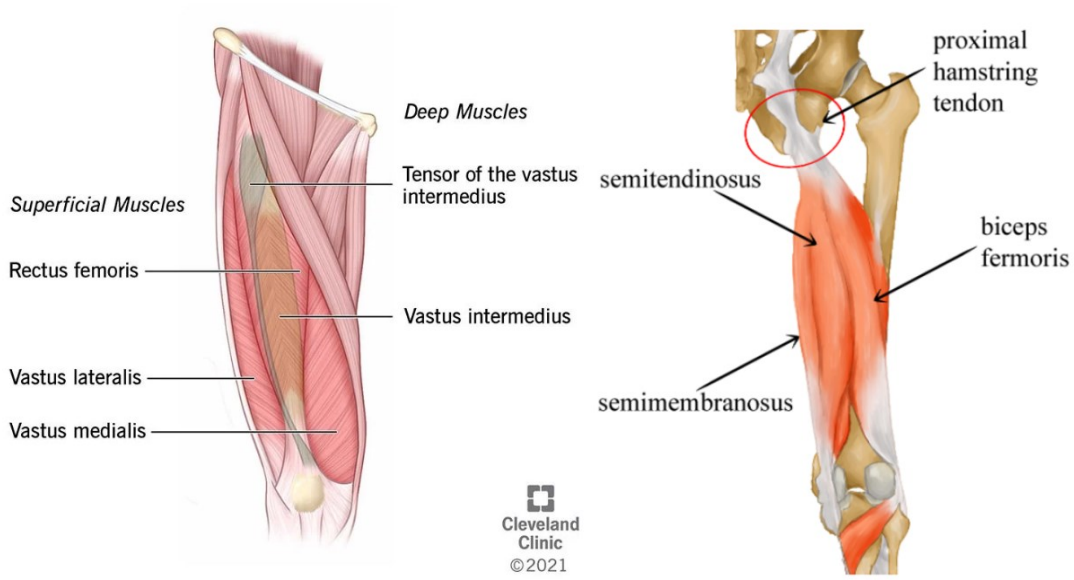

Figure 1.7 Quadriceps muscles (left) and Hamstring muscles (right) [38], [39]

1.2 Knee joint biomechanics

The knee this joint is one of the most complex joints in the human body, that allows many different movements essential to have a healthy life. Therefore, the study of its biomechanics has become indispensable to improving the prevention and treatment of its disorders and injuries [40].

1.2.1 Movements

The wide range of movements allowed by the knee joint is due to its 6 degrees of freedom that allow three translations and three rotations along the axes [41] as shown in **Figure 1.8**.

Rotations are [42], [43]:

- flexion/extension from -15° to 140° around the medio-lateral or epicondylar femoral axis;
- axial rotation or internal/external between 25° to 30° around the tibial longitudinal axis;

- varus/valgus or adduction/abduction between -6° and 8° around the floating axis perpendicular to the tibia mechanical axis.

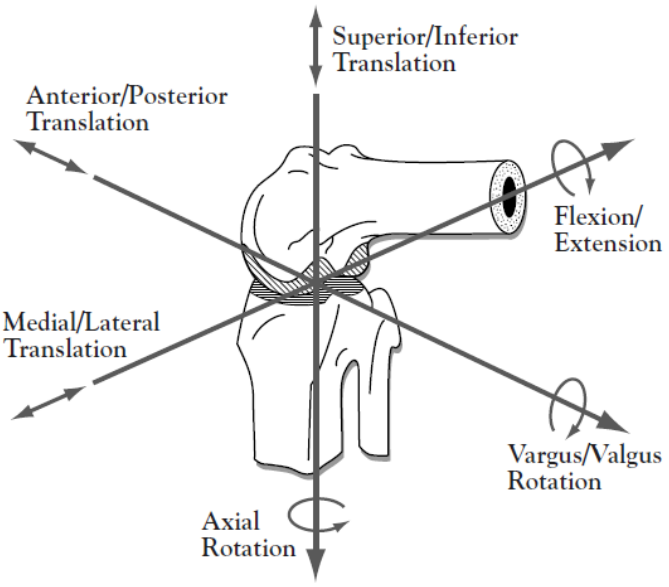

Figure 1.8 Knee joint six degrees of freedom: 3 rotational and 3 translational moments [43]

In particular, the flexion-extension involves both a sliding and rolling between the femoral condyle surfaces and the corresponding arear of the tibia plateau. The rolling is the principal visible movement when the knee joint is in the extended position and then when the angle of flexion increases the slipping become predominant to be then the only one during the final phase of the flexion [43].

Translations are [42], [43]:

- anterior/posterior from 10 to 15 mm being so the highest one occurs along the floating axis perpendicular to the tibia mechanical axis;
- medial/lateral from 2 to 5 mm along the epicondylar femoral axis;
- superior/inferior or proximal/distal along the tibial longitudinal axis.

1.2.2 Alignment of the lower limb

The reciprocal alignment of femur and tibial bone results then fundamental in matter of stability and functionality of the knee joint. The in-use method to determine the correct alignment is given by the orientation of an anatomical/mechanical axis of the tibia and the mechanical axis of the femur.

The mechanical axis of the lower limb, also named load-bearing axis, is the line that extend from the center of the femoral head to the center of the ankle joint. From the frontal plane, the mechanical axis of the femur results coincident with the anatomical/mechanical axis of the tibia, while the femoral anatomical axis instead present 6° degrees angle from the femoral mechanical axis [44]. So, the knee joint in healthy conditions results to be in a neutral configuration in which the mechanical axis of the femur and of the tibia are aligned and form an angle that range in 172°-177° [25], [44].

If the knee joint is not in a physiologically aligned condition, there is the presence of a malalignment in which the knee centre is shifted medially or laterally with respect to the mechanical axis of the knee. This malalignment can be either of a varus or valgus type.

In the valgus deformity there is a knock-kneed appearance of the joint since the distal part of the tibia is turned outward respect to the femur. While in the varus deformity a bowlegged configuration can be noticed since the tibia is turned inward with respect to the femur. It was scientifically demonstrated that both this knee malalignment contributes to the progression of important diseases such as the osteoarthritis [45], [46] due to the increase the amount of stress per unit area in the overloaded compartments [25]. Therefore, the restoration of the femoral and tibial alignment is fundamental to be achieved for an optimal functioning of the knee joint [47].

1.2.3 Articular Forces

The knee joint is subjected to important articular forces that are physiologically transferred thanks to the soft tissues such as the menisci and articular cartilages. The articular forces are transferred as contact stresses between the articular surfaces of the knee and can be divided into lateral tibio-femoral, medial tibio-femoral and patella-femoral. Moreover, they vary depending on the type of activity that is performed. Indeed, the forces transmitted across the knee joint during the gait is of two or three time the BW, while during running it range from four to seven time the BW [48].

These multiplications of the transmitted forces respect the body weight are due to the kinetics of body acceleration and to the contraction of muscles of the lower limb [48].

1.2.4 Gait Cycle

The main activity of the knee joint, that is the one taken in consideration in the present study, is the Gait Cycle (GC). It is the time interval between two successive supports of the same foot on the ground during walking. It is generally convenient to use the instant at which one-foot contacts the ground. It is possible to start the GC with

right or left foot, obtaining the same cycle but the action of the other leg (no starting leg) will be displaced in time by half a cycle. The duration of a complete GC is known as the cycle time (100% GC) which is divided in two phases (stance and swing) and composed of 7 main events which divide the stance phase into 4 periods and the swing phase into 3 periods as shown in **Figure 1.9** [49]:

1. Stance phase (60% of GC): the phase in which the foot is on the ground. It is divided into 4 periods:
    - Loading response (LR) (0-10%): from initial contact (IC) to opposite toe off (OT)
    - Mid-stance (MSt) (10-30%): from OT to heel rise (HR)
    - Terminal Stance (TSt) (30-50%): from HR to opposite initial contact (OI)
    - Pre-swing (PSw) (50-60%): from OI to toe off (TO)
2. Swing phase (40% of GC): the phase in which the foot is moving forward through the air. It is divided into 3 periods:
    - Initial swing (ISw) (60-73%)): from TO to feet adjacent (FA)
    - Mid-swing (MSw) (73-87%): from FA to tibia vertical (TV)
    - Terminal swing (TSw) (87-100%): from TV to new initial contact (IC)

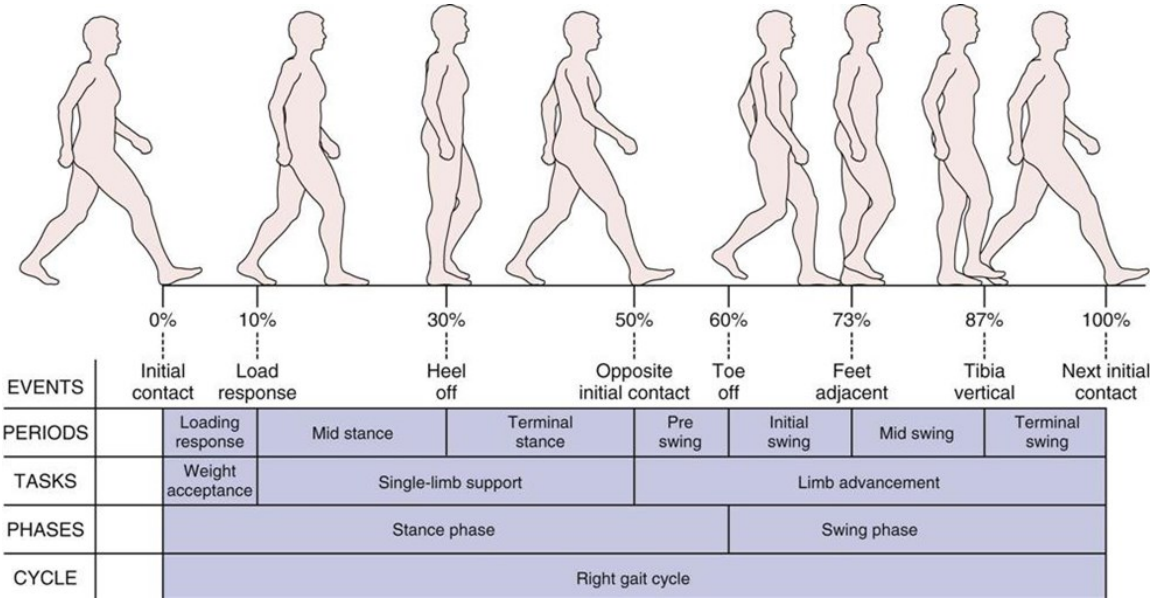

Figure 1.9 A normal gait cycle divided in two phases (stance and swing) and in seven periods [49]

1.3 Knee joint injuries and diseases

The physiological functions of the knee joint can be compromised by degenerative, inflammatory, and traumatic diseases [50].

The most common one is osteoarthritis, a degenerative disease affecting joints and leading to joint cartilage loss. This disease affects 3.3% of the world's population and is the 11th of the most impairing diseases worldwide [51] having so a very negative impact on the quality of life [3], [52].

The pathological consequences of osteoarthritis in the knee joint are [50] (**Figure 1.10**):

- Articular cartilage degradation provoking a femur-tibia bones contact;
- Subchondral bone thickening;
- Osteophytes formations;
- Synovium inflammations;
- Ligaments and menisci degeneration;
- Joint capsule hypertrophy.

It is therefore noticeable that the OA compromises the knee joint physiological biomechanics leading to its misalignment. Consequently, the loads and functional stresses will increase on the side of the knee that is affected whereas, on the opposite side, the ligaments will be overstretched [53]. The main risk factors that lead to OA development include obesity, joint injury caused by sports activities, age, and anatomical factors [51].

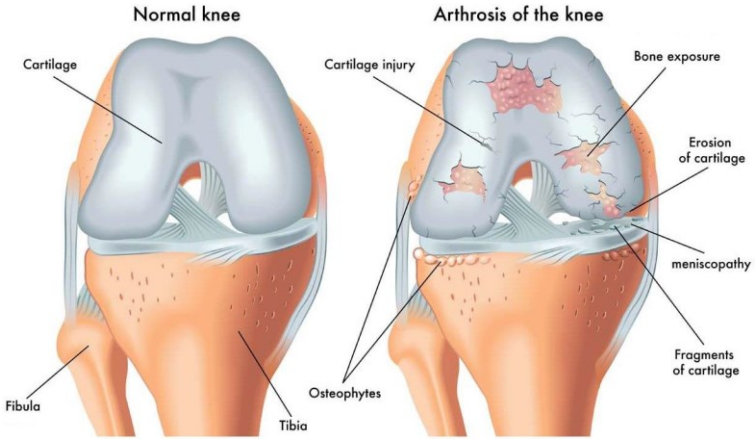

Figure 1.10 Normal knee vs knee affected by osteoarthritis [54]

1.4 Knee Arthroplasty: Total knee vs Unicompartmental

The degenerative processes induced in the knee joint from OA result to be irreversible if not properly treated [55].

A first attempt is to manage them through rehabilitative therapies, anti-inflammatory or pain medications, and a healthier lifestyle. But when these non-invasive or minimally invasive treatments result to be no longer effective in the relief of the symptoms, it is necessary to surgically operate the knee joint to restore as much as possible the physiological functionality of the joint improving so the quality of life of the patients. Indeed, nowadays it has not been possible to create a knee prosthesis capable of fully restoring the kinematics of a healthy knee joint [25].

Arthroplasty is nowadays the most common surgical procedure in a knee joint replacement with an artificial joint [56]. Knee joint arthroplasty is suitable for a wide

range of patients of different ages and conditions even if the majority of arthroplasty is performed on patients between the age of 55 to 80 [57].

Each patient situation is evaluated by a team of surgeons to decide which is the most appropriate arthroplasty to perform, depending on the patient's bones and soft tissue conditions [58].

The most important differences between arthroplasty can be grouped as follows [59]:

- Total Knee Arthroplasty (TKA) or Unicompartmental Knee Arthroplasty (UKA);
- Fixed Bearing (FB) or Mobile Bearing (MB);
- Cemented or Cementless.

TKA (**Figure 1.11**) is generally used when both the lateral and medial sides of the knee joint are injured, and if the ligaments result to be damaged [59].

UKA (**Figure 1.11**) instead, is a particular type of knee prosthesis that partially replaces the knee joint; in fact, it is successfully used to treat anteromedial and anterolateral osteoarthritis [60]. UKA results to be a more conservative alternative to the Total Knee Arthroplasty (TKA) in terms of bone and ligament sparing, in patients presenting a single-compartment degeneration of the knee, thus allowing an earlier post-operative recovery [56], [61]. UKA results fundamentally also in the slowing of arthritis progression in the unaffected compartments of the knee joint providing a long-term symptom relief if this kind of arthroplasty is performed early in the disease process [62].

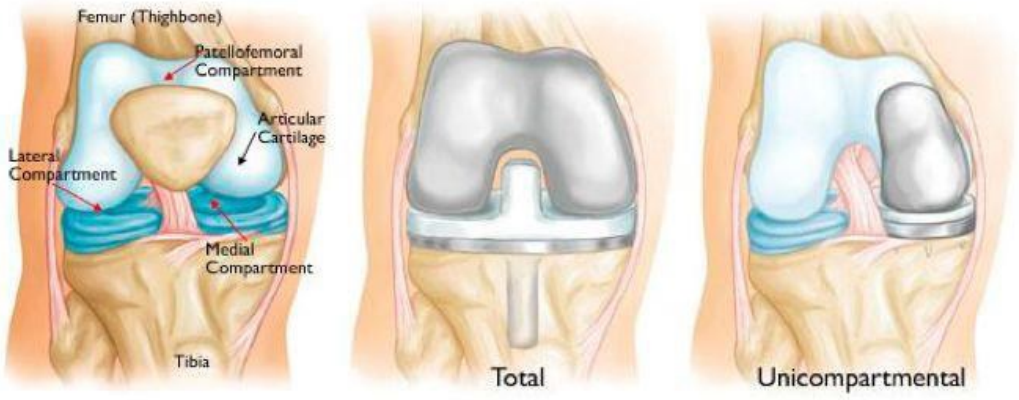

Figure 1.11 Healthy knee (left), knee with TKA (centre), knee with UKA (right) [63]

Independently from the different kinds of designs of knee prostheses, all of them must satisfy three relevant requirements as listed below.

a. Anatomical requirements: undesired contacts between the different anatomical parts must be avoided thereby complying with the anatomical joint space;
b. Mechanical requirements: implant-bone interfaces and contact areas between prosthesis components must ensure an adequate and uniform load distribution to all the involved parts. Moreover, the implant stability must be reliable as well as long-lasting lifetime;
c. Biological requirements: low invasiveness level is required in this kind of surgical procedure during which the knee femur and tibia bones must be cut as less as possible. Finally, just as much important is the requirement of biocompatibility that must be met by all components.

In the present work, the focus will be just on the study of biomechanical performances of the knee after a UKA implant in both FB and MD designs.

1.4.1 UKA successes, failures, and limitations

The basic goal of the UKA is to restore the proper functions of the knee joint, for a properly selected gamma of patients, and to reduce pain [61], [64].

In the literature are present multiple clinical studies reporting that the UKA can reproduce the physiological motion of the healthy knee [62], [65], [66]. These results were then confirmed by several authors reporting very good results at 10 years of follow-up [67], [68]. But despite these optimal results, some cases of failure are also reported in the literature [69], [70]. Indeed, UKA represents a technically challenging surgical procedure, which requires a lot of attention to the correct sizing of the components, bone cuts, and postoperative alignment as overstuffing or understuffing [64]. The main post-operative issues highlighted were:

- Prosthesis wear, especially of the polyethylene bearing component [71], [72].
- OA progression in the preserved compartment and due to incorrect UKA positioning leading to an incorrect stress pattern in the bone/cartilage [73];

- Loosening of the tibial and/or femoral UKA component, caused by the stress shielding in the joint bones [74]–[76].
- Misplacement of UKA components, with a possible strain increase in the soft tissue structure resulting in a tightening or a slackening behaviour [77].

Moreover, UKA presents some other limitations since it is not recommended when the patient presents [61]:

- Obesity;
- Varus/Valgus deformities exceeding 15°;
- Improper function of the Ligaments, especially of the ACL;
- Previous infection localized in the affected part of the joint;
- Damage to the articular cartilage of the preserved compartment;
- Lacking a proper femur or tibial bone stock.

Results so that if there is a failure of UKA, the life quality of the patient is not improved, and the performed arthroplasty has not reached its purpose, and therefore it is important to understand the reasons for these failures to prevent them[78].

1.4.2 Economic Profile

The global market of orthopedic devices size in 2020 was valued at US$ 46.1 billion according to Vision Research Reports [79]. It is expected to reach approximately US$ 57.7 billion by 2030. It is estimated to increase at an annual Compounded Average Growth Rate (CAGR) of 3.1% from 2022 to 2030. Orthopedic knee devices occupy the most significant part of this global market, with a broader market share of 28.2% in 2021 with a growth compound annual growth rate (CAGR) of 5.67% by 2030 (**Figure 1.12**).

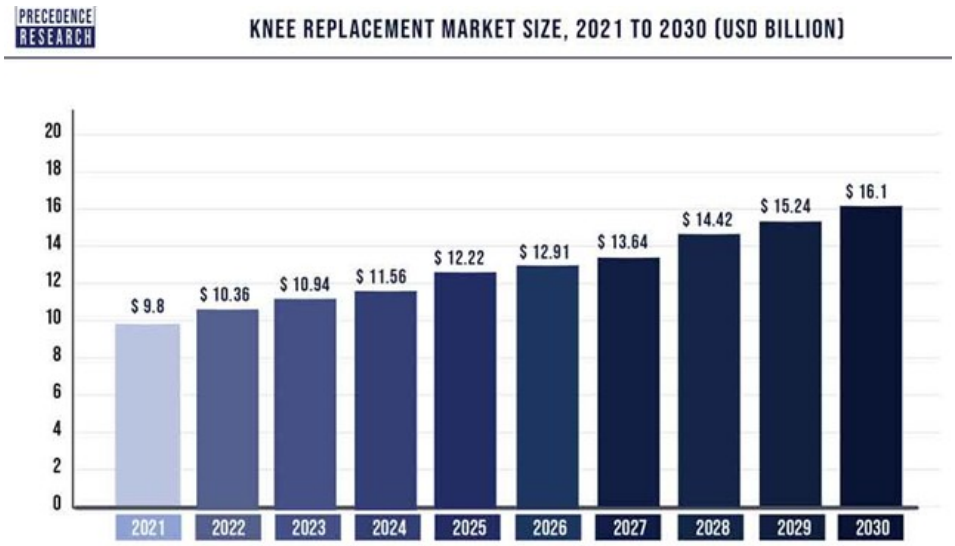

Figure 1.12 Knee replacement market size from 2021 to 2030 [80]

The driving factors of orthopedics devices are the rapid increase in the aging populations with the consequent increase of degenerative diseases such as osteoarthritis and osteoporosis and the musculoskeletal disorders caused by obesity and a sedentary lifestyle.

However, some challenging factors slow down its growth. These factors are associated with high-cost arthroplasty and stringent regulatory guidelines that these medical devices are obliged to follow [81].

According to the Orthopedic Design and Technology [82], some key players operating in the orthopedic devices market include DePuy Synthes, Stryker Corporation, Zimmer-Biomet Holdings, Smith and Nephew PLC, and Medtronic PLC.

Even if the TKA represents the greatest part of the knee arthroplasty market, the UKA, thanks to its conservative properties, easier revisions, and cost-saving compared with TKA [83], is increasingly taking place in the global market of orthopedic devices. This trend is confirmed by the National Joint Replacement registries; they state that UKA nowadays is performed among 5% to 11% of the total knee replacement with a growing rate in the last 10 years [84]. It is easily noticeable that orthopedic device replacement, led by knee joint replacement, covers a large part of the healthcare financial market. Therefore, is requested to improve the current knee replacement systems to achieve better and better results of performance and economic profile.

1.5 Aim of the study

It was highlighted that a proper understanding of knee joint biomechanics results essential to enhance the prevention and different kind of treatments of its pathological conditions and injuries. Numerical methods, such as the Finite Element Analysis (FEA), represent robust tools to simulate knee biomechanics. These methods indeed results to be reliable to [2], [24]:

-predict the effects of different parameters involved;

-predict the consequences of degenerative pathologies and traumatic events;

-predict surgical repair and replacement strategies

-provide information otherwise difficult to obtain from experiments.

Thus, this project aims to analyse, in terms of kinematic, bone stresses, and ligament length, the difference in knee biomechanics performances after a UKA implant with different configurations by analysing a mobile-bearing and a fixed-bearing UKA during the dynamic daily tasks of gait. Moreover, given the importance of overstuffing and understuffing configurations correlated with the success of a UKA implant, a study to quantify their effect on the biomechanics performances of the two prostheses taken into consideration was carried out.

To reach this goal eighteen Finite Element models of the knee joint were modelled to evaluate the effects induced by considered surgical design parameters.

2 Unicompartmental knee prosthesis

Nowadays exist principally three main types of UKA depending on where the OA symptoms are localized. They are:

1. Medial UKA is performed on the diseased medial compartment of the knee joint. It represents the majority of performed UKAs with a percentage of 90-95% [84].
2. Lateral UKA is performed on the diseased lateral compartment of the knee joint. However, an isolated lateral OA is a relatively rare condition. Indeed, it has a 10-time lower incidence lower than the medial compartment representing just the 5-10% of the UKAs totality [61], [84].
3. Bi-unicompartmental UKA (bi-UKA) [84] is performed on both tibial-femoral compartments using two femoral and two tibial components using two femoral and two tibial components and the preserved part is limited just to the tibial eminentia. The presence of a healthy or well-functional ACL is mandatory for this kind of UKA since it allows a knee kinematic reinstatement closer to the physiological one. In particular, the external tibia rotation during a total extension, femoral rollback, and gait are improved by the preservation of ACL [85]. Patello-femoral instability or malalignment represents an important contraindication to the bi-UKA [84].

Another important distinction for UKA prosthesis is the type of bearing. Indeed, UKA exists in the fixed and mobile-bearing versions. In the present study to simulate their characteristics were used:

1. Physica Zuk fixed-bearing UKA by Lima Corporate [61];
2. Oxford Partial Knee mobile-bearing UKA by Zimmer Biomet [86].

2.1 Patient selection

For all the above-mentioned types of UKA what is very important is the correct patient selection to achieve expected clinical outcomes after UKA [87]. Indeed, not all the patients affected by OA are appropriate for UKA implant.

Focusing of the medial part of the knee joint, the characteristics of an ideal medial UKA patient are [86], [88]:

1. Bone-on-bone contact due to an anteromedial OA;
2. Cartilage defect in the lateral and medial side of the medial compartment. This can be detected in an easy and reliably manner using radiographic images;
3. Intact cruciate (ACL and PCL) and collateral ligament (MCL and LCL) to guarantee the stability of the prosthesis;
4. Pain location should be limited to the only medial compartment;
5. All the soft tissues of lateral compartment must be unaffected by the OA or nearly to. Indeed, is often seen during surgery that the medial side of the lateral condyle is affected by marginal osteophytes and localized erosions of the cartilage. These factors are classified as grade 1 of cartilage defect do not pose a contraindication to medial UKA;
6. Varus deformity induced by wear must be passively correctable.

Other factors such as patients age, weight, activity level or patella-femoral joint damage, do not seem to represent contraindications for the treatment outcomes [88].

2.2 Fixed bearing vs Mobile bearing UKA

Nowadays the fixed FB and MB UKA are routinely used [89] even if there is still an open debate on which of the two carry out better performs related to e.g., revision rate decreasing duet to loosening, or survivorship improving [90].

The most characterizing difference between the FB and MB UKA design is in the polyethylene meniscal bearing. Indeed, in the FB it is fixed into the metallic tibial component, enabling flexion, extension, and roll-back movements, while in the MB it is mobile with respect to the tibial component, allowing in addition some degree of tibial rotation respect the femur [89].

The FB UKA (**Figure 2.1**) presents a round on flat contact assumed like a point on a plane leading to low congruency and so the articular geometry offers no guided knee motion [91]. In this configuration the force exerted by the knee articulation it is focused on a very small contact point leading to a probable accelerated wear due to the focusing of a higher pressure in a small contact point on the bearing component [92].

The MB UKA (**Figure 2.1**) instead present a high congruency contact between the femoral component and the polyethylene mobile bearing component, due to shape assumed to be like a sphere on a sphere. Thus, there is a larger contact area that leads to less pressure in just one point and consequently less wear of the polyethylene meniscal bearing [93].

Regarding the survival rate FB UKA showed better biomechanical performances respect the MB UKA. In addition, MB design present a higher revision rate (almost double) related to implant loosening facing also early failure due to bearing dislocation [90]. Technical errors play an important role in these failures [94]. On the other hand, MB UKA has been shown to have better kinematic performance respect to the FB UKA, even if this behaviour was not confirmed by the clinical scores [95].

Despite these discoveries, from a general point of view, nowadays it is still not possible to indicate that one design insures better performances over to the other [89]. Therefore, the personal experience of the surgeons combined with the patient's clinical status remain the focal points when deciding between FB and MB UKA [96].

Figure 2.1 Fixed bearing UKA characteristics: non-congruous articular surface, small contact area, large point contact force, and polyethylene insert fixed to base plate. Mobile bearing UKA characteristics: ultra-congruent articular surface, large contact area, small point contact force, and mobile polyethylene insert [56]

2.2.1 Physica ZUK FB UKA

The FB UKA is the one produced by Lima corporate named Physica ZUK and sold within the European Economic Area (EEA) and the Swiss markets since 2015 [97]. The first design of this model was primarily introduced in 2004 as the Zimmer Unicompartmental High Flex Knee system, based on the design of the Zimmer Miller/Galante Uni introduced in 1987 [98].

The Physica ZUK (**Figure 2.2**) presents a design that wants to replicate as much as possible the kinematics of the natural knee. Indeed, it resembles the anatomical shape of the epicondyle and consequently is positioned using an anatomical technique with the intent to replace what is resected by the surgeon. The three components are [61]:

Figure 2.2 Physica ZUK Fixed Bearing UKA design by Lima Corporate in two different view [61]

1. Femoral component made of Cast Cobalt Chromium Molybdenum (Co-Cr-Mo) alloy is wear-resistant, strong, and biocompatible.

   Its Round-on-flat articulation design aimed to enable a varus/valgus tilt of +/- 8° without loading excessively the edges. The external curved surface presents a posterior condyle that allows accommodating high flexions up to 155°, while the internal surface presents three planar spaces, two of them which accommodate the two angled femoral pegs that will provide an optimal fixation to the bone. Indeed, their angulation is designed to provide resistance to losing forces when the prosthesis undergoes flexion up to approximately 120°. Finally, to match optimally the femoral anatomy of the patient, the femoral component presents seven different sizes varying from 40 mm to 60 mm, according to the antero-posterior measure for a total of 7 sizes.
2. Fixed polyethylene insert is a semicrystalline compression molded ultra-high molecular weight polyethylene (UHMWPE) used for its high resistance to abrasion, low friction coefficient, and high chemical resistance. It is used as a bearing articulate surface [99] fixed on the superior surface of the tibial tray

through a locking mechanism. Consequently, it presents six different sizes to match the underlying tibial size; for each size, there are six thicknesses, ranging from 8 mm to 14 mm presenting a 1 mm thickness increment.

3. Tibial tray, made of Ti6Al4V alloy, presents a carved chamber on the superior surface to allow the positioning of the polyethylene insert. On the bottom are present two pegs and one fin to shield from shear and rotational forces. Moreover, these three parts are fundamental for the mechanical stability of the prosthesis allowing fixing the tibial tray on top of the properly shaped tibial bone. The tibial tray is available in six sizes depending on the antero-posterior and medio-lateral measures, ranging from 41x23 mm to 56x33mm.

The Femoral component and the Tibial tray are designed to be cemented into the patient's bone; indeed, this is a mandatory aspect to ensure the Physica ZUK UKA biomechanical performances [61].

2.2.2 Oxford Partial Knee MB UKA

The MB UKA used in this study is the Oxford Partial Knee (OPK) produced and sold by Zimmer Biomet Inc. [86].

It does not present an anatomical design as the FB but requires a functional implant technique primarily aimed to ensure stability. The OPK was designed to allow sweeping sliding and rolling movements of the knee joint and to avoid the development of shear stress which could provoke the loosening of the components; for this reason, the components, if well positioned should apply just compressive stress [100].

Moreover, the muscles and mainly the ligaments work as a constraint of this MB UKA that otherwise, given its conformation, could exit its location [100].

The OPK (**Figure 2.3**) is composed by the same three components the Physica ZUK [86], [101]:

Figure 2.3 Oxford Partial Knee Mobile Bearing UKA design by Zimmer Biomet [86]

1. Femoral component (**Figure 2.4**) is made of Co-Cr-Mo alloy to reach the required properties of wear resistance, strength, and biocompatibility. Its external surface presents a spherical curvature while the internal part has two femoral pegs that serve to anchor it to the diseased femoral condyle after an accurate surgical cut. It is available in five parametric sizes that present corresponding radii of curvature to provide an optimal fit based on the patient size.

Figure 2.4 Oxford Partial Knee 5 femoral component size [86]

2. Mobile polyethylene insert (**Figure 2.5**) made by UHMWPE, presents a superior spherical concave surface to permit an ultra-congruent fitting with the spherical curvature of the femoral component. The underside is flat and in direct contact with the flat superior face of the tibial tray over which it

moves without constraints. This insert can be chosen between five distinct bearing sizes to match the radii of curvature of the five different femoral component sizes. Moreover, for each size are available seven different thicknesses varying from 3 mm to 9 mm.

Figure 2.5 Oxford Partial Knee 6 size polyethylene bearing insert [86]

3. Tibial tray (**Figure 2.6**) is also made of Co-Cr-Mo alloy. Its design ensures optimal bone coverage, avoiding a component overhang anteromedially. The superior surface is flat to allow the free moving of the mobile polyethylene insert; while the underside presents a big peg with rounded shape corners that permit a good anchorage to the tibia. Finally, it is available in seven different sizes to optimally fit the tibial dimension for a wide range of patients.

Figure 2.6 Oxford Partial Knee 6 size Tibial tray [86]

As seen for the Physica ZUK, also for OPK is mandatory that both the femoral component and the tibial tray be cemented into the patient's bones [86].

2.2.3 Surgical technique

The surgical technique guidelines followed by the surgeons to position both Physia ZUK and OPK are provided by the corresponding manufacturers[61], [86] . Since both are UKAs, the suggested surgical steps are very similar; they differ only in some part that will be specified below.

As a prior step the surgeon must choose the right size of the UKA using x-rays taken to the affected knee in the lateral and antero-posterior (AP) standing weight-bearing. Then patient must be positioned in a supine position to test the range of knee flexion that must achieve at least 120° to create sufficient exposure of the knee, otherwise a larger incision is necessary. To follow, a deep medial parapatellar skin incision with the knee flexed at 90° is made and the knee joint disease level is visually evaluated by the surgeon. Finally, as last step before the beginning of bone resections intercondylar and peripheral osteophytes along with the one usually presented in the medial tibial section of the lateral condyle, are removed [61], [86].

Then the following surgical step are performed:

1. Tibial Plateau Resection: the femoral sizing spoon is inserted to help in the choosing of an appropriate femoral component; indeed, it depends on the relationship between the front of the spoon and an estimate of the cartilage surface position preceding arthritis. Then the tibial saw guide is applied with the shaft parallel to the tibia longitudinal axis. For the FB the tibia saw guide is positioned with 7° of posterior slope, while the MB at 5°. The femoral sizing spoon along with the tibial saw guide are locked with a clamp and this last is pinned. Then the femoral sizing spoon and the clamp are removed.

   The right level of proximal tibial resection should be checked for both FB and MB UKA. Now, being careful to not touch the ACL insertion, a vertical cut is performed with a surgical blade starting from the intercondylar notch. Then a horizontal cut is performed at the desired level after putting a retractor to protect the MCL from any accidental resection.

Finally, after the bone resection (**Figure 2.7**) all the tibial guide assembly is removed.

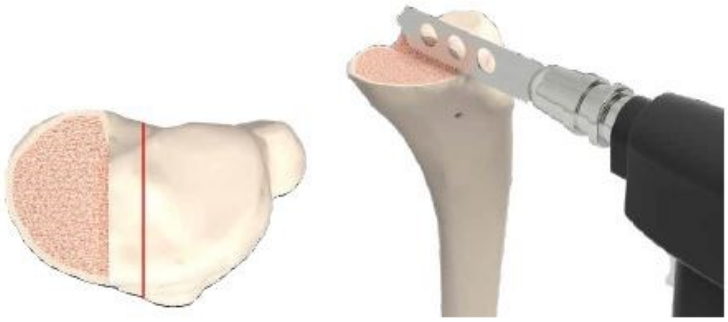

Figure 2.7 Vertical and horizontal bone resection in the affected tibia plateau [61]

2. Distal Femoral Resection: performed differently in the Physica ZUK FB and OPK MB.

- Physica ZUK FB [61]: the knee is fully extended, and a space block of 8 mm is inserted into the joint space to be sure that the fair amount of distal femoral bone will be cut. Other size of the space Block is available until thickness of 14 mm to perform this kind of arthroscopy on a wide range of patients. Moreover, the Spacer Block is angled at 5° to guarantee that the distal femoral resection is made perpendicular to the longitudinal femur axis. The joint space in then checked also by flexing the knee at 90°. This passage is important since it avoid unwanted imbalances that that could manifest themselves in the final step of implantation. Femoral Cutting Guide is then inserted into the joint, flush with the bone, to be sure that was choose the proper size of femoral component. The femoral bone is then resected following the femoral cutting guide. Subsequently, the posterior condyle is examined to find and removed any osteophytes left avoiding a possible inhibition of the extension or flexion.
- OPK MB [86]: the knee is flexed about 45° and a hole for the first peg of the femoral component is made in the femur intramedullary canal anteriorly to the PCL insertion position. Then the knee is carefully flexed 90° and a femoral drill guide is inserted to assess if the gap thickness is of the right dimensions.

The posterior resection guide is inserted into the drilled holes along with a retractor to protect MCL and ACL. The femur anatomical resection is then performed, and the posterior resection guide is removed. Any eventual posterior bone fragment is removed cutting completely the posterior horn as shown in **Figure 2.8**.

Figure 2.8 Bone fragment removal in the posterior affected epicondyle section, where the femur component will be located [61].

The knee is flexed to 100° and a tibial template is inserted along with the twin peg femoral trial component and the trial bearing insert to ensure that the joint gap has the right measure. After that the knee was moved in a fully range of motion, ensuring that there is not any presence to ensure there is no unwanted piece of bone left.

3. Tibia sizing and finishing: tibial sizer is inserted to ensure that the correct size of the tibial tray was selected and the holes necessary for the tibial pegs are drilled. Then the correct thickness of the polyethylene bearing insert is chosen to provide the desired alignment a to not give rise to an excessive stress in the ligaments, especially the collaterals one. In this stage particular care must be taken to avoid an overstuffed conformation that will overload the preserved lateral compartment of the knee joint.
4. Implant Final Components: as a final step the tibial tray and the femoral component are cemented to the bone and the polyethylene insert is in the

right position. Starting from the tibial tray for both the MB and FB, the cement is applied to both the tibial tray and to the tibia cut surface. Then the tibial tray is inserted in the bone and pressed. A cement remover is used to eliminate any excess cement. The same procedure is applied to the femoral component and femoral bone. Once that these two components are settled, the chosen bearing insert is placed between them (**Figure 2.9**).

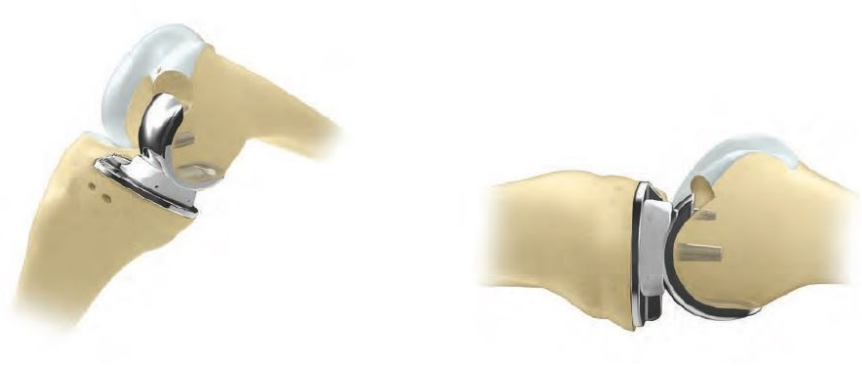

Figure 2.9 UKA succesfully implanted into the affected medial compartment of the knee joint [86]

5. Closure: the incision is closed and covered with sterile bandages.

3 State of the art

Unicompartmental knee arthroplasty was pioneered in the 1970s when Marmor [102] performed the first contemporary UKA, resurfacing just the impaired compartment of the tibia and femur. Despite the advantage of preserving the non-affected compartment, due to inconsistent early results, the TKA was preferred in the majority of arthroplasty [103]. Insall and Walker [104] found that just for a conversion rate of 28% the UKA presents good results in comparison with TKA. Indeed, the number of patients that undergoes revision before 10 years of the implant was higher than 30% [105]. The reasons were identified as the rapid wear of the polyethylene insert and tibial component loosening due to prosthesis malposition [106].

Then Kozinn and Scott [77], in 1989, proposed to use some inclusion criteria to limit the UKA implant just to a selected core of patients, to try to improve the initial disappointing outcomes. Some of the original criteria regarding the patient include the recommended age higher than 60, weight lower than 82, movement-related pain symptoms, varus-valgus deformity lower than 15°, a knee pre-operative flexion higher than 90°, and both cruciate ligaments in healthy conditions.

Consequently, greater improvements were detected starting from Berger et al [66] which reported a survivor rate of 98% within a 10-year follow-up, and the clinical outcomes that were graded as excellent reached 78% of patients. Berger et al, used the Miller-Galante UKA design by Zimmer, introduced in 1987, which is the ancient Physica ZUK fixed-bearing prosthesis used in the present study.

Also, Murray et al. [62] reported a rate of 97% concerning the survivorship of a UKA after a 10-year follow-up. The arthroplasty in this case was performed on the medial knee compartment of 143 patients using in this case the Oxford mobile bearing by Zimmer Biomet Inc, which is the second UKA design used in this study. Over the course of the years, the understanding of the knee biomechanics [40] and UKAs modes of failure allows for improved initial outcomes [107].

In addition to the overcited strict criteria in patient selection, other crucial factors to improve were found to enhance the performance of UKA and laid the groundwork for increased use of UKA. These factors regard the implant design, surgical instrumentation, and techniques. Indeed, in selected patients with the currently improved implant designs and surgical technique, the surgical procedure has become simpler to perform with an easier and faster recovery for the patient [108].

Mancuso et al. [109] highlighted another important aspect concerning UKAs and related to ACL deficiency as one of the major causes of failure for this kind of prosthesis. Indeed, ACL-deficient knees can lead to tibial loosening with a high revision rate. This is probably related to the proper function of the ACL which is a primary static stabilizer preventing the translation of the tibia on the femur [110].

Also the cement or cementless fixation of UKA results is an important factor to consider. Initially, both types were used, but since the cementless design presented a failure rate of up to 20% within the 10 years after the surgery, the cemented design was decided as the standard technique still in use nowadays [111]. Indeed, cemented UKAs demonstrated to have higher survivorship along with good functional outcomes [112]. Campi et al. [113] instead highlighted that the cementless UKA, concerning the cemented one, has a shorter surgical time, reliable fixation, and prevents cementation errors. But despite these outcomes, a follow-up over a long period should be assessed to confirm their results.

Nowadays the UKA is surgically implanted using a mobile-bearing or a fixed-bearing insert. This last design was the earliest available version of the UKA present a flat tibial articular surface that during flexion led to an increase in point loading on the surface as a result [114]. As is understandable this led to higher stress on the polyethylene and so to a high wear rate [114]. To avoid this, in 1986, Goodfellow and O'Conner [115]designed a mobile bearing UKA. This design presented a small contact stress due to a larger contact area. Consequently, the wear rate decreased, and the forces decouple at the implant interfacing the bone [115]. Nevertheless, due to its mobile nature, the mobile-bearing UKA presents some issues related to its possible dislocation and cruciate ligament impingement [107].

Both mobile-bearing and fixed-bearing despite their design differences are found to be similar concerning the survivor rate and functional outcomes both in the mid and long-term as reported by Whittaker et al. [116] and Parrette et al [117]. These similar outcomes were also reported by the national arthroplasty registries, leading so to the conclusion that neither of the two designs presents a conclusive advantage of one design over the other.

Also surgical techniques have seen a great improvement over these years [107]. Over the last few years, the surgical variables that can be controlled intraoperatively have started to be considered. These regard the component alignment, joint line maintenance, lower leg alignment, and balanced soft tissues [118]–[120]. To better control all these surgical factors, robot-assisted UKAs surgery started to be used [121]. Indeed, the goal of these systems is to be minimally invasive, highly precise, and patient-specific [107]. Indeed, compared to conventional manually performed UKA surgery techniques, these computer-aided systems demonstrate to assess a better component and lower leg alignment [122] and surgical accuracy minimizing arthroplasty failures due to the surgeon's workload [123]. But an important drawback of this robot-assisted technique is the high overall costs even if Moschetti et al. [124] reported that the costs of robot-assisted arthroplasty are comparable to conventional UKA when more than 94 surgeries are performed per year. Nevertheless, longer follow-up needs to be assessed to suggest the additional value of this kind of UKA surgery.

Another important tool that assists surgeons in the decision-making for a correct UKA surgery is represented by the finite element analysis (FEA). It is a numerical process performed by computer software capable to solve engineering problems by

subdividing an important and large problem into smaller and simpler parts named finite elements [125].

In the knee prosthesis field, the FEA results are widely used due to their effective costs and the possibility to simulate by the software a different range of loadings and configurations to evaluate which could be the best outcomes to apply in UKAs surgery.

This is possible thanks to the intrinsic capability of FEA to predict and measure parameters such as displacements, stress, strain, and abnormal force transmissions leading so to a possible failure of both mobile and fixed-bearing UKA prosthesis. Several studies have applied FEM to both this UKA design simulating different daily activity movements such are gait and squat. These studies intend to highlight possible complications that can lead to failures in order to prevent, reducing also the revision rate, and improve patient satisfaction.

Many FEM-based studies suggest that the principal cause of failure of UKAs should be searched in the coronal malalignment of the tibial tray that led to abnormal stress and strain in the tibia bone [126]–[128]. Iseka et al. [126] and Sawatari et al. [127] have detected that slight valgus inclination of the tibia is preferable when a tibial tray is positioned. While Innocenti et al. [129] suggested that a slight tibial varus alignment of 3° is preferred basing the outcome of different clinical follow-ups. However, there is currently no biomechanical justification for confirming the suitability of different alignment positions. Always in this context, but referring to the femoral condyle, Hopkins et al. [130] found that varus-valgus misalignment up to 10° did not induce highly improper kinematics for a mobile bearing UKA.

Concerning the mobile and fixed bearing designs in the literature different results can be found. For example, Emerson et al. [131] observed that the higher failure rate in fixed-bearing UKA was due to polyethylene insert wear while the mobile-bearing UKA was due to osteoarthritic degeneration in the preserved compartment. While

Kwon et al. [132] at the opposed found that the mobile-bearing UKA presents better results in the OA in the lateral compartment.

In general, in the literature, according to the knowledge of the literature acquired so far for the present study, there is no present research that highlights a marked behavior positively or negatively of one of these designs over the other one, that was performed in the FEA environment simulating the gait movement.

There are just two other studies carried out using FEA in static conditions before this study [133], [134] to confirm that no significant differences have been found among fixed and mobile bearings. The only annotation that they considered to be

relevant was the high sensitivity of the polyethylene-bearing inserts to the posterior slope. The other important outcome found was correlated with the material of the tibial tray that can change how the stress is distributed among the tibia bone.

Even though the previous works have largely applied the FEA in the field of knee prosthesis, some aspects remain unknown or unclear and controversies about UKA's way to improve biomechanical performances still exist. Thus, the present work aims to apply the FEA in both Mobile and Fixed UKA during gait, under the same conditions, by changing several important parameters that could compromise the biomechanics of this type of arthroplasty. This was done to assess which are the parameters that can influence mostly the UKA biomechanical performances and to give input regarding the improvements that can be made.

4 Materials and methods

The purpose of the present work was to perform a comparative FEM analysis of knee biomechanics performances after a FB and MB UKA implant with different configurations during the gait.

To accomplish this purpose, a total of eighteen three-dimensional (3D) Finite Element models of the knee joint after the FB and MB UKA implant were implemented: nine for the Physica ZUK FB UKA and nine for the OPK MB UKA. Then after an accurate analysis setup, the FEA was performed for all the different models. All the numerical steps were done using the FEA software ABAQUS/ Explicit version 2019 of Dassault Systemes [135] that thanks to its five core software products permit to perform both the modelling and analysis of mechanical components and assemblies allowing also to visualise the result of the finite element analysis [136].

Before starting with the analysis setup another important factor was considered to have an analysis as more reliable as possible. This regarded the choice of the optimal size components of both the UKAs. From the literature [137], [138] and the master thesis reports of the colleagues Altamore V. [133] and Fiore S. [134] was possible to state that the size of the most frequent components used by the surgeons for the two analysed UKAs models are:

- Physica ZUK FB UKA: the C-size for the femoral component and UHMWPE Insert, and the 3-size for the tibial component;
- OPK MB UKA: the M-size for the femoral component and UHMWPE Insert, and the C-size for the tibial component.

Then, these sizes were confirmed as the optimal ones, to perform the FEA in both previous studies [133], [134]and in the present one, by Prof. Dr. Thomas Luyckx [139].

In **Figure 4.1,** the different sizes for both prostheses can be noticed. The ones highlighted in yellow are the chosen size for the Physica ZUK FB and the OPK MB UKA [133], [134].

Size correspondance chart					
Fixed Bearing			**Mobile Bearing**		
Tibial component (+ disk)			**Tibial component**		
SIZE	**AP [mm]**	**ML [mm]**	**SIZE**	**AP [mm]**	**ML [mm]**
#	#	#	AA	38	26
1	41	23	A	41	26
2	44	25	B	44	28
3	47	27	C	47	30
4	50	29	D	50	32
5	53	31	E	53	34
6	56	33	#	#	#
Fixed Bearing			**Mobile Bearing**		
Femoral component			**Femoral component (+disk)**		
SIZE	**AP [mm]**		**SIZE**	**R [mm]**	**AP [mm]**
A	40		XS	20.3	38.34
B	42.5		S	22	41.6
C	45		M	23.8	45.01
D	48		L	25.6	48.42
E	51.5		XL	27.5	52.48
F	55.5		#	#	#
G	60		#	#	#

Figure 4.1 Different size present in the market for the Physica ZUK FB and the OPK MB UKA for the Femural Component, polyethylene bearing inserts and the tibial tray. The sizes are shown in in Antero Posterior (AP) and Medio Lateral (ML) direction [133], [134]

4.1 Analysis setup

The first step of the analysis setup was to decide the correct parameter to change based on the principle to understand which of them could influence, in a more relevant manner, the biomechanics of both the FM and MB UKA.

The considered parameters are five, three based on geometrical factors and two on mechanical factors. All the parameters were varied one at the time within a certain range of values. Both analysed implants have undergone the same procedures considering the corresponding differences due to their geometrical construction and requirements.

Then based on these parameter changes, different configurations were analysed to achieve the goal of the present study.

4.1.1 Parameters

The three changes in parameters based on geometric factors are the tibial AP slope angle, tibial cut error, and UHMWPE inserts thickness. Instead, the material of the tibial tray and friction coefficient are the two parameters based on mechanical factors.

All the parameter changes are explained below and reported in **Table 4.1**.

Table 4.1 Five type of parameter changed in this study to perform the different configurations.

PARAMETERS					
Tibial slope	Tibial cut error	Insert thickness		Tibial tray material	Friction coefficient
		FB	MB		
3°	-2 mm	5 mm	4 mm	Ti6Al4V	0.05
5°	0 mm	6 mm	5 mm	CoCrMo	0.2
7°	+2 mm	7 mm	6 mm	-	-

4.1.1.1 Tibial slope

This parameter regards the slope angle, in the AP direction, used to cut the tibia to allow an anatomic positioning of the tibial tray on the tibia bone. The suggested slope for the Physica ZUK is of 5° [61] while for the OPK is of 7° [86]. Of course, greater is the AP tibial slope angle, larger will result the amount of bone removed. Regarding this parameter different approaches can be implemented. So, depending on the patient's joint conditions, the surgeon must evaluate if a change in the slope inclination, respect the suggested one, is necessary.

So, in the present study, for both the evaluated designs, 3 different AP tibial slope angles are considered:

- 3° posterior slope angle for a more conservative and natural approach;

- 5° posterior slope angle suggested for the Physica ZUK FB UKA;
- 7° posterior slope angle is suggested for the OPK MB FB UKA.

4.1.1.2 Tibial cut error

This important parameter is due to an error done by the surgeons during the transverse cut of the affected tibial plateau. Indeed, can happen that the tibia is cut in excess or defect respect the cut needed to perform the UKA positioning respecting the provided surgical guidelines. This kind of error can affect the overall biomechanical performance of the implant since it can lead to an abnormal stress distribution on the bones and on the soft tissues of the knee.

Starting from a standard total cut [61], [86], defined as the sum of the tibial tray and UHMWPE insert thicknesses chosen for the two analysed UKAs, two different tibial cut errors in the longitudinal direction were simulated:

- Less deep cut equal to -2 mm respect the standard total cut. This new configuration is named understuffing configuration.
- Deeper cut equal to +2 mm respect the standard total cut. This new configuration is named overstuffing configuration.

4.1.1.3 UHMWPE insert thickness

As stated in subchapters 2.2.1 and 2.2.2 of the second chapter, the UHMWPE insert thickness are offered in different thicknesses for each size. The surgeon has the responsibility to choose the right option based on the conditions of the specific patient.

As concern the Physica ZUK design, the 6 mm configuration, used in the reference configuration model [**Table 4.2-4.3**] was provided [133] while the 5 mm and the 7 mm configurations were obtained by removing and then adding 1 mm the baseline thickness. These geometrical changes were performed in the computer-aided engineering environment (CAE) of the Abaqus software.

While the UHMWPE insert thickness analysed for the OPK were 4 mm, 5 mm, and 6 mm. The configuration of 4 mm was provided and the other two thickness obtained, as for the Physica ZUK 3D CAD model.

4.1.1.4 Tibial tray material

The tibial tray in the knee prostheses undergoes a high level of stress. So, analysis with different materials results to be an interesting parameter to consider in the analysis of the stress magnitude. Moreover, also the loads withstanding are expected to differ when different materials are coupled.

In the beginning, the standard configurations were evaluated and then the material is switched. Indeed, in the beginning, the Pyhisica ZUK was tested with the standard material (Ti6Al4V alloy) and then with the standard material of the OPK (CoCrMo alloy). The opposite was done with the OPK MB UKA.

4.1.1.5 Friction coefficient

The different materials that characterise the UKAs components lead to different friction coefficients when they come into contact. The materials of interest for the present study were the Ti6Al4V alloy, CoCrMo alloy, and the UHMWPE. So, the dynamic friction coefficient for the Ti6Al4V - UHMWPE and CoCrMo - UHMWPE contact where searched in the literature [140]. Based on the founded results two different friction coefficients were decided to be analysed: 0.05 and 0.2 [141].

4.1.2 Configurations

Two reference models were defined with their specific reference values.

The reference model for the Physica ZUK FB UKA parameters:

- UHMWPE insert presents a thickness of 6 mm, corresponding to the most used size;
- 0 mm tibia cut error stating an ideal hypothesis of no errors done by the surgeons respect the standard total cut;
- friction coefficient 0.05 corresponding to the Ideal hypothesis as lowest one;
- tibial tray realized with the standard material Ti6Al4V alloy by Lima Corporate [61];
- AP slope angle of 5° for the tibial cut as suggested by Lima Corporate [61].

The reference model for the OPK MB UKA parameters:

- UHMWPE insert presents a thickness of 4 mm;
- 0 mm tibia cut error;
- friction coefficient 0.05;
- tibial tray realized with the standard material CoCrMo alloy by Zimmer Biomet Inc. [86];
- AP slope angle of 7° for the tibial cut as suggested by Zimmer Biomet Inc. [86].

Considering all the parameters mentioned in the above subchapter, and the appropriate combinations, a total of eighteen configurations were defined as shown in **Table 4.2** for the Physica ZUK, and **Table 4.3** for the OPK comprehensives of the 2 reference ones.

Table 4.2 Nine different configurations implemented for the Physica ZUK FB UKA. The parameter highlighted represent the parameter changed respect the Reference configuration.

Physica ZUK UKA Configurations					
Name	Tibial tray material	Friction coefficient	Insert thickness	Tibial cut error	Tibial slope
Reference	Ti6Al4V	0.05	6 mm	0 mm	5°
1st	Ti6Al4V	0.05	***5 mm***	0 mm	5°
2nd	Ti6Al4V	0.05	***7 mm***	0 mm	5°
3rd	***CoCrMo***	0.05	6 mm	0 mm	5°
4th	Ti6Al4V	***0.2***	6 mm	0 mm	5°
5th	Ti6Al4V	0.05	6 mm	***-2 mm***	5°
6th	Ti6Al4V	0.05	6 mm	***+2 mm***	5°
7th	Ti6Al4V	0.05	6 mm	0 mm	***7°***
8th	Ti6Al4V	0.05	6 mm	0 mm	***3°***

Table 4.3 nine different configurations implemented for the OPK MB UKA. The parameter highlighted represent the parameter changed respect the Reference configuration.

Oxford Partial Knee UKA Configurations					
Name	Tibial tray material	Friction coefficient	Insert thickness	Tibial cut error	Tibial slope
Reference	CoCrMo	0.05	4 mm	0 mm	7°
1st	CoCrMo	0.05	***5 mm***	0 mm	7°
2nd	CoCrMo	0.05	***6 mm***	0 mm	7°
3rd	***Ti6Al4V***	0.05	4 mm	0 mm	7°
4th	CoCrMo	***0.2***	4 mm	0 mm	7°
5th	CoCrMo	0.05	4 mm	***-2 mm***	7°
6th	CoCrMo	0.05	4 mm	***+2 mm***	7°
7th	CoCrMo	0.05	4 mm	0 mm	***5°***
8th	CoCrMo	0.05	4 mm	0 mm	***3°***

4.2 FEA analysis

4.2.1 Introduction

FEA is a numerical procedure that is currently used to solve a vast class of engineering problems such as structural/stress analysis that can be static or dynamic and Linear or nonlinear, electromagnetism and fluid flow or heat transfer, biological cells growth, etc [142].

To solve these engineering problems, mathematical models are elaborated to represent a specific physical situation [142]. These models are represented by partial differential equations, identified by a set of related initial and boundary conditions, and derived using fundamental laws and principles of nature to the represented system.

An important aspect of these systems is the "approximation" factor that very often is applied to the FEA. These approximations are necessary because usually the

engineering problems present a high level of complexity in the differential equations or the initial and boundary conditions. So, to have exact solutions or a completely realistic models, result to be almost impossible and then numerical approximations are needed. Therefore, it is possible to state that these numerical models are used to predict which will be the behaviour of a part or assembly under certain imposed conditions. The results of a FEA-simulation- based are then usually represented using a colour scale that depict the result sough.

The basic steps of FEA are mainly three [46], [143](**Figure 4.2**):

1. Pre-processing phase. A model of the analysed system is constructed, and its geometry is subdivided in several sub-regions, called 'elements' (as suggested by the name FEA) or mesh, connected at discrete points, named 'nodes'. The model usually is obtained from a CAD draw that may be included or not in FEA software, but also other techniques such is the reverse engineering technique can be used. This last allows to model a real object from imaging data or object measures.
2. Processing or analysis phase. Is a computational procedure performed so by the software with the interactions of the user. Here, the prepared dataset in the first phase is then given as input to the finite element code itself. Then a system of linear or nonlinear algebraic equations are constructed, assembled, and solved giving in output the solution of the analysed problem. It is assumed that the solution is given by an approximate continuous function for each element of the system.
3. Postprocessing phase. The data of interest are obtained in output and presented as graphic concepts to allow any comparisons; nowadays, the modern FEA software permit to display overlays coloured contours that represent the data levels (e.g., strain or stress) on the analysed model.

Then the results are analysed to understand if any modification must be performed (initial geometries, boundary conditions, etc.) to have more reliable results affected as less as possible by errors.

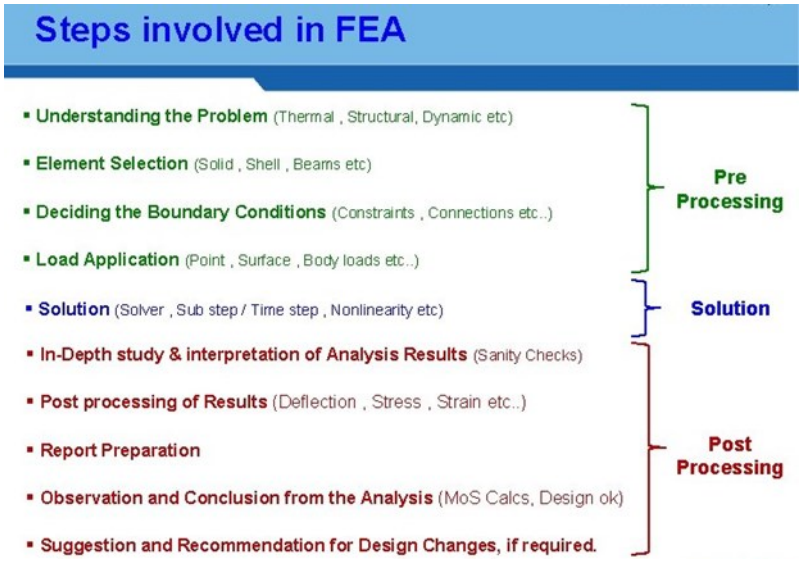

Figure 4.2 A more detailed passages involved in each of the three FEA main steps [144]

4.2.2 FEA in Orthopaedic Biomechanics

In orthopaedic biomechanics the two more used numerical approaches. The first is the multi-body-dynamics used in the musculoskeletal research and the secondo is the structure-mechanical approach. The first analyse the kinematics of the muscle activity and skeletal system, while the second is based on the stress and strain analysis of bone, load bearing implants and joints analysis. The present study relates to this second structure-mechanical approach that use FEA to solve numerically problems related to the orthopaedic biomechanics [125]. The major players involved in the entire process are engineers, that take care of the numerical simulations and the clinicians that must state if the obtained results have a clinical relevance. A clear communication between the engineers and the clinicians is so very important to ensure reliable results based on clear and certain clinical information[145].

Moreover, the analysed structure in biomechanics is strongly patient-specific depending on a lot of subjective factors such as the age, healthiness of the structures, physiologic loads, etc. this is an important factor to keep in mind when face with biological structures such as bones. Indeed, when an arthroplasty is performed, the bones of the knee joint undergo different mechanical load processes, respect the ones in a healthy knee joint[146]. With FEA is possible to analyse the behaviours of the knee

joint bones and correlated soft tissues when an arthroplasty is performed. In this way, different settings concerning the prosthesis or knee joint morphologies can be set virtually in the software to simulate or predict different clinical situations that may lead to failure or complications of the arthroplasty [147]. As a final step, the stress and strain distribution on an implant-bone compound are evaluated and the best configuration is chosen and surgically performed on the real knee joint.

To resume, the reliability of the numerically constructed models depends both on a proper geometrical reconstruction and a thorough mathematical description of the involved biological tissues behaviours; also the interactions of these structures with the surrounding environment it is of basilar importance [24].

4.2.3 Assembly

The virtual numerical models necessary for this study are so composed:

- 3D CAD model of a native knee composed of femur and tibia with the relative articular cartilage, and all the soft tissues proper of a knee joint.
- 3D CAD model of Physica ZUK FB UKA;
- 3D CAD model of OPK MB UKA.

In relation to the last two, the 3D CAD geometry of the Physica ZUK FB and OPK MB UKAs were already available from previous studies developed by former students at the Beams department of the Université Libre De Bruxelles (ULB)[148], under the supervision of Professor Bernardo Innocenti [149] in collaboration with Prof. Dr. Thomas Luyckx [139] that supervised also the present work in some passages related to the clinical aspects of the study.

4.2.3.1 Native knee model

A right leg from a healthy patient was considered to represent the geometric native knee model. The 3D CAD model was already available and was taken as a reference for the development of a more realistic model's geometry. Indeed, an initial problem was encountered due to the absence of the physiological separation between cortical

and cancellous bone, both on the tibia and femur.

Thus, this cortical-cancellous subdivision was obtained by importing the 3D CAD model of the knee joint in the Abaqus software environment where an operation of remodelling was performed on the tibia and on the femur. To do this operation, guidelines [150], [151] related to the proper width of cortical bone in a healthy human leg were followed to obtain a model as much realistic as possible.

This operation was performed in both tibia and femur of the original model.

Finally, the new "entry-level" model obtained was used to perform the virtual implantation of the MB and FB UKA. Is important to state that the muscles, the patella, and relative ligaments were not considered and so were removed from the virtual model. This has been done because this study regards the gait movement, and their presence does not influence in a relevant manner the simulations and the FEA results.

The finite element model included different "Part" that define the geometry of the individual components and are called the building blocks of the ABAQUS/CAE model. These are:

- femoral bone comprehensive of articular cartilage;
- tibial bone comprehensive of articular cartilage;
- patellar bone;
- left and right menisci;
- MCL divided into two constituent bundles: anterior (aMCL) and posterior (pMCL);
- LCL is defined as a single linear element.

While the ACL, divided into anterior (aACL) and posterior (pACL) bundle, and the PCL also divided into anterior (aPCL) and posterior (pPCL) bundle, are constructed as "Connectors" that don't belong to the "Part" module but are performed in the "Assembly" module to the Abaqus. These connectors are used to connect the femur to the tibia, as in a real knee, and the attachment points were decided following the literatures indications [1]. This concept to represent the cruciate ligaments as connectors is completely new and was developed in the Beams department of the ULB [148].

4.2.3.2 Fixed Bearing UKA virtual implantation

After the definition of the "entry-level" model, the second step was to follow the surgical technique guidelines of the manufacturer's [61](Chapter 2.2.3) to recreate in the FEM virtual environment an identical configuration of the knee joint that the surgeon accomplishes on the knee joint of a patient in the operating room environment So, the tibia and the femur were cut and prepared to host respectively the tibial tray and the femoral component

Moreover, the tibia was cut distally while the femur proximally. These cuts consist in cutting 30 % of the total length of the two parts. This quantity was decided since after 30% of the total length the section can be considered constant with a constant stress distribution [134]. This passage was done to reduce the computational cost.

Then the provided 3D CAE model of the Physica ZUK FB UKA was uploaded in the same Abaqus environment. It is constituted by the femoral component, the UHMWPE insert fixed to the tibial tray, and the tibial tray itself (**Figure 4.3**).

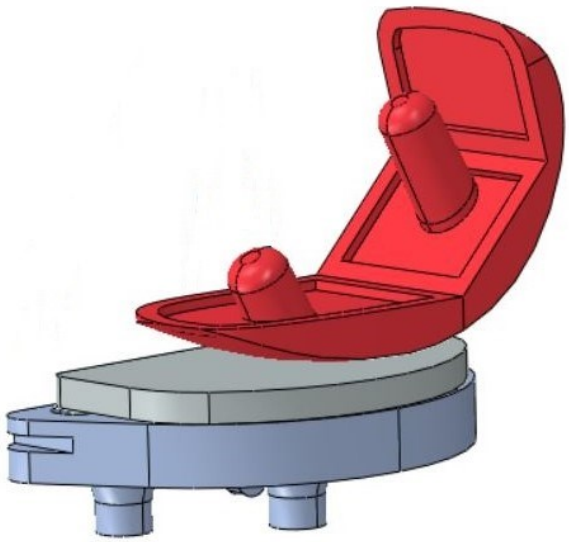

Figure 4.3 Fixed Bearing (Physica ZUK UKA) 3D CAE Abaqus model composed of femoral component (red), fixed-bearing insert (grey), and tibial tray (light blue)

Starting from the tibia and then from the femur model bone, the FB UKA was virtually implanted in the reference configuration with the parameters specified in **Table 4.2**. Then the polyethylene component was correctly positioned on the carved chamber in the superior surface of the tibial tray. Consequently, the femoral

component was positioned on the predisposed part of the femur that will host it. To circumvent interference problems, the tibial tray and the femoral component were positioned on the respective shaped bones and then were virtually implanted with the cut/merge function of Abaqus realizing so the holes for the peg of the tibia.

The prosthesis size resulted to be optimal for the size of the reference model, so there was no need to scale the femur or tibial bone model to adjust it to the chosen dimensions of the FB UKA.

Finally, in **Figure 4.4** it is possible to appreciate the final model with the FB UKA virtually implanted.

Then the other eight configurations were obtained changing the parameters one by one as shown in **Table 4.2**. All the new configurations were obtained starting from the reference one. So, the tibial and femur cut were performed from the beginning following the same process described a few lines above. Then placing the FB UKA was placed in the correct position for all the configurations.

The only two configurations on which were not repeated all the cut process were the 3rd and the 4th ones since for these was necessary to change respectively the tibial tray material from Ti6Al4V to CoCrMo, and the friction coefficient, from 0.05 to 0.2. Indeed, to actuate these mechanical changes in the Abaqus environment it only takes to go to the "Part" module and change these quantities assigning the new material to the tibial tray and the new friction coefficient to the respective part in contact.

Once that the final models were developed for all the nine configurations, the implementations and simulations were performed in the FEM analysis environment to obtain the results.

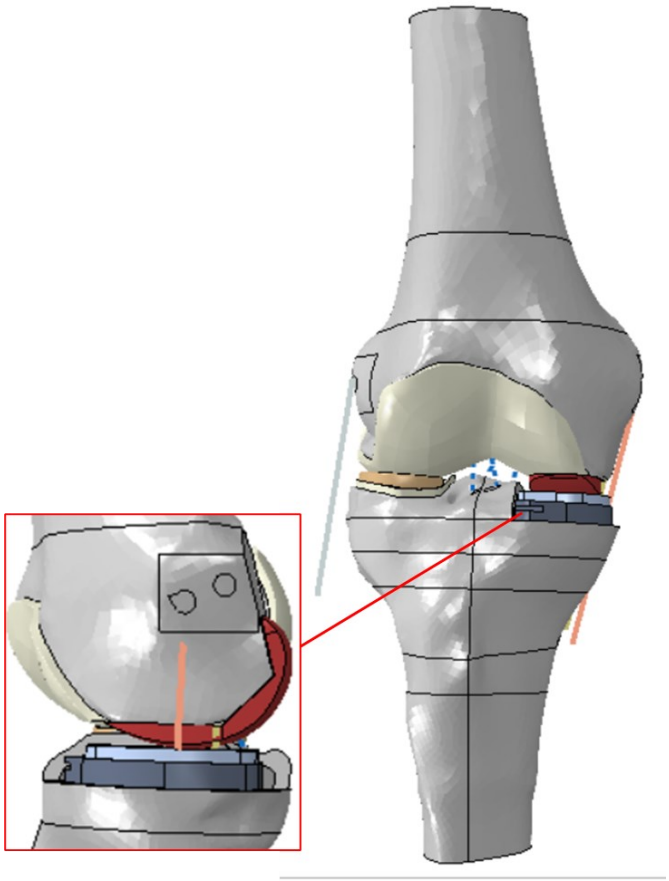

Figure 4.4 Fixed Bearing (Physica ZUK UKA) implanted on the reference model, following the manufacturer's guidelines surgical technique [61]. It consists of tibial and femoral bones (grey), cartilage layers (cream-colored), lateral meniscus (light brown), lateral collateral ligament (light grey), anterior medial collateral ligament (pink), posterior medial collateral ligament (dark grey), cruciate ligaments (blue dotted lines), femoral component(red), tibial tray (dark grey), and polyethylene fixed bearing insert (light blue).

4.2.3.3 Mobile Bearing UKA virtual implantation

The same procedures followed for the FB UKA implantation were adopted to perform also the OPK MB UKA virtual implantation. Thus, starting from the same "entry-level" model, the manufacturer's surgical guidelines [86] were followed, and then the chosen prosthesis was virtually positioned.

In **Figure 4.5** the only design of the used MB UKA is shown. As the FB is composed of the femoral component, the UHMWPE insert, and the tibial tray with the difference

that here the bearing insert is only supported and not anchored to the tibial tray being so free to move accordingly with the femoral component.

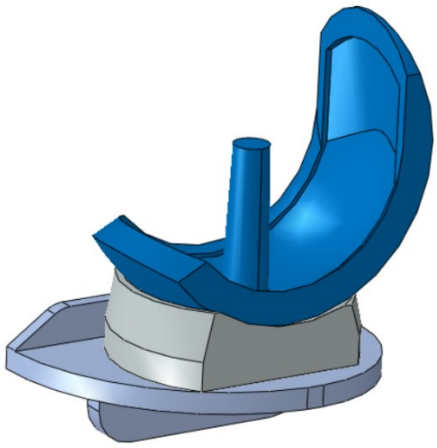

Figure 4.5 Oxford Partial Knee 3D CAE Abaqus model composed of femoral component (blue), mobile-bearing insert (grey), and tibial tray (light blue)

Then the other eight configurations were obtained changing the parameters one at the time as shown in **Table 4.3**. Almost all the new configurations were obtained by repeating all the cut process on "entry-level" model. This was necessary since a

major part of the parameter changing regards geometrical factors such as the tibial slope. of the reference one that was obtained implanting the OPK prosthesis following

the suggested configuration by the Zimmer Biomet Inc. for the posterior slope, the deepness of the longitudinal cut on the tibia [86]. The only two configurations for which the parameter change concerned mechanical and not geometrical factors are the 3rd and the 4th of **Table 4.3**. Indeed, they represents the models in which were changed respectively the tibial tray material from CoCrMo to Ti6Al4V (opposite to the 3rd configuration regarding the change of the tibial tray material), and the friction coefficient that was simulated to increase from 0.05 to 0.2.

Once that the final models were developed for all the nine configurations, the implementations and simulations were performed in the FEM analysis environment to obtain the results.

As for the MB, also for the FB UKA the prosthesis size resulted to be optimal for the size of the reference model, without performing any scale of the femur or tibial bone model.

Finally in **Figure 4.6** it is possible appreciate the final model with the FB UKA virtually implanted.

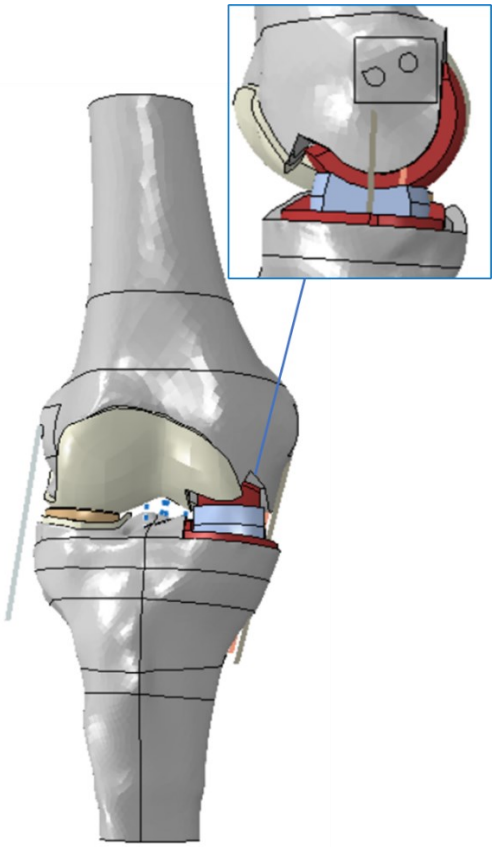

Figure 4.6 Mobile Bearing (Oxford Partial Knee UKA) implanted on the reference model, following the manufacturer's guidelines surgical technique [86]. It consists of tibial and femoral bones (grey), cartilage layers (cream-colored), lateral meniscus (light brown), lateral collateral ligament (light grey), anterior medial collateral ligament (dark grey), posterior medial collateral ligament (pink) cruciate ligaments (blue dotted lines), femoral component and tibial tray (red) and polyethylene mobile bearing insert (light blue).

4.2.4 Material Properties

For the present study was necessary to define the mechanical properties of the materials of all the single parts used. It was chosen to define most of the materials as linear elastic isotropic since they result to give a good approximation of the mechanical proprieties of the knee when a stress analysis needs to be carried out.

Table 4.4 reports all the values needed to describe the mechanical properties of the materials used. They were taken from data available in literature [129], [152], [153].

Table 4.4 Values used to define the mechanical properties of all the material used in this study. This value has been taken from the literature. For the cortical bone, E_1, E_2, and E_3 represents respectively the radial, circumferential, and axial direction. Abbreviation used: aMCL anterior bundle of the medial collateral ligament, pMCL posterior bundle of the medial collateral ligament, LCL lateral collateral ligament.

Material	Model	Young's Modulus (MPa)	Poisson's Ratio	% Initial strains at full extension	Density [g/cm³]
Cortical bone	Transversely isotropic	E_1 = 11,500 E_2 = 11,500 E_3 = 17,000	ν_{12} = 0.58 ν_{13} = 0.31 ν_{23} = 0.31	---	1.85
Cancellous bone	Elastic isotropic	2130	0,31	---	0.29
Menisci	Elastic isotropic	59	0,49	---	11
Cartilage	Elastic isotropic	13	0,475	---	10
aMCL	Elastic isotropic	332	0,45	0,03	0.31
pMCL	Elastic isotropic	332	0,45	0,04	0.31
LCL	Elastic isotropic	345	0,45	0,08	0.31
CoCrMo alloy	Elastic isotropic	220,000	0,30	---	10
Ti6Al4V alloy	Elastic isotropic	110,000	0,30	---	4,51
UHMWPE	Elastic isotropic	685	0,40	---	0.97

For the Cortical bone of the tibia and femur a linear elastic transversely isotropic model was developed since it is more suitable when a stress analysis is performed. As visible from the data reported in **Table 4.4**, the cortical bone is characterized by a Young's Modulus that presents significant variation along the longitudinal axis while on the transversal and sagittal ones this variation is lower. So, the direction E_3 represents the tibial mechanical axis.

On the contrary, the cancellous bone has a neglectable variation of Young's Modulus and so isotropic, linear, and elastic with a constant thickness of 2,5 mm for both the

femur and it was modelled as linear elastic isotropic.

Articular cartilage that covers distal epicondyle part of the femur and the proximal part of the tibia, is considered isotropic, linear, and elastic with a constant thickness of 2,5 mm for both femur and tibia.

Also the menisci are modelled as linear elastic isotropic with E = 59 MPa and $\upsilon = 0.49$.

Regarding the mechanical properties of the UKA components materials results clearly that they present Young's modulus value very high if compared with the ones of the menisci and cartilage. This is a very important aspect and particular attention should be given to this difference in stiffness between the interactions of healthy-soft-tissue of the lateral compartment and metal–UHMWPE of medial one since this is one of the causes that damage both the tibia, by increasing its stress, and the ligaments leading to an increase in strain (especially for MCL and the ACL).

Also the three collateral ligaments (aMCL, pMCL, and LCL), are modelled as linear elastic materials since when they are in healthy conditions and no load is applied to them, these ligaments are never in an unloaded configuration. This condition is present because when the motion of the joint is simulated, the knee is usually considered in an extended position. In this state, even if there is no external load, the ligaments are strained and therefore already sustaining a tensile load, which is called reference strain, initial strain, pre-strain, or in situ strain [129], [152].

Instead, the pre-strain for the Cruciate ligaments is zero values since both are unloaded when there is not any load applied on the knee.

Concerning the behaviour of the ACL and PCL, during tensile loading can be noticed a first phase in which the ligament is almost unloaded presenting so a non-linear pattern during the toe region. Therefore, both the cruciate ligaments present a non-linear stress-strain curve described by the following function [154]:

$$f = \frac{1}{4} k \frac{\varepsilon^2}{\varepsilon_l}, \qquad 0 \leq \varepsilon \leq \varepsilon_l$$

$$f = k(\varepsilon - \varepsilon_l), \qquad \varepsilon > 2\varepsilon_l$$

$$f = 0 \qquad \varepsilon < 0$$

With f representing the axial force sustained by the ligament, k is a stiffness parameter that differ between the bundles, ε is the strain and $2\varepsilon l$ is the threshold strain indicating the passage from the toe to the linear region εl (**Figure 4.7**) and is set at a value of 0.03 for all the bundles [154], [155].

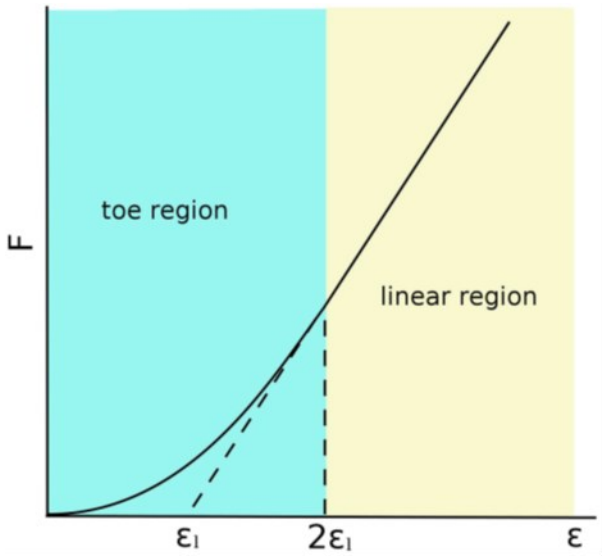

Figure 4.7 Force–strain behaviour of a generic ligament following the model described by Blankevoortetal. in the 1991 [154]. The threshold strain $2\varepsilon l$ indicates the change from the toe to the linear regions.

The stiffness parameters used in the equation for the cruciate ligaments were taken from the literature and listed in **Table 4.5** [154], [156]**.**

Table 4.5 Stiffness parameters used in the equation. Abbreviations used: aACL anterior bundle of anterior cruciate ligament; pACL posterior bundle of anterior cruciate ligament; aPCL anterior bundle of posterior cruciate ligament; pPCL posterior bundle of posterior cruciate ligament.

Ligaments	Stiffness [N]
aACL	1500
pACL	1600
aPCL	2600
pPCL	1900

4.2.5 Constraints

The constraint in all the models presented in this study was applied to the femur, tibia, ligaments, articular cartilages, lateral meniscus, and all the UKAs components.

The femur center of rotation was constrained in all the degrees of freedom with two Kinematic coupling constraints, to the lateral and to the medial femoral epicondyle as shown in **Figure 4.8**. In this way, the body of the femur varies according to the center of rotation at which the Amplitude and loads are applied.

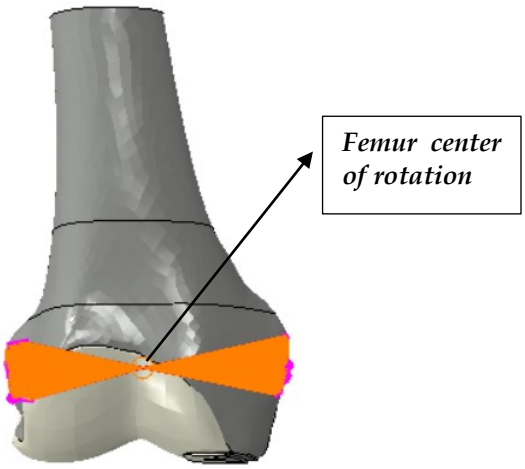

Figure 4.8 Femur 3D CAE model in Abaqus. The orange bundles represent the constraints applied between the femur center of rotation and both the lateral end medial epicondyle.

All the ligaments were constrained both to the femur and to the tibia, in the respective point of insertions, with Kinematic coupling constraints of just the three degrees of freedom related to the translations, while the rotations were not constrained.

The only applied constraint that was not a kinematic, but a tie constraint is the one between the horns of the lateral meniscus and the articular cartilage of the tibia to simulate the physiological behaviour found in a healthy knee. Indeed, the rest of the semilunar part of the lateral meniscus was not constrained and was free to move and follow the knee movements.

4.2.6 Interactions

A surface-to-surface interaction type is established between almost all the components that enter in contact and that is possible to divide into three main categories as reported in the following **Table 4.6** with the corresponding dynamic friction coefficient assigned following the literature indications[141], [152].

Table 4.6 Three type of interaction present in the UKAs model. Abbreviation used: UKA unicompartmental knee arthroplasty.

Interaction	Dynamic Friction Coefficient
Tibio- Femoral	0,1
Bone-UKA	0,4
UKA-UKA	0,05

The interaction was set between the following couples of surfaces:

- Articular Cartilage of femur and tibia
- Articular Cartilage of femur and superior section of the lateral meniscus;
- Femoral component and UHMWPE bearing insert;
- UHMWPE bearing insert and Tibial tray;
- Tibial tray and tibial bone.

Is important the remember that the chosen models of the UKAs are cemented, so in the interaction between the femoral component and tibial tray with the respective bones. This factor was considered and given as input information that in the Abaqus environment was done by setting a dynamic friction coefficient equal to 0.4 that according to the literature [141] mimics the functions of cement.

4.2.7 Boundary conditions

The boundary conditions applied to all the eighteen models was four.

1. Encastre of the distal face of the tibia generate by the transverse cut that reduced the tibia to 30% of its original length. This was done to ensure the tibia to the ground and so to fix it in all directions. The moving part of the model that was chosen to set free to move to perform the gate movement, is the femur. Indeed, this last does not present any type of encastre boundary condition.
2. Displacement/rotation boundary condition type was applied to the extremity of the LCL that usually insert into the proximal part of the fibula. But in the present study, the fibula is not present, since is not relevant for the final goal. Thus, it was bounded to the ground n the three translational degrees of freedom.
3. Flexion- Extension rotation applied directly to the femoral center of rotation along the y-axes of our reference system, but in the opposite direction to perform the right gait movement.
4. Internal-External rotation is also applied directly to the femoral center of rotation along the z-axes in the same direction.

The amplitudes for the Flexion- Extension and Internal-External angles were provided by previous studies.

4.2.8 Loading conditions

Only two loads were applied to the center of rotation of the femur:

1. Axial load applied to the femoral center of rotation along the z-axes but in the opposite direction to mimic the gravity force.
2. AP load applied always to the femoral center of rotation along the x-axes of the reference system but in the opposite direction.

The amplitude for the axial and AP load were provided by previous studies.

Since dynamic FEAs for a gait cycle were performed in the present study, the loads and the rotational angles were given in input as Amplitudes, and so as values that

change in time. More precisely during 1 second that is the duration of a gait cycle. Instead in static analysis, just a value is settled because of course it does not change with respect the time.

4.2.9 Finite Element Model

As written in Chapter 4.2, the FEA principle is based on the subdivision of the complex geometry of a solid into smaller finite elements connected through nodes, that form the finite element mesh. Then a solution is obtained for each finite element rather than obtaining an analytical solution for the whole model. This kind of approach brings an approximate result to the complex problem and by using mesh refinement, the obtained approximate results will approach the true result.

The difficulty in meshing finite element models involves achieving the best balance between analysis accuracy and speed.

In all the studied models the mesh dimensions have been varied along the vertical direction both for the femur and tibia. This permits us to obtain solutions more reliable in the regions of interest (ROIs) where the mesh was set to have a low and more precise dimension. Indeed, small elements permit a better discretization allowing to fit better the original shape, also presenting a higher number of nodes that will improve the accuracy of the results. This higher accuracy of course will increase the computational time due to a higher number of differential equations that the software needs to solve.

While for the rest of the regions the dimension was higher. From a general point of view, the usage of bigger elements brings to important approximations of the model structure, leading so to changes between the boundaries of two contiguous structures.

Also the distance between the nodes of the element and the interpolation error will increase affecting negatively the accuracy of the results. But, even if the regions that were not of interest for the present study were set with a bigger element dimension with respect the one for the ROIs, no significant accuracy impairs were observed. This is probably due to the particular attention putted to combine in a correct way the difference in dimension on the border regions to match them.

So, this element dimension variation along the vertical direction allows to reduce

the computational time of the simulations that is already high in this study due to the intrinsic complexity of the model that replicates the complexity of the knee joint, even if some approximations have been made.

To realize the meshes on the totality of the model structure, a tetrahedral element shape was used. Different element sizes were made until the right balance between accuracy and computational time was reached. The results of the final mesh for all the parts of the model can be seen in **Figure 4.9** while in Table **4.7** is reported the totality of tetrahedral 3-D elements used for each of them during the simulations.

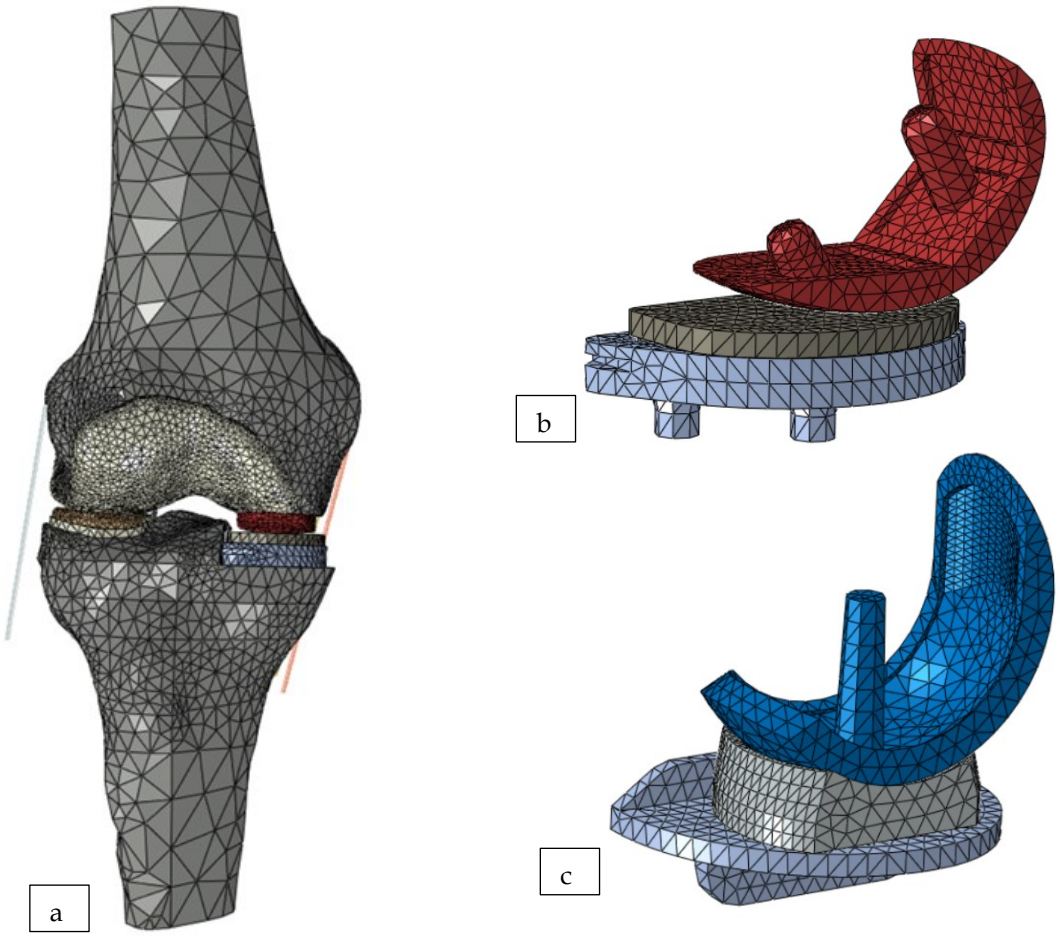

Figure 4.9 a) Complete model constituted by Mesh of different dimensions according to the identified ROIs. It consists of tibial and femoral bones (grey), cartilage layers (cream-colored), lateral meniscus (light brown), lateral collateral ligament (light grey), anterior medial collateral ligament (pink), posterior medial collateral ligament (dark grey), cruciate ligaments (blue dotted lines), femoral component(red), tibial tray (dark grey), and polyethylene fixed bearing insert (light blue).
b) Physica ZUK design Mesh: femoral component (red), fixed-bearing insert (dark grey), and tibial tray (light blue).
c) Oxford Partial Knee design: femoral component (blue), fixed-bearing insert (grey), and tibial tray (light blue).

For the components of the UKAs, the collaterals, and the lateral menisci the total number of tetrahedral elements does not change since their morphology does not change. While for the tibia and the femur this number changes with the change of the analysed configuration due to the different cuts made. Just the number of the tibia and femur elements for the reference configurations for the FB and MB are reported in the **Table 4.7** this is because the geometrical differences of the other configurations with respect to the reference one are not so deep to suddenly combine the total number of elements. Thus, the totality of elements in the tibia and femur respect all the configurations is approximately the same.

Table 4.7 Elements and nodes numbers for the finite element model of the different instances used in the reference models for the MB and FB UKA. Abbreviation used: FB fixed bearing, MB mobile bearing, aMCL anterior bundle of the medial collateral ligament, pMCL posterior bundle of the medial collateral ligament, LCL lateral collateral ligament

Part	N° of elements	N° of nodes
Femur of FB reference model	81,079	16,102
Tibia of FB reference model	23,554	4,757
FB UKA femoral component	3,324	960
FB UKA UHMWPE insert	4,056	993
FB UKA tibial tray	4,216	1,197
MB UKA femoral component	4,145	1,215
MB UKA UHMWPE insert	4,191	1,036
MB UKA tibial tray	3,214	912
Femur of MB reference model	154,895	28,323
Tibia of MB reference model	32,447	6,404
Lateral meniscus	1,155	443
aMCL	16	17
pMCL	16	17
LCL	13	14

4.2.10 Regions of interest

The ROIs for the present study were defined in the tibia used then to obtain the average von-Mises stress in these regions. Whereas for the femur three regions were defined to perform a variable mesh sizing, but no stress analysis was carried out on them in the present study.

The ROIs defined on the tibia [133], [134], and used for all the eighteen models, are five as shown in **Figure 4.10**:

- Two local regions close to the tibial tray in the medial and lateral proximal zone: 10 mm depth were investigated starting from the tibial surface in contact with the lower surface of the tibial tray;
- Two global regions, lateral and medial, located at 20 mm from the tibia tray and so in the distal part of the tibia. Starting from this 20 mm distance, a total depth of 30 mm was investigated both for the medial and lateral part.
- Subchondral lateral region was also investigated in all the analysed models. It is in the proximal lateral part of the tibia immediately beneath its articular cartilage.

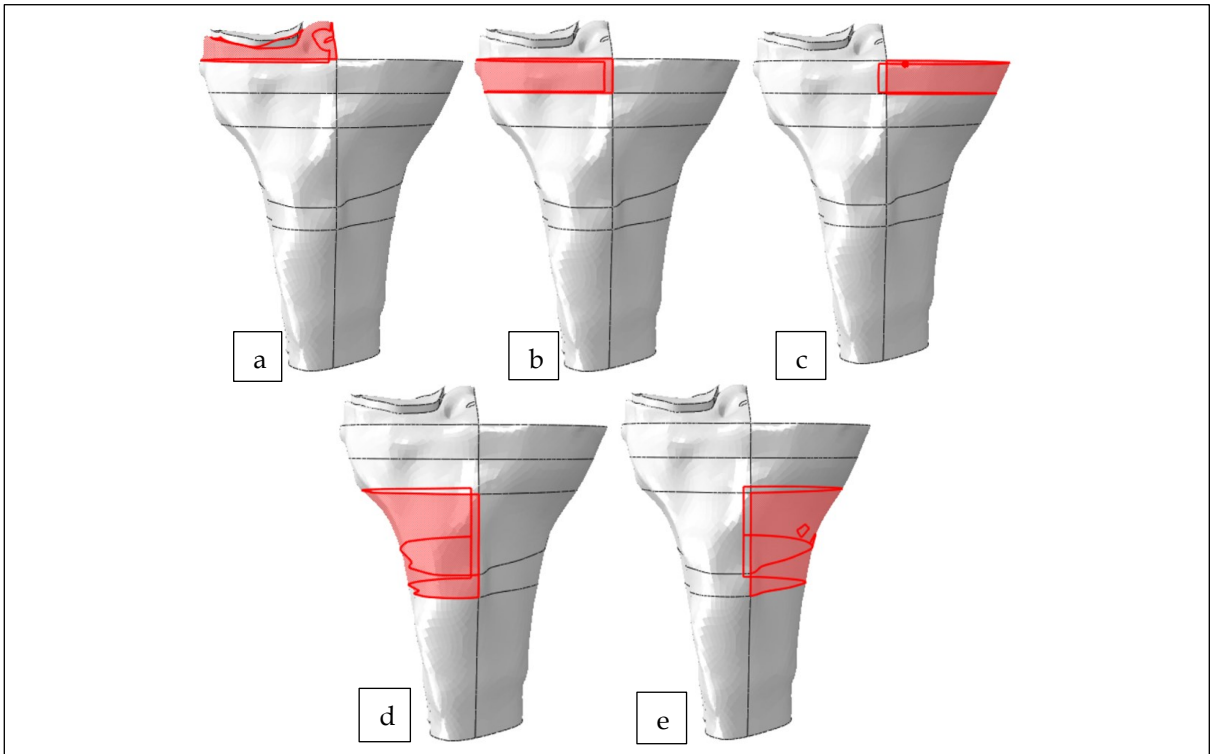

Figure 4.10 Region of interest defined in the Tibia: a) Subchondral lateral ROI, b) Proximal Lateral ROI, c)Proximal Medial ROI , d) Distal Lateral ROI and e) Distal Medial ROI

4.2.11 Mass scaling

A dynamic explicit analysis needs a mass scaling factor, that how suggested by the name, is necessary to scale the mass of the whole model at the beginning of each step. What happen is that when the mass scaling factor is implemented, the masses of the elements presenting a time increment inferior to the one that is supplied by the user are scaled. This means that the time increment of those elements becomes

equal to the time increment supplied.

In beginning, the simulations were carried out on the reference model presenting the FB UKA implant and then on the reference model presenting the MB UKA implant. The first mass scaling supplied to both the models was equal to 1e-05 to see if the gait movement was correctly performed and no errors were done. Then the final mass scaling supplied to the FEA software was set at 1e-06 for all the nine models presenting the FB UKA. For the FB UKA instead, some vibrational behaviour could have been noticed so a further upgrade was performed and set at 1e-07 for all the nine models presenting the MB implants.

Of course, lower is the mass scaling and more computational effort and time is required. So, one simulation with the mass scaling set at 1e-06 required around 36 hours to converge to a solution, while the time required when with the mass scaling of 1e-07 approximately was of 72 hours or even more.

Thus, in general, the golden rules is to find a mass scaling value for which convergence is reached within an adequate simulation time, without presenting noticeable vibrational behaviours.

4.2.12 Output of interest

The outputs of interest, used to compare the biomechanical performance of the different UKA implant considered, were eight as follow:

- Femoral Antero-Posterior (AP) translation;
- Femoral Internal-External (IE) rotation;
- Contact Area on UHMWPE Insert surface;

- AP and ML Contact Point on UHMWPE Insert surface;
- UHMWPE Insert average von-Mises Stress;
- Tibial ROI average von-Mises Stress;
- Cruciate Ligament Length;
- Collateral Ligament Length.

5 Results

The results obtained by the simulations of all the evaluated models are presented in this paragraph. For each output of interest are reported 3 graphs organized as follows:

A. 1st graphs depict the difference in the MB and FB reference models presenting the specific geometrical parameters suggested by the manufacturers, as previously reported in the **Table 4.2** and **Table 4.3**. The blue curve always represents the MB UKA while the red one represents the FB UKA.

B. 2nd graphs show the most relevant results obtained with respect to the MB reference configuration reported in the 1st graph.

C. 3rd graphs show the most relevant results obtained with respect to the FB reference configuration reported in the 1st graph.

In all the graphs is present a black vertical line positioned at 0.6 s representing the passage from the stance to the swing phase that characterize the gait cycle as shown in **Figure 1.9**.

5.1 Femoral Antero-Posterior (AP) translation

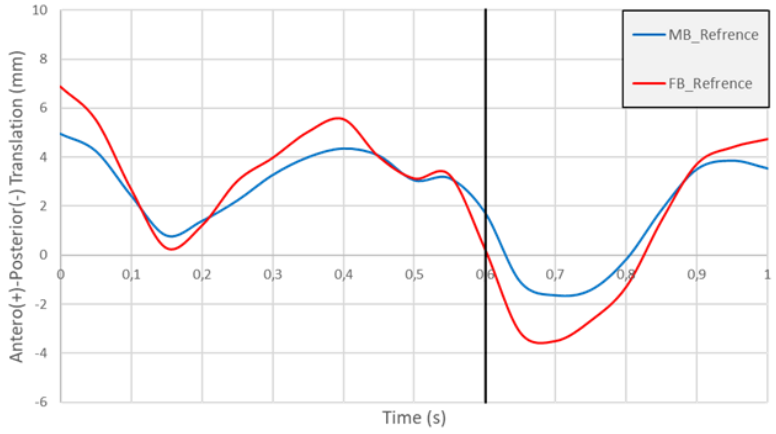

Figure 5.1 Antero posterior translation of femur centre of rotation in the reference configurations MB and FB

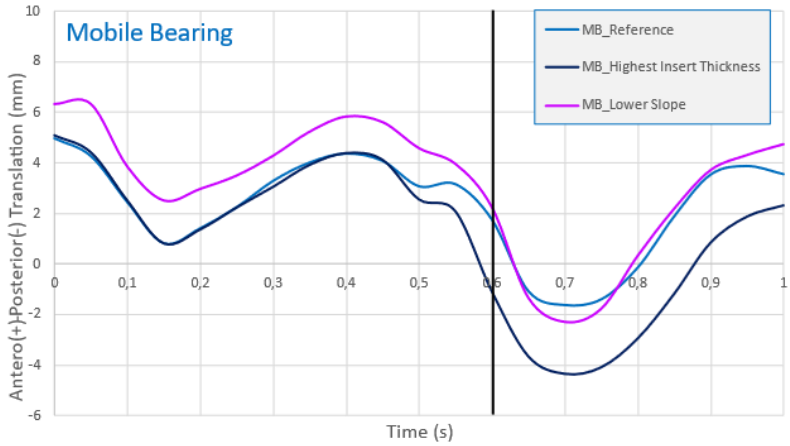

Figure 5.2 Most relevant difference respects the AP translation of the femur centre of rotation for MB UKAs

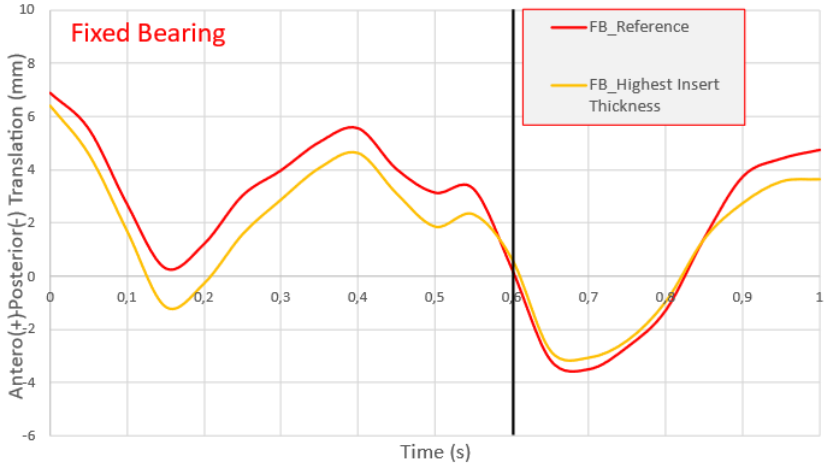

Figure 5.3 Most relevant difference respects the AP translation of the femur centre of rotation for FB UKAs

5.2 Femoral Internal-External (IE) rotation

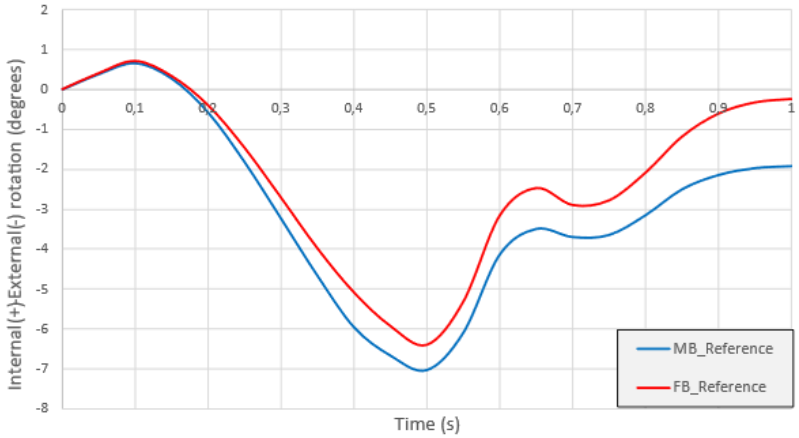

Figure 5.4 Femoral center of rotation internal-external rotation in the reference configurations MB and FB

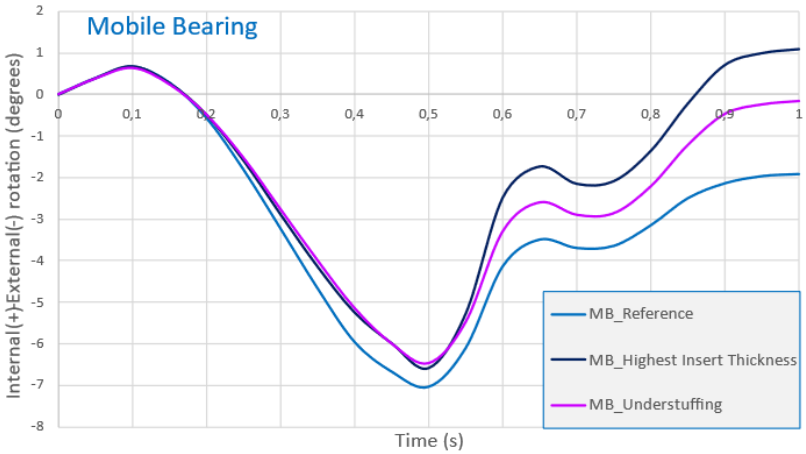

Figure 5.5 Most relevant difference respects the Femoral center of rotation internal-external for MB UKAs

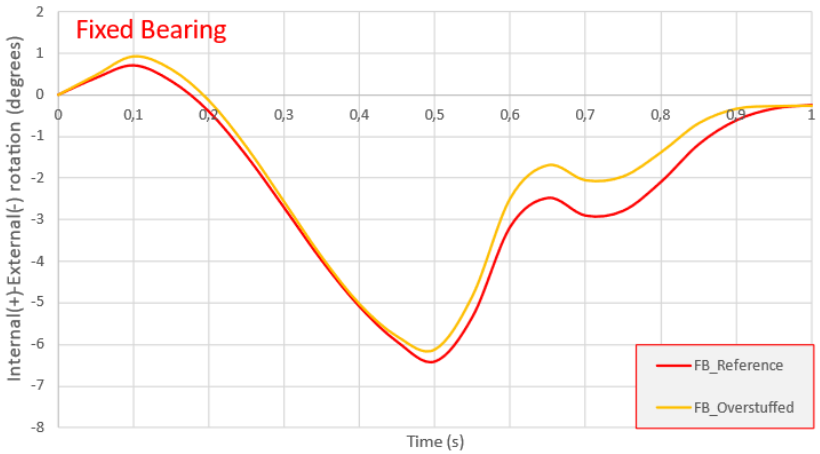

Figure 5.6 Most relevant difference respects the Femoral center of rotation internal-external for FB UKAs

5.3 Contact Area on UHMWPE Insert surface

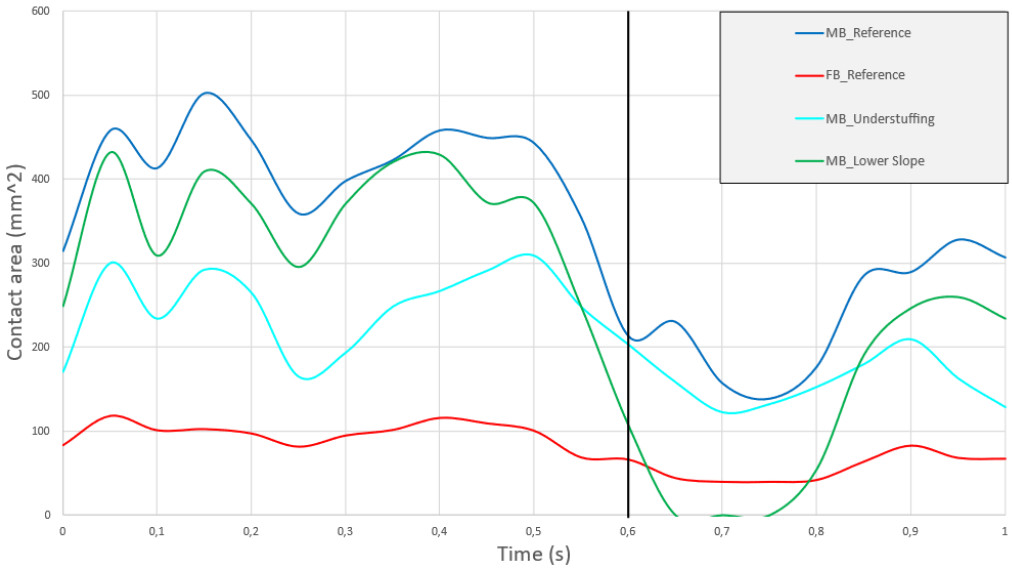

Figure 5.7 contact area un the superior UHMWPE Insert surface. The contact area for the reference configuration of FB and MB UKA are reported along with the most relevant differences respect the contact area of the MB UKAs.

5.4 AP Contact Point on UHMWPE Insert surface

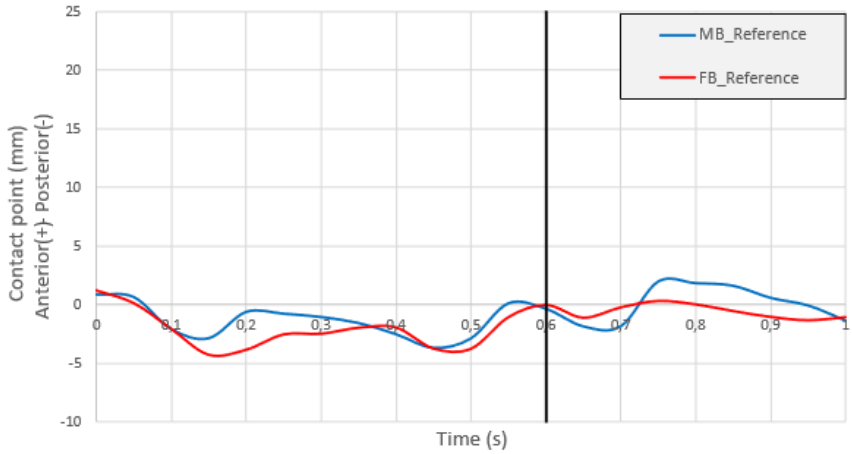

Figure 5.8 AP Contact Point on UHMWPE Insert surface in the reference configurations MB and FB

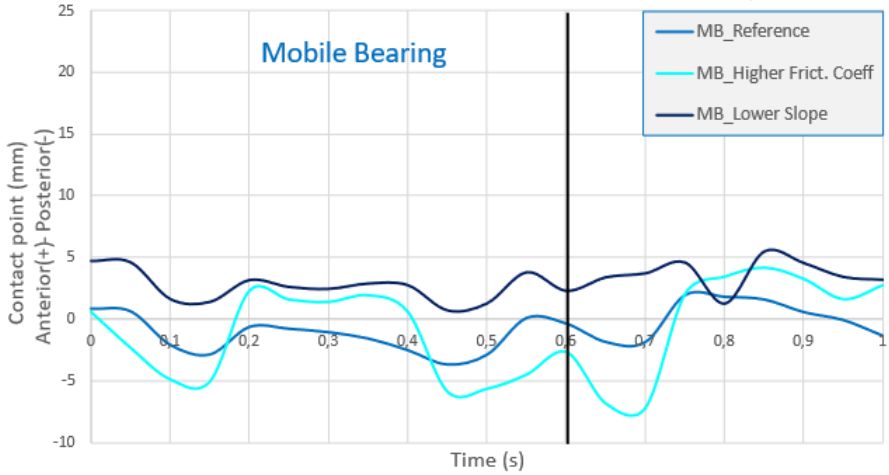

Figure 5.9 Most relevant difference respects the AP Contact Point on UHMWPE Insert surface for MB UKAs

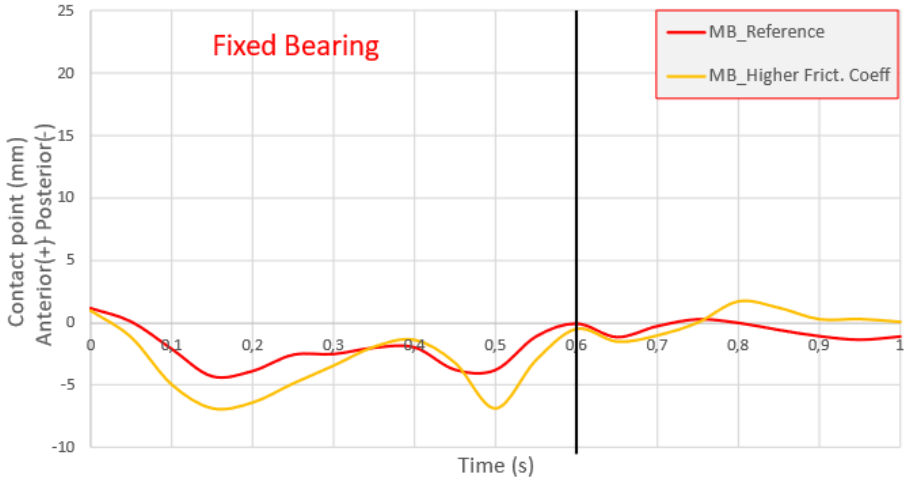

Figure 5.10 Most relevant difference respects the AP Contact Point on UHMWPE Insert surface for FB UKAs

5.5 ML Contact Point on UHMWPE Insert surface

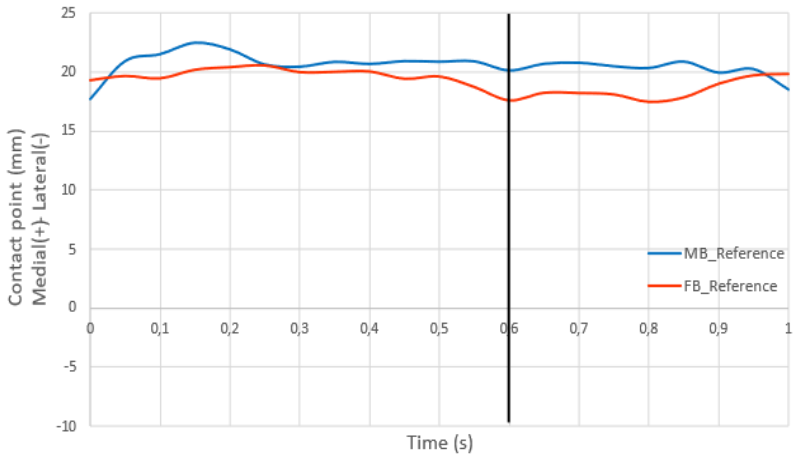

Figure 5.11 ML Contact Point on UHMWPE Insert surface in the reference configurations MB and FB

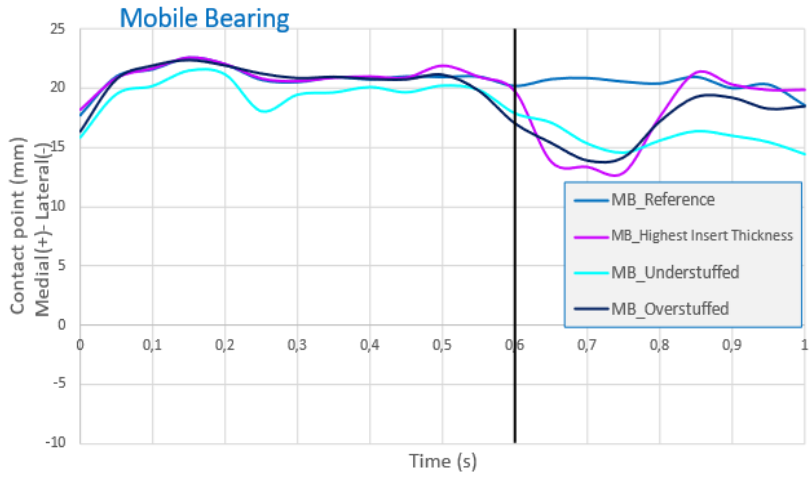

Figure 5.12 Most relevant difference respects the ML Contact Point on UHMWPE Insert surface for MB UKAs

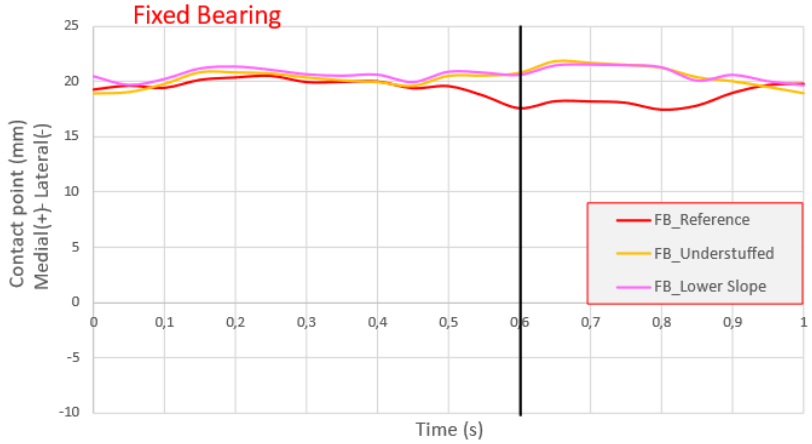

Figure 5.13 Most relevant difference respects the ML Contact Point on UHMWPE Insert surface for MB UKAs

5.6 UHMWPE Insert average von Mises Stress

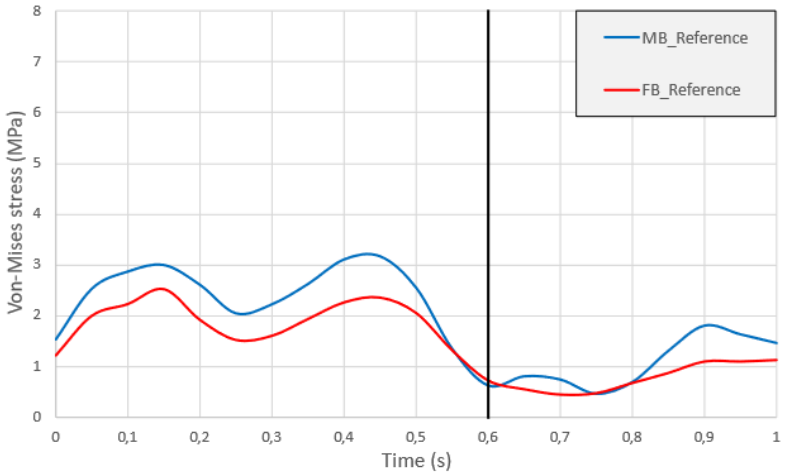

Figure 5.14 Average von Mises stress for UHMWPE Insert in the reference configurations MB and FB

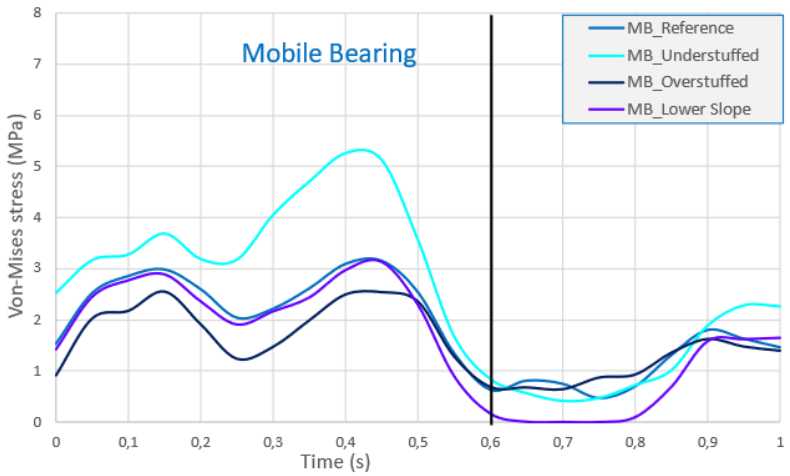

Figure 5.15 Most relevant differences for UHMWPE Insert in average von Mises stress for MB UKAs

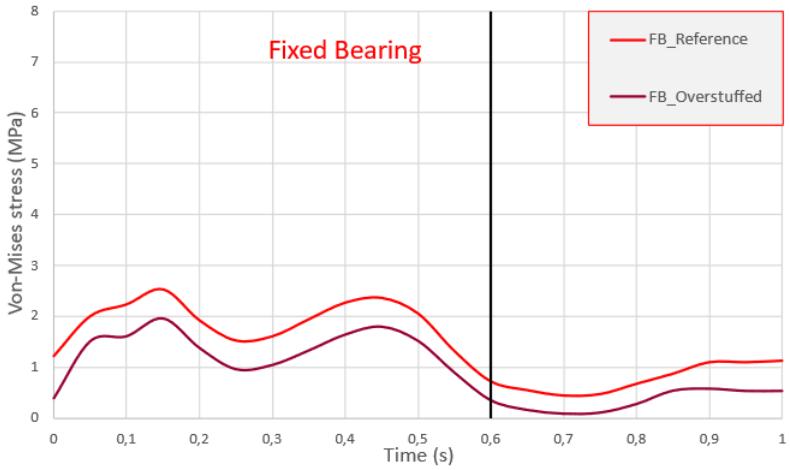

Figure 5.16 Most relevant differences for UHMWPE Insert in average von Mises stress for FB UKAs

5.7 Tibial ROI Stress

5.7.1 Subchondral Lateral ROI average Von Mises Stress

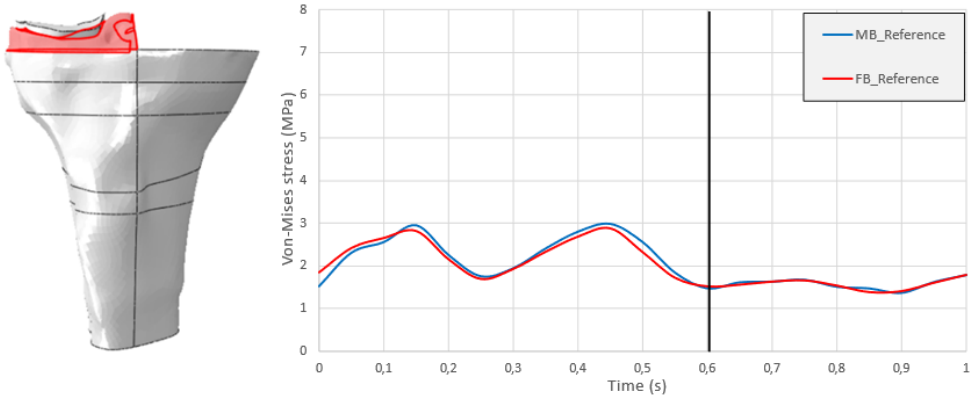

Figure 5.17 Subchondral lateral Roi(left) and average von Mises stress in the lateral subchondral in the reference configurations MB and FB (rigth)

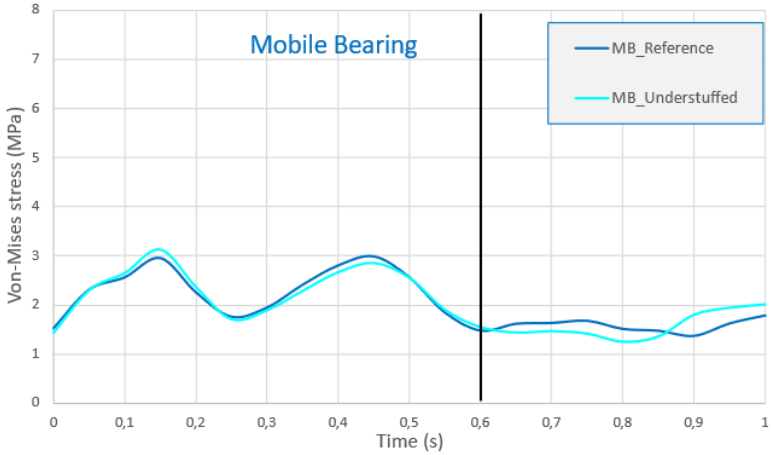

Figure 5.18 Most relevant differences for average von Mises stress in the lateral subchondral for MB UKAs

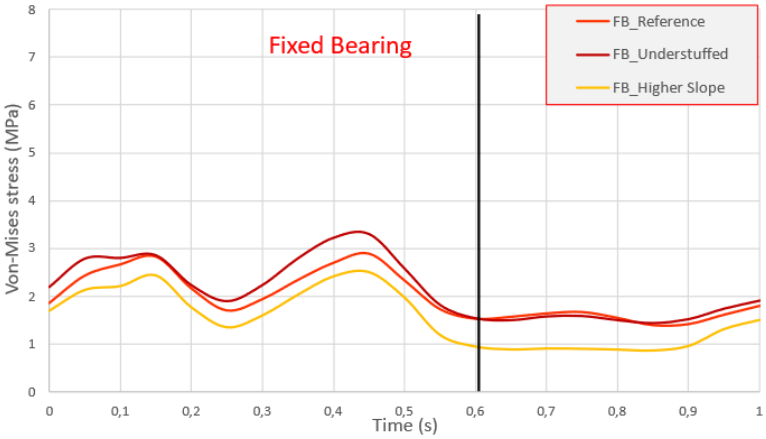

***Figure** 5.19 Most relevant differences for average von Mises stress in the lateral subchondral for FB UKAs*

5.7.2 *Proximal Lateral ROI average Von Mises Stress*

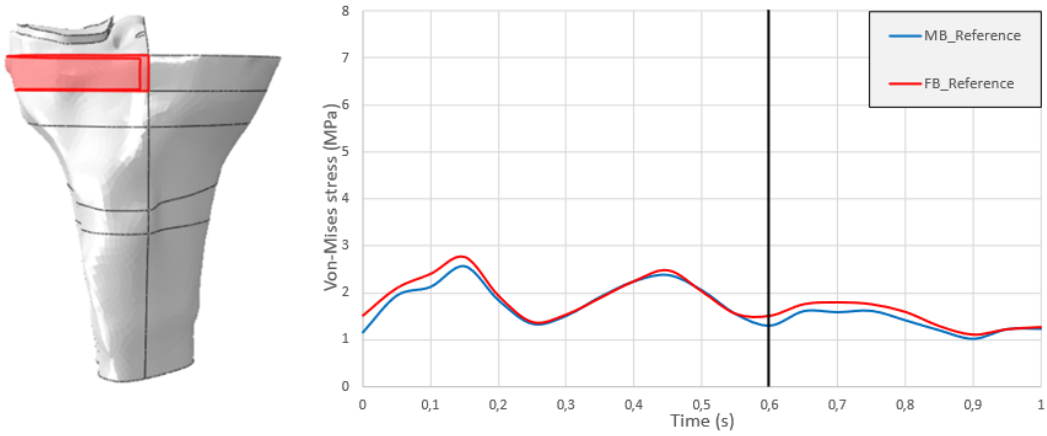

Figure 5.20 Proximal lateral Roi(left) and average von Mises stress in the proximal lateral tibia in the reference configurations MB and FB (right)

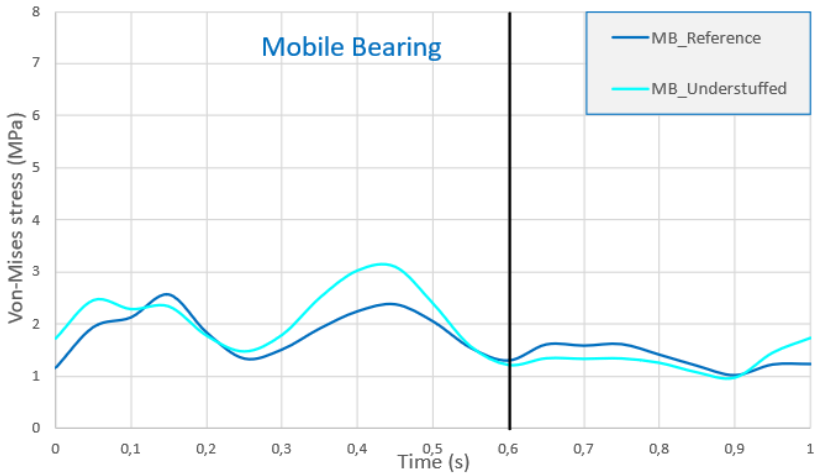

Figure 5.21 Most relevant differences for average von Mises stress in the proximal ROI for MB UKAs

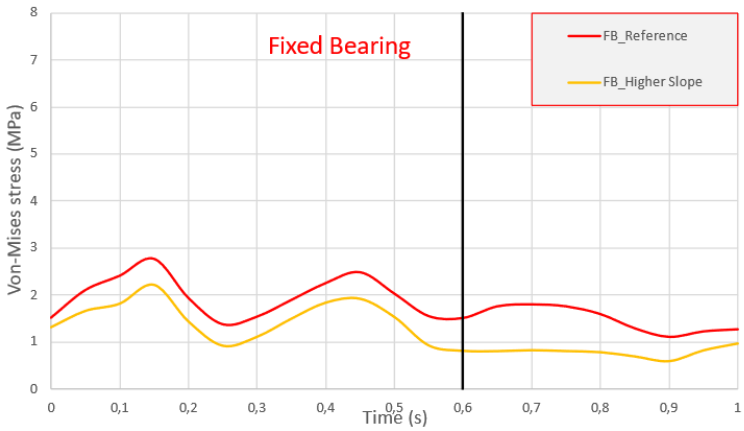

Figure 5.22 Most relevant differences for average von Mises stress in the proximal ROI for FB UKAs

5.7.3 Distal Lateral ROI average Von Mises Stress

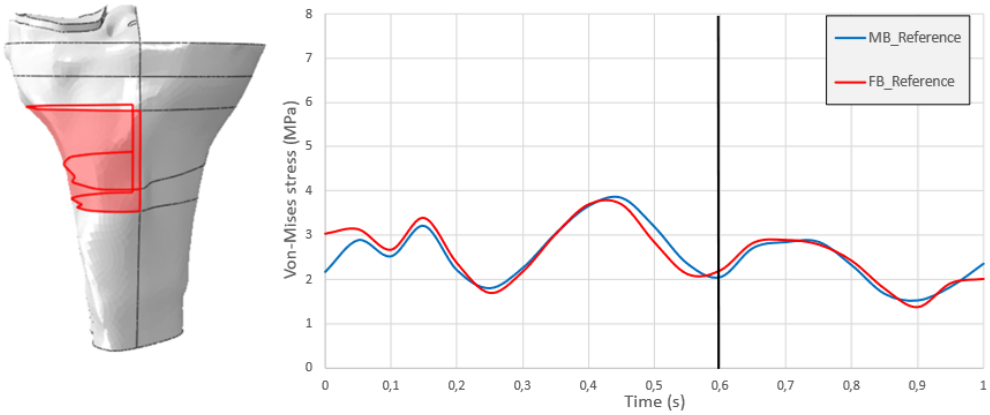

Figure 5.23 Distal lateral Roi(left) and average von Mises stress in the proximal lateral tibia in the reference configurations MB and FB (rigth)

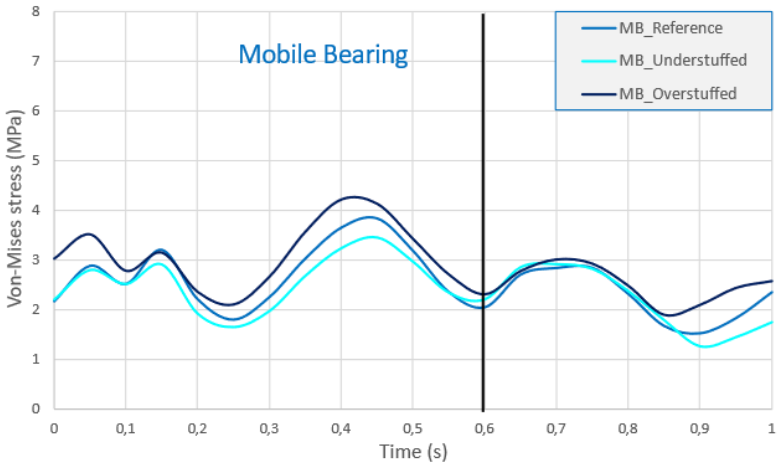

Figure 5.24 Most relevant differences for average von Mises stress in the distal ROI for MB UKAs

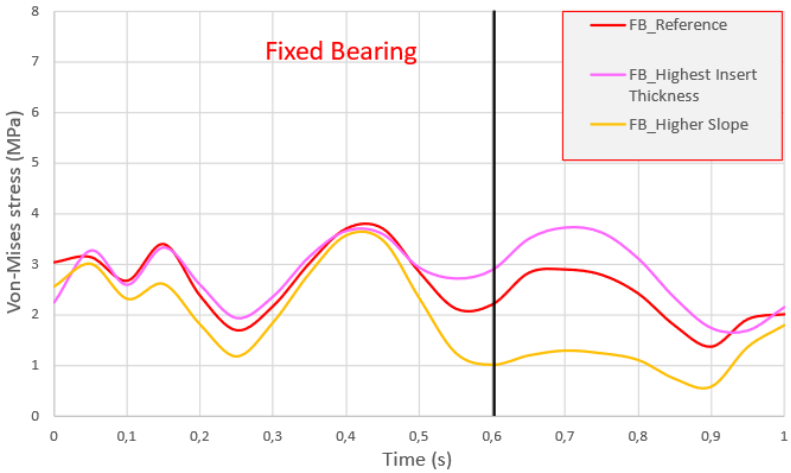

Figure 5.25 Most relevant differences for average von Mises stress in the distal ROI for MB UKAs

5.7.4 Proximal Medial ROI average Von Mises Stress

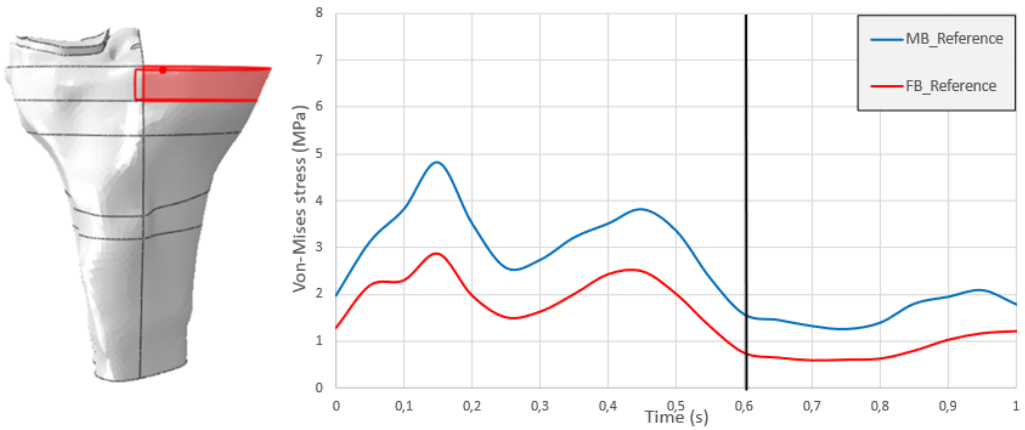

Figure 5.26 Proximal Medial Roi(left) and average von Mises stress in the proximal lateral tibia in the reference configurations MB and FB (rigth)

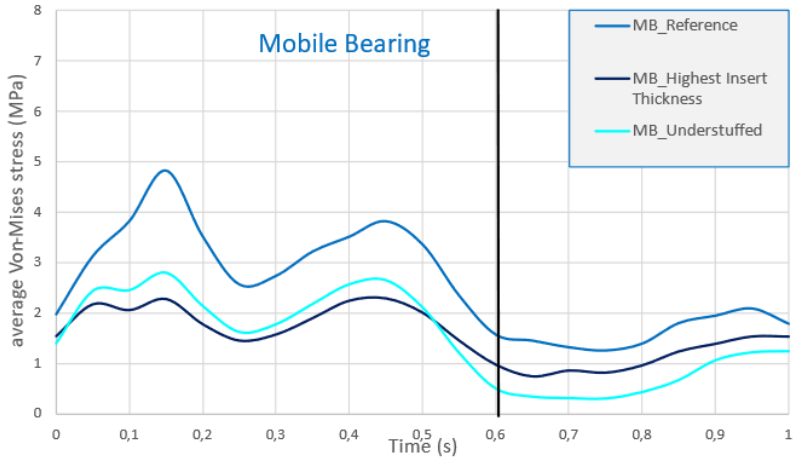

Figure 5.27 Most relevant differences for average von Mises stress in the Proximal Medial Roi for MB UKAs

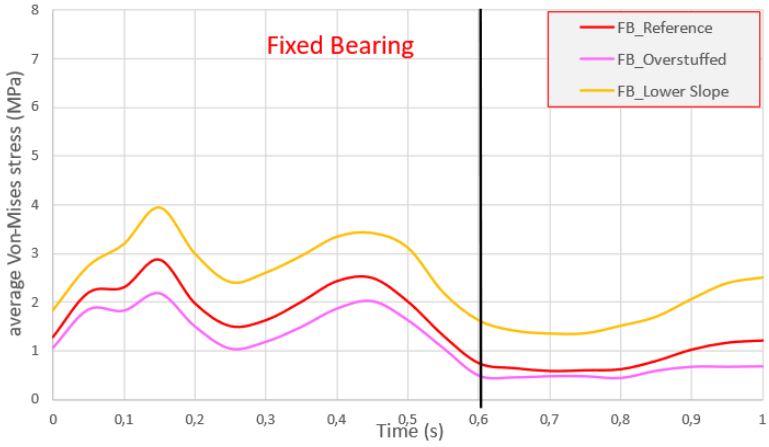

Figure 5.28 Most relevant differences for average von Mises stress in the Proximal Medial Roi for FB UKAs

5.7.5 Distal Medial ROI average Von Mises Stress

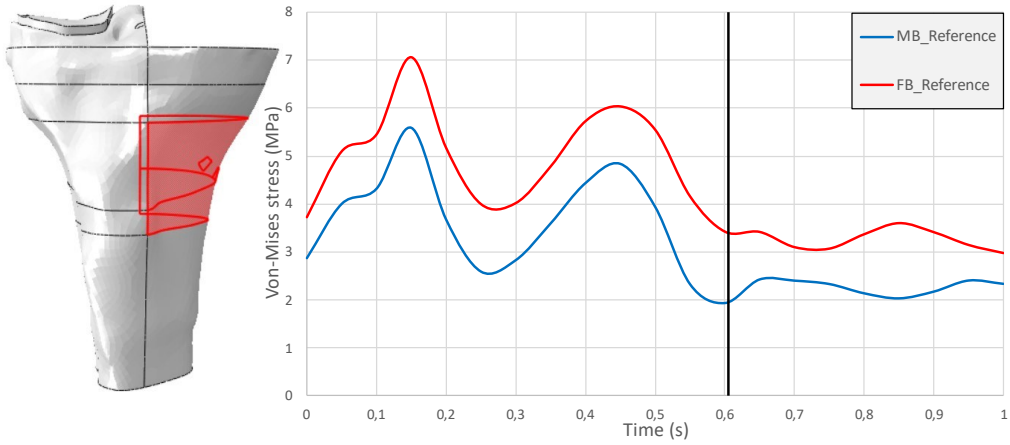

Figure 5.29 Distal Medial Roi(left) and average von Mises stress in the proximal lateral tibia in the reference configurations MB and FB (rigth)

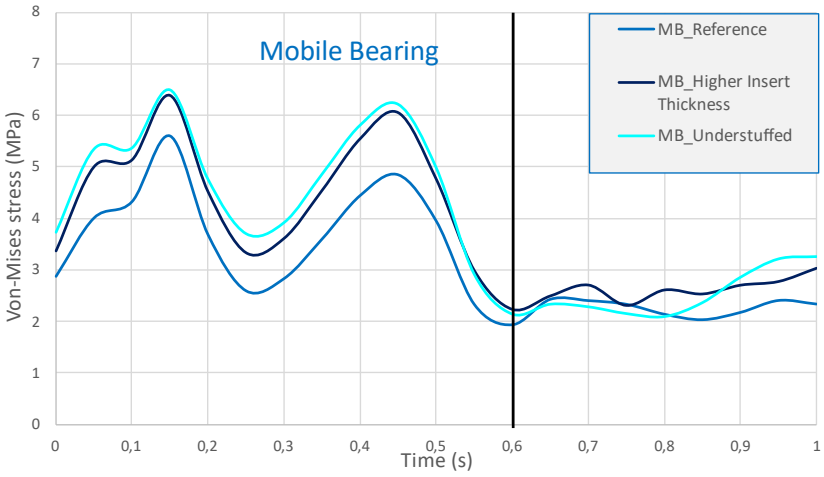

Figure 5.30 Most relevant differences for average von Mises stress in the Distal Medial Roi for MB UKAs

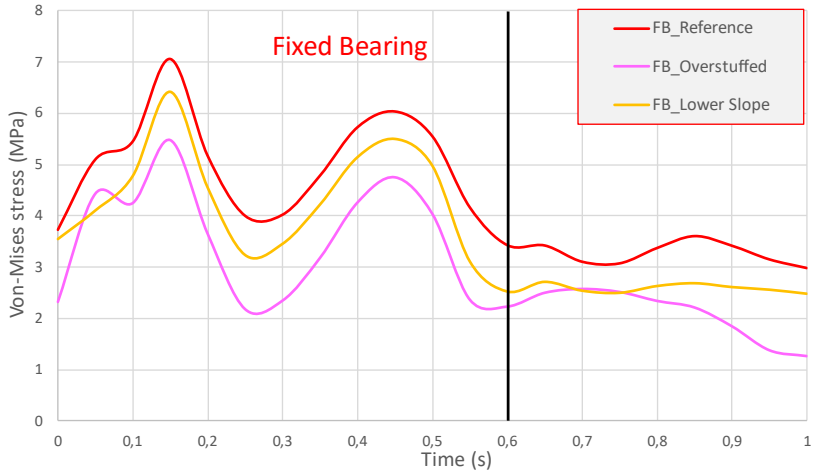

Figure 5.31 Most relevant differences for average von Mises stress in the Distal Medial Roi for FB UKAs

5.8 Cruciate ligament length

5.8.1 ACL length

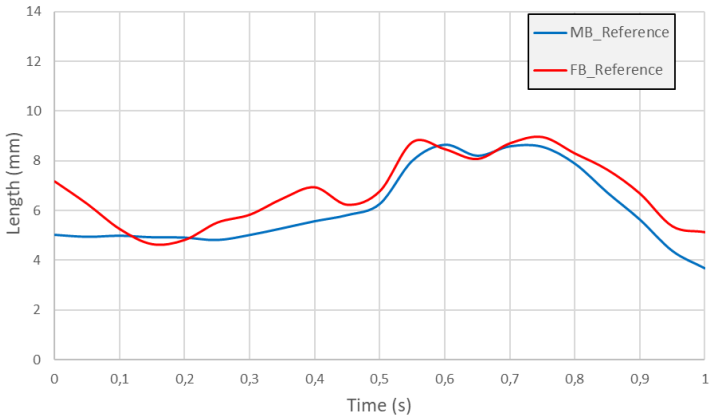

Figure 5.32 ACL Length change for the reference configurations MB and FB

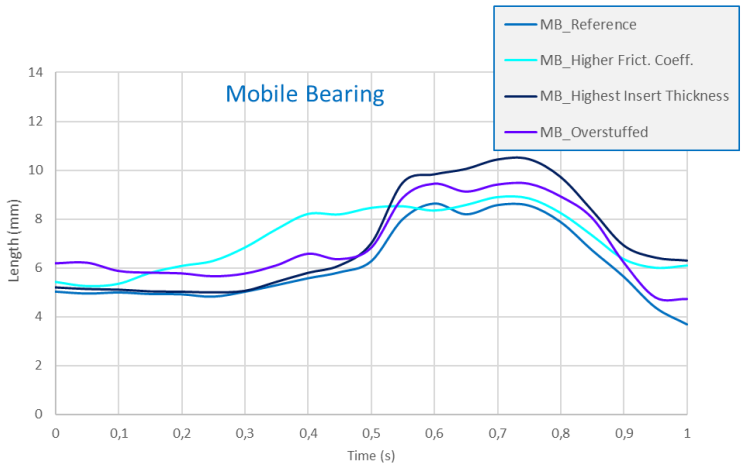

Figure 5.33 Most relevant differences for ACL length change in the MB UKAs

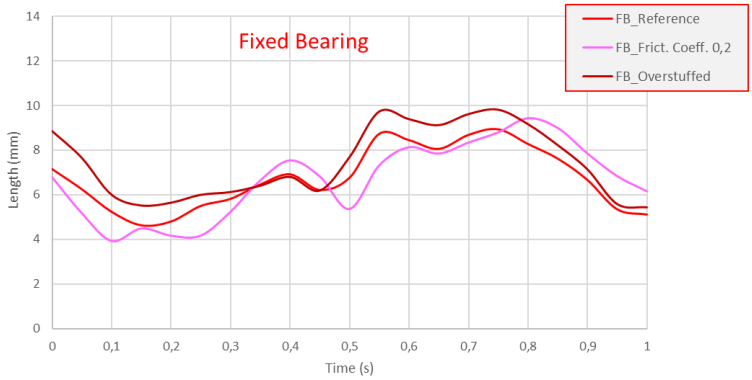

Figure 5.34 Most relevant differences for ACL length change in the MB UKAs

5.8.2 PCL length

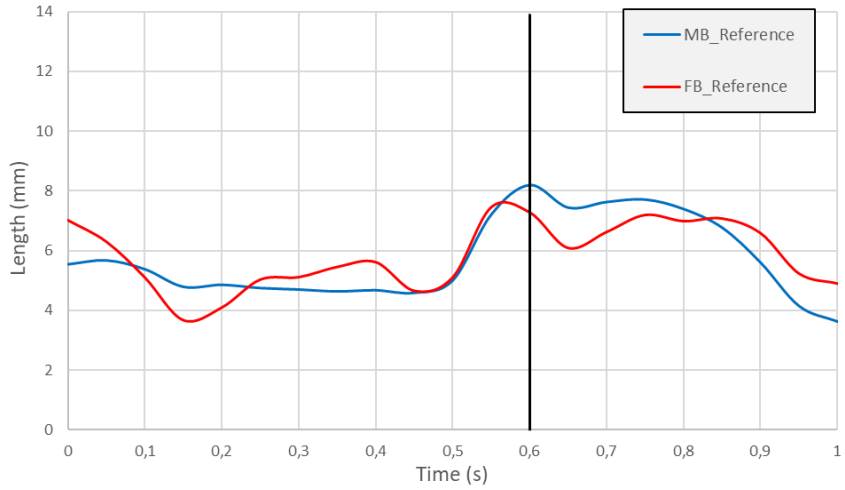

Figure 5.35 PCL Length change for the reference configurations MB and FB

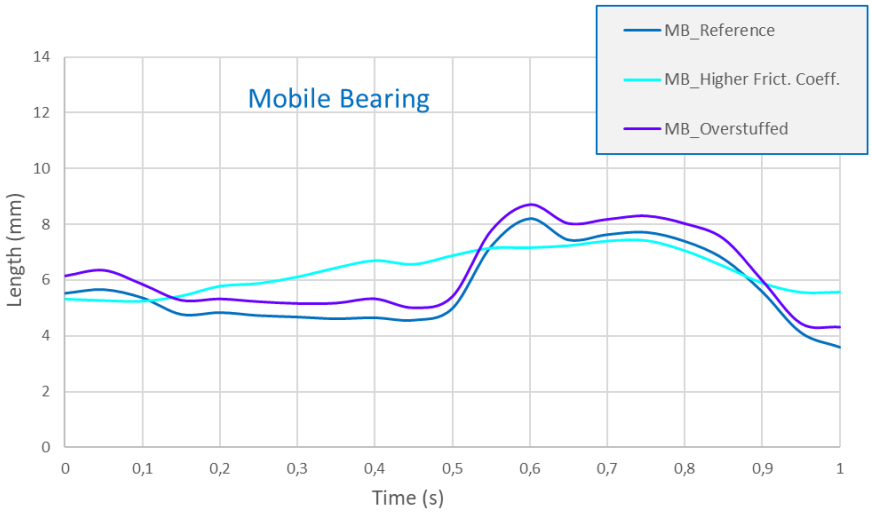

Figure 5.36 Most relevant differences for PCL length change in the MB UKAs

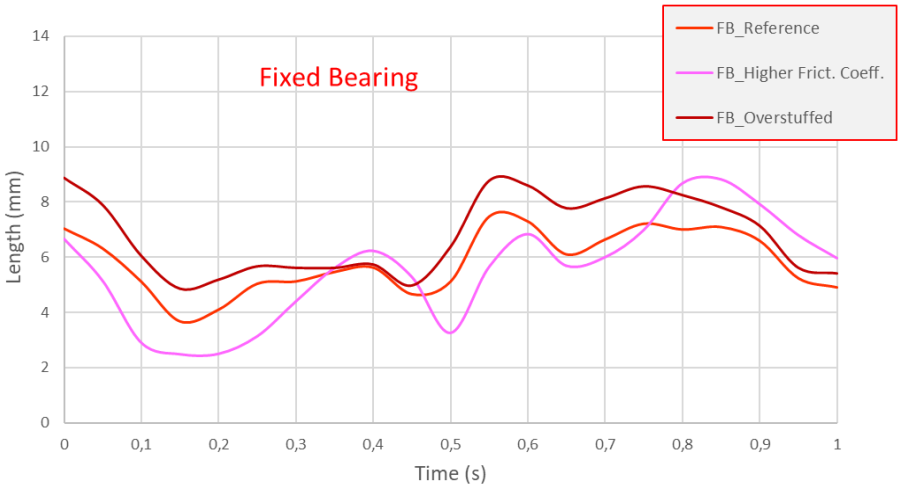

Figure 5.37 Most relevant differences for PCL length change in the FB UKAs

5.9 Collateral ligaments length

5.9.1 aMCL length

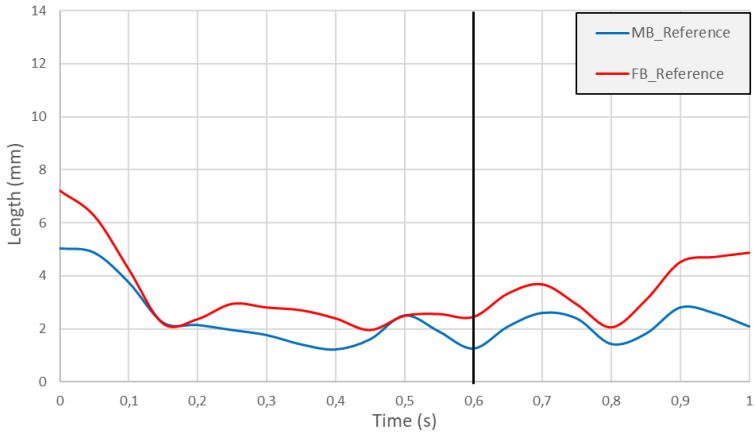

Figure 5.38 aMCL Length change for the reference configurations MB and FB

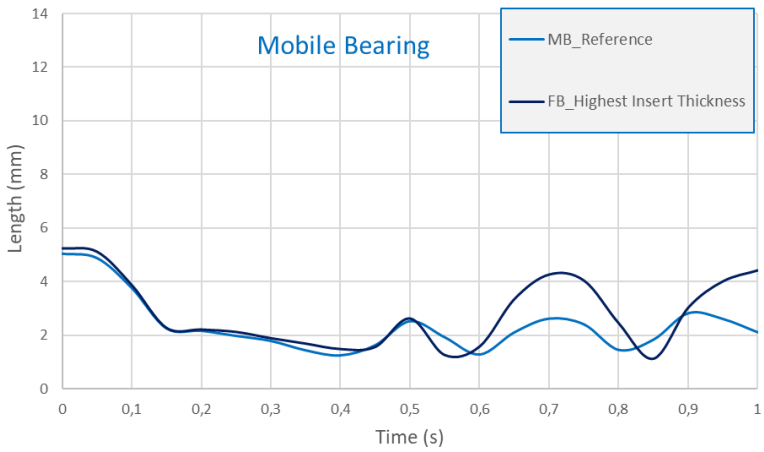

Figure 5.39 Most relevant differences for aMCL length change in the MB UKAs

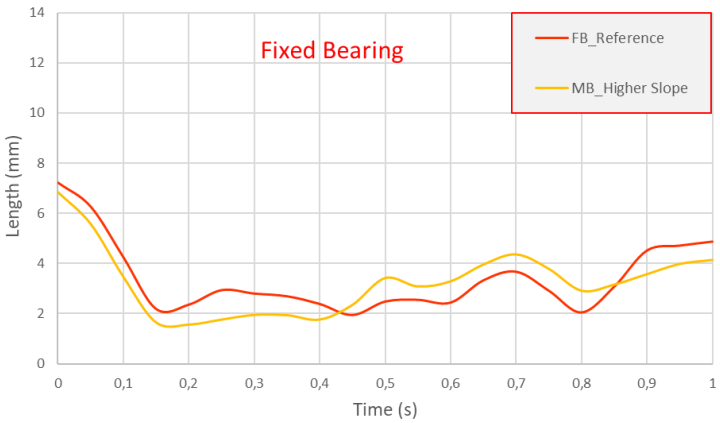

Figure 5.40 Most relevant differences for aMCL length change in the FB UKAs

5.9.2 pMCL length

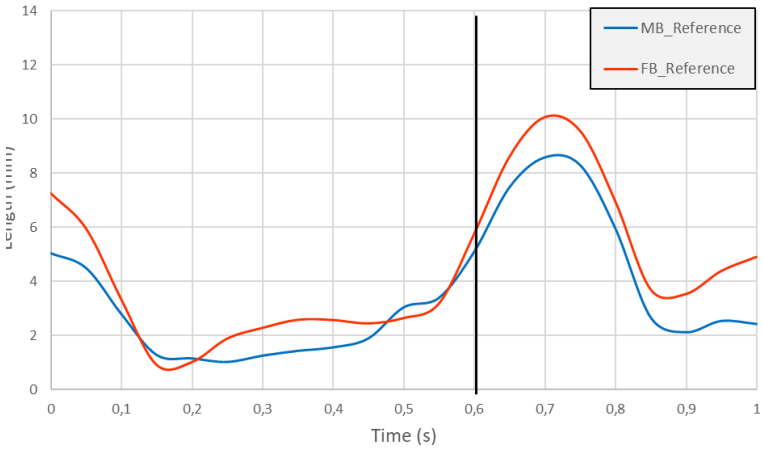

Figure 5.41 pMCL Length change for the reference configurations MB and FB

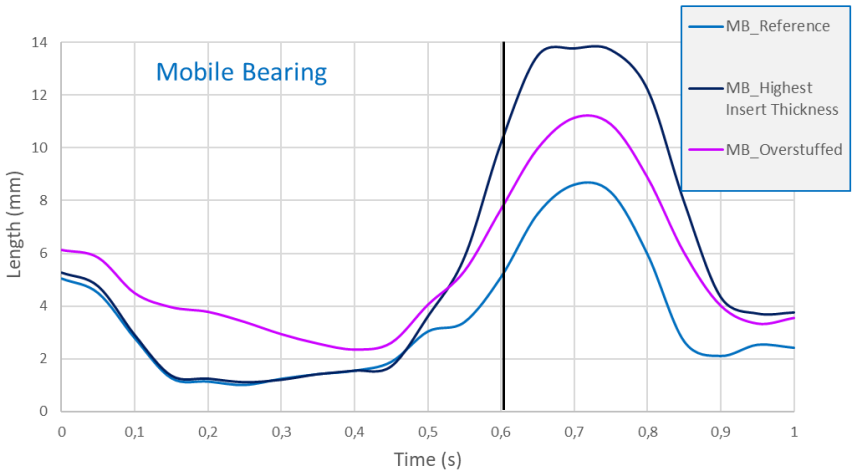

Figure 5.42 Most relevant differences for pMCL length change in the MB UKAs

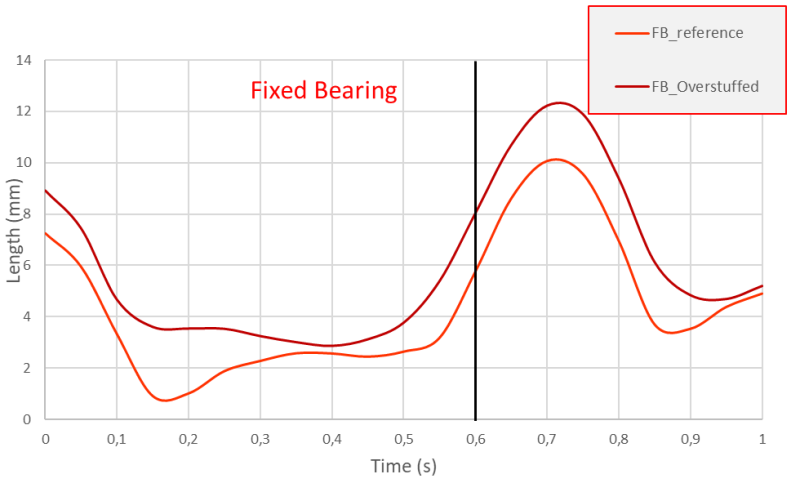

Figure 5.43 Most relevant differences for pMCL length change in the FB UKAs

5.9.3 *LCL length*

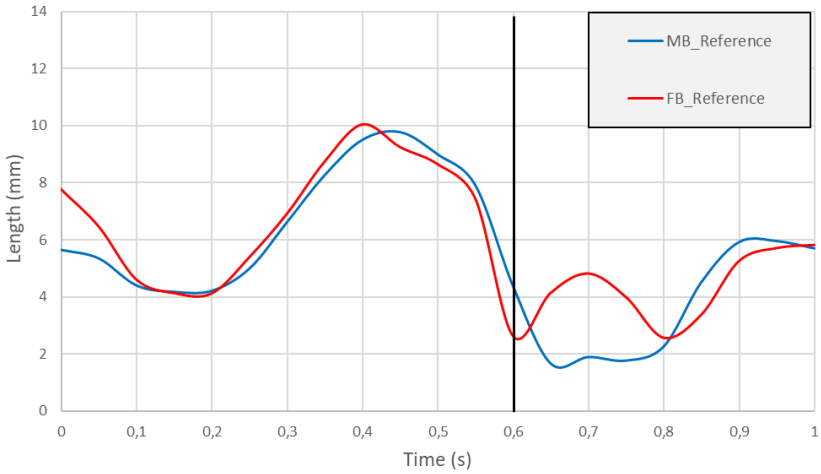

Figure 5.44 LCL Length change for the reference configurations MB and FB

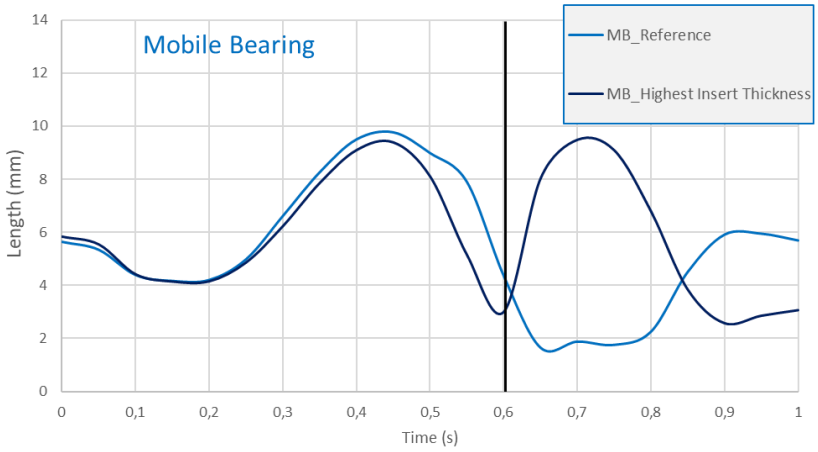

Figure 5.45 Most relevant differences for LCL length change in the MB UKAs

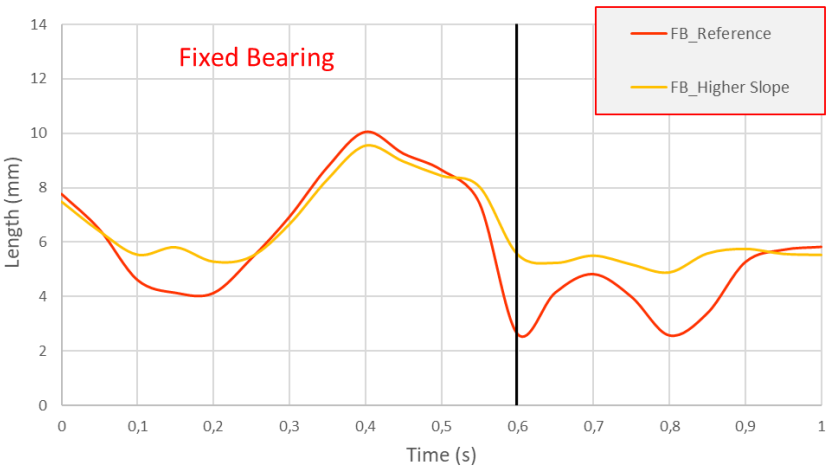

Figure 5.46 Most relevant differences for LCL length change in the FB UKAs

6 Discussions

Unicompartmental knee arthroplasty (UKA), is becoming one of the most successful surgeries in orthopedics used to treat anteromedial and anterolateral osteoarthritis [60]. Due to their relatively major conservative when compared to the Total Knee Arthroplasty (TKA) [56], is becoming increasingly common in arthroplasty surgeries when the patient's condition allows it as seen in Chapter 2.1.

Therefore, a targeted study on its biomechanics performance is necessary to understand in a more detailed way what can be improved to allow an optimal stress/strain distribution.

In the present study was chosen to compare the biomechanics performance after a UKA implant with different configurations by analysing a mobile-bearing and a fixed-bearing UKA during the dynamic daily tasks of gait that is one of the most relevant movements of daily life.

To compare their biomechanical performances, different output was analysed.

Starting from the Femoral translation of the femur rotational center (**Figure 5.1**) was seen that the behaviour of the MB and the FB is pretty much the same. The difference is that the FB presents a more an initial posterior translation higher during the stance and a second one during the swing respect to the MB. This is probably since the femur in the FB it's freer to move. Respect the reference configuration of the MB (**Figure 5.2**), was seen that the configuration with a lower slope presents a lower initial posterior translation but a greater anterior translation during the stance phase, while during the swing presents the same behaviour. The configuration with the higher insert thickness instead is identical during the stance but more unstable during the stance with a greater posterior and then an anterior translation respects the reference configuration. Respect the FB reference configuration (**Figure 5.3**) instead was noticed that the configuration with the higher insert thickness has a slightly higher posterior translation during the stance phase.

The second output analysed was the internal-external rotation of the femoral center of rotation. The MB reference configuration presents a higher external rotation during the stance phase resulting in a more instable rotation respect to the FB; but the internal rotation presents a lower average (**Figure 5.4**). Respect the MB reference configuration (**Figure 5.5**) the greater differences are given by the understuffed and the highest insert thickness configurations that result in a lower range for the internal rotation, so are more stable. For the FB (**Figure 5.6**) the same behaviour can be seen with the Overstuffed configuration that has a slightly lower internal rotation during the stance.

Then the polyethylene surface in contact with the femoral component were considered to evaluate the contact area on the insert superior surface during the movement. How is clearly depicted in **Figure 5.7**, the MB being ultra-congruent has a much larger contact area than the FB which has a very small area and that is almost a single point. Therefore, the more relevant difference in these configurations regards the MB UKA. In detail is possible to notice that a lower slope configuration has a similar contact area during the stance but decreases it by an important amount during the stance and this can compromise the stability of the UKA in this phase. For the understuffed configuration instead, there is a general decrease in all the gait cycle.

Regarding the AP contact point on the polyethylene insert both the UKAs show a good behaviour with the FB that present a higher contact point due to the morphology (**Figure 5.8**). For the MB configurations (**Figure 5.9**) the one with the higher friction coefficient present a greater range in the Anterior and posterior contact point during all the gait cycle resulting in a less balanced configuration. A lower slope instead seems to increase the stability since this curve has a less oscillatory path. For the FB configurations (**Figure 5.10**) just the higher friction coefficient configuration destabilises the balance of the femur even if in the FB result less destabilized respect to the MB.

Also the contact point in the ML directions (**Figure 5.11**) was analysed and the results show a lower range difference respect to the AP contact point. Indeed, the contact point moves more medially respect the FB during the stance phase.

For the MB configurations is possible to notice in **Figure 5.12** that the higher insert along with a higher insert thickness and an understuffed configuration moves the contact point in a rapid way laterally resulting in a more unbalanced movement. The FB instead just for the understuffed and the lower slope configurations present a greater contact point in the lateral part of the bearing insert (**Figure 5.13**).

One of the most important outputs to analyse is the stress on the bone and on the polyethylene insert. Starting from this last one in **Figure 5.14** can be seen that the average von Mises stress on the polyethylene insert of the MB is higher respect the one of the FB. Since the area of contact in the ultra-congruent MB is much higher respect to the one of the FB the results should be the opposite since the applied force is the same. But in the MB UKA is present a double friction, between the femoral component and the insert, and between the insert and the tibial tray. This double friction could be the reason that induces a higher stress level in the MB even if the area of contact is much higher with respect to the FB in which the stress is more concentrated in a limited zone. For the MB (**Figure 5.15**) the understuffed configuration presents an average stress that is almost doubled with respect to the reference configuration, while for the overstuffed presents a decrease of stress. Moreover, when a lower slope configuration is performed, there is no stress during the stance phase indicating that there is no contact between the femoral component and the polyethylene insert, becoming so a potential negative configuration. For the FB instead, the only one noticeable difference is given by the overstuffed configuration (**Figure 5.16**) that such as for the MB decrease the stress on the insert.

Then a completely new output was considered i.e., the average von Mises stress on the subchondral lateral ROI. As reported in **Figure 5.17, f**rom a clinical point of view the fact that the stress curves present the same trend for the MB and the FB means that the stress in the subchondral lateral ROI is the same for both the UKA meaning so that neither of the two UKA damages this region more than the other. The principal differences for the MB are really neglectable (**Figure 5.18**). Indeed, just a very small increase in the stress during the swing phase can be seen for the configurations that

present a smaller slope, while the understuffed one decrease a little bit the stress during the stance phase. Also for the FB (**Figure 5.19**) the understuffed configuration increase the stress, while, the increase in the slope, decrease the stress especially during the stance phase.

Then the literature based tibial ROIs considered were considered [133], [134]. Starting from the proximal lateral ROI (**Figure 5.20**) and the results, a behaviour like the subchondral area with the MB and FB UKA was seen. Indeed, they show an identical stress pattern throughout the gait. For the MB configuration (**Figure 5.21**) the only remarkable difference can be noticed in the understuffed configuration that increases the stress during the stance phase. For FB (**Figure 5.22**) instead when the slope is increased, the stress level is decreased especially during the swing phase.

Going down longitudinally on the tibia we selected the distal lateral ROI (**Figure 5.23**), the third and last ROI in the lateral compartment of the tibia. Also here, as we saw for the previous two lateral regions, the behaviour of the MB and of the FB is the same and the stress continues to have a maximum that is lower than 4 MPa. For the MB (**Figure 5.24**) the understuffed configuration shows a slight decrease in the stress in the stance phase while the overstuffed configuration manifests an increase in the stress in the same stance phase. Regarding the change in parameters of the FB UKA (**Figure 5.25**), there is the highest insert thickness configuration that shows an increase during the swing phase of the gait; the opposite happens for the configuration that presents a higher slope.

On the medial side of the tibia instead, two ROIs are considered to analyse the von Mises stress. The first one is the proximal medial ROI that in **Figure 5.26** report a sudden increase in stress compared to that seen for the proximal lateral area since the

stress level go from a maximum of 3 MPa to 5 MPa and this happens for various reasons. The most important of course is that just above this ROI is located the prosthesis and therefore the stress increases. In the MB (**Figure 5.27**) configurations the average von Mises stress decrease for the configurations that have a higher insert

thickness, are and a tibia cut error of – 2 mm (understuffed configuration). In the **FB** (**Figure 5.28**) instead, an overstuffed configuration tend to decrease the stress, while in

a similar way seen for the MB, when there is a decrease in the slope, the stress gets higher.

The second medial and last considered ROI for the average von Mises stress was the distal medial ROI. What was immediately noticeable from **Figure 5.29,**

Figure 5.30, and **Figure 5.31**, is that moving distally in the tibia, the stress increases even more because of three important reasons:

1. moving from the proximal zone to the distal one, the cortical section in the distal region becomes thinner.
2. in the distal section there is the insertion of collateral that also bring a certain amount of stress.
3. in the medial part is positioned the prosthesis.

In the MB (**Figure 5.30**) the configurations that show a different behaviour are the ones that have higher insert thickness and the understuffed and all these increases the stress quantity. In the FB (**Figure 5.31**) instead the overstuffed and the lower slope configurations decrease the stress level.

Then the change in the length of the ligaments was carried out, both for cruciate and collaterals.

Starting from the ACL, Figure **5.32** which show the reference configurations, during the stance phase both the trends are practically flat since there is not a variation of length that can be clearly visible during the stance phase. This confirms what can be found in the literature [25]. For the MB configurations (**Figure 5.33**), the higher friction coefficient, the highest insert thick, overstuffed decrease the range of variation of the length for the ACL. While in the FB (**Figure 5.34**) configurations a higher friction coefficient presents a greater range variation with respect to the reference one resulting in a bad behaviour for the ACL that changes its length in a rapid and strict time. The overstuffed configuration instead results in a behaviour that is like the balanced one but with a higher change in the ACL length during the stance phase.

Also for the PCL (**Figure 5.35**) during the stance phase, the graphs are practically flat since there is not a variation of length that is more visible during the swing phase. Even if the FB presents more variation in the Stance phase. For the MB configurations,

(**Figure 5.36**) the higher friction coefficient presents a more controlled and linear variation in the length which is a good behaviour for this ligament. Instead, the overstuffed decrease the range of variation of the length for the ACL. The FB higher friction coefficient (**Figure 5.37**) has a greater range variation with respect to the balanced one so this results in a bad behaviour for the PCL that changes its length in a rapid and strict time. The FB overstuffed configuration instead results in a behaviour that is like the balanced one but with a higher change in the ACL length during the stance phase.

Then the collateral ligaments were analysed in their length. Starting from the aMCL for the reference configurations (**Figure 5.38**) its length changes less in the reference MB with respect to the FB UKA. For the MB (**Figure 5.39**) we have both the configurations with highest insert thickness that present a higher length for the aMCL in the stance phase. Instead, for the FB configurations (**Figure 5.40**) instead the higher slope results in a more change in length during all the gait cycle.

As concern the pMCL (**Figure 5.41**) length there is a change in the beginning of the stance, stay flat for the rest of the stance and rapidly increase in the swing phase. In detail, the MB has a higher average in the length change for the swing phase.

For MB configuration can be noticed in **Figure 5.42** that the highest insert thickness, the overstuffed configurations show a higher range of variation during the stance phase, and this is not a positive factor for the pMCL because can brings to an increase in its strain. More stable results instead the FB UKA (**Figure 5.43**) for which just the overstuffed configuration presents a similar variation in range with respect to the reference configuration.

Finally, the last output that was analysed is the LCL length. From a general point of view, the LCL is more mobile than MCL. Indeed, during the stance phase, (**Figure 5.44**) we can notice a greater change in the stance phase that for what was noticed for the aMCL which was almost flat. In this phase, the FB and the MB did not present notables differences. In the swing phase instead, the FB presents a change in the length. This behaviour can be seen also in the highest insert thickness and the lower slope configurations of the MB UKA (**Figure 5.45**). FB higher slope results more improved

especially during the swing phase (**Figure 5.46**).

In summary, the present work has reached its purpose: FEA has been applied in medial UKA for both the two important types that are present nowadays in the orthopedic market: fixed bearing and mobile bearing UKA. The parameter changes were successfully performed, and their results were critically analysed. In conclusion, the present work could be a starting point for further investigations aimed to improve the UKA biomechanical performances.

7 Conclusions

The results obtained from this study pointed out some important factors outlining that from a general point of view, kinematic changes that were found during loaded motion are probably due to:

- Loss of the conforming medial meniscus and the mismatch in geometry and stiffness introduced by UKA.
- Malpositions of the UKA components, especially of the tibial tray.

And from the comparisons between the Fixed Bearing and Mobile Bearing UKA was stressed out that:

- A-P translations in the MB show a more general stability but for the I-E rotations the FB that is more stable.
- Average von Mises stress on UHMWPE insert shows that an overstuffed configurations results in a less quantity of stress for both the presented UKA, even if in a general point of view the FB responds better to the stress.
- Average von Mises stress on the tibia is lower in FB for most of the analysed ROIs. For both types of UKA was found that the understuffed configurations tend to increase the level of stress in some ROIs while the Overstuffed to reduce it.
- But the Overstuffed configuration seems to be a very challenging configurations for both the Cruciate ligaments since their length tend to increase; this overstretching can lead to a probable rupture of them.
- Collaterals in the Overstuffed and Higher Slope configurations tend to increase their length especially in the stance phase and this can be dangerous because this overstretching can lead to serious consequences arriving to a probable rupture of them.

So far, the present work represents a first approach but a very promising study for the analyses and comparisons, during gait, of the two types of UKA presented, the Mobile Bearing and the Fixed Bearing, aimed at highlighting the specific characteristics that each of them presents. Even if some limitations are present i.e, :

- Only 1 patient's anatomy has been considered;
- Potential malalignments of the femur are not included in this analysis. They could be investigated in future studies analysing the effect of mixed femoral/tibial component malalignment.
- Ligament pre-strain was taken from the literature, making the simulations less patient-specific inducing so some degrees of error.

Thus, to resolve the drawbacks of this study, future works should carry out the FEA of this study on a wider range of patients with a model having its own ligaments pre-strain and a natural cortico-cancellous bone separation. Moreover, they should also focus on the study of other important daily tasks such can be the squat to have a more in deep knowledge of the behaviour of these two types of prostheses and improve biomechanical performance in order to extend the life expectancy of a UKA.

8 References

[1] J. D. Hassebrock, M. T. Gulbrandsen, W. L. Asprey, J. L. Makovicka, and A. Chhabra, "Knee ligament anatomy and biomechanics," *Sports Med. Arthrosc.*, vol. 28, no. 3, pp. 80–86, Sep. 2020, doi: 10.1097/JSA.0000000000000279.

[2] S. Pianigiani, D. Croce, M. D'Aiuto, W. Pascale, and B. Innocenti, "Sensitivity analysis of the material properties of different soft-tissues: implications for a subject-specific knee arthroplasty," *Muscles. Ligaments Tendons J.*, vol. 7, no. 4, p. 546, Oct. 2017, doi: 10.11138/MLTJ/2017.7.4.546.

[3] L. Zhang *et al.*, "Knee Joint Biomechanics in Physiological Conditions and How Pathologies Can Affect It: A Systematic Review," *Appl. Bionics Biomech.*, vol. 2020, 2020, doi: 10.1155/2020/7451683.

[4] V. Deshmukh, S. Bhand, M. Dangat, M. Urit, and R. Raskar, "A Review on Biomechanics of Knee Joint," *Int. Res. J. Eng. Technol.*, 2020, Accessed: Dec. 03, 2022. [Online]. Available: www.irjet.net.

[5] "Anatomy of the Knee - Comprehensive Orthopaedics." https://comportho.com/anatomy/anatomy-of-the-knee/ (accessed Dec. 04, 2022).

[6] S. Koo and T. P. Andriacchi, "The Knee Joint Center of Rotation is Predominantly on the Lateral Side during Normal Walking," *J. Biomech.*, vol. 41, no. 6, p. 1269, 2008, doi: 10.1016/J.JBIOMECH.2008.01.013.

[7] S. Pianigiani, L. Labey, W. Pascale, and B. Innocenti, "Changes in Tka Kinematics and Contact Forces Induced By Mal-Configurations: a Numerical Study," *J. Biomech.*, vol. 45, no. 1, p. S321, 2012, doi: 10.1016/s0021-9290(12)70322-6.

[8] B. Innocenti, E. Truyens, L. Labey, P. Wong, J. Victor, and J. Bellemans, "Can medio-lateral baseplate position and load sharing induce asymptomatic local bone resorption of the proximal tibia? A finite element study," *J. Orthop. Surg. Res.*, vol. 4, no. 1, p. 26, 2009, doi: 10.1186/1749-799X-4-26.

[9] R. W. Liu, D. G. Armstrong, A. D. Levine, A. Gilmore, G. H. Thompson, and D. R. Cooperman, "An anatomic study of the distal femoral epiphysis," *J. Pediatr. Orthop.*,

vol. 33, no. 7, pp. 743–749, Oct. 2013, doi: 10.1097/BPO.0B013E31829D55BF.

[10] P. G. J. Maquet, "Biomechanics of the Knee," 1984, doi: 10.1007/978-3-642-61731-7.

[11] S. Affatato, "Biomechanics of the knee," *Surg. Tech. Total Knee Arthroplast. Altern. Proced.*, pp. 17–35, Nov. 2014, doi: 10.1533/9781782420385.1.17.

[12] J. Kirkup, "Mechanics of the human walking apparatus," *undefined*, 1993.

[13] J. F. Abulhasan and M. J. Grey, "Anatomy and Physiology of Knee Stability," *J. Funct. Morphol. Kinesiol. 2017, Vol. 2, Page 34*, vol. 2, no. 4, p. 34, Sep. 2017, doi: 10.3390/JFMK2040034.

[14] D. G. Eckhoff, "Functional anatomy of the knee," *Total Knee Arthroplast. A Guid. to Get Better Perform.*, pp. 18–24, 2005, doi: 10.1007/3-540-27658-0_3/COVER.

[15] M. Biščević, M. Hebibović, and D. Smrke, "Variations of femoral condyle shape," *Coll. Antropol.*, vol. 29, no. 2, pp. 409–414, 2005.

[16] "Femur | Definition, Function, Diagram, & Facts | Britannica." https://www.britannica.com/science/femur (accessed Dec. 04, 2022).

[17] "The Knee Joint - Articulations - Movements - Injuries - TeachMeAnatomy." https://teachmeanatomy.info/lower-limb/joints/knee-joint/ (accessed Dec. 04, 2022).

[18] M. A. Cacko and J. D. Keener, "Total Knee Arthroplasty," *Orthop. Phys. Ther. Secrets Third Ed.*, pp. 560–565, 2017, doi: 10.1016/B978-0-323-28683-1.00072-2.

[19] "Tibia | Encyclopedia | Anatomy.app | Learn anatomy | 3D models, articles, and quizzes." https://anatomy.app/encyclopedia/tibia (accessed Dec. 03, 2022).

[20] "Fibula | Definition, Anatomy, Function, & Facts | Britannica." https://www.britannica.com/science/fibula-bone (accessed Dec. 04, 2022).

[21] C. F. Cox, M. A. Sinkler, and J. B. Hubbard, "Anatomy, Bony Pelvis and Lower Limb, Knee Patella," *StatPearls*, Aug. 2022, Accessed: Dec. 03, 2022. [Online]. Available: https://www.ncbi.nlm.nih.gov/books/NBK519534/.

[22] S. L. Y. Woo, S. D. Abramowitch, R. Kilger, and R. Liang, "Biomechanics of knee ligaments: injury, healing, and repair," *J. Biomech.*, vol. 39, no. 1, pp. 1–20, 2006, doi: 10.1016/J.JBIOMECH.2004.10.025.

[23] A. J. Sophia Fox, A. Bedi, and S. A. Rodeo, "The Basic Science of Articular Cartilage: Structure, Composition, and Function," *Sports Health*, vol. 1, no. 6, p. 461, Nov. 2009, doi: 10.1177/1941738109350438.

[24] E. Peña, B. Calvo, M. A. Martínez, and M. Doblaré, "A three-dimensional finite

element analysis of the combined behavior of ligaments and menisci in the healthy human knee joint," *J. Biomech.*, vol. 39, no. 9, pp. 1686–1701, 2006, doi: 10.1016/J.JBIOMECH.2005.04.030.

[25] E. Vaienti, G. Scita, F. Ceccarelli, and F. Pogliacomi, "Understanding the human knee and its relationship to total knee replacement," *Acta Biomed.*, vol. 88, pp. 6–16, 2017, doi: 10.23750/abm.v88i2-S.6507.

[26] K. MESSNER and J. GAO, "The menisci of the knee joint. Anatomical and functional characteristics, and a rationale for clinical treatment," *J. Anat.*, vol. 193 (Pt 2, no. Pt 2, pp. 161–178, Aug. 1998, doi: 10.1046/J.1469-7580.1998.19320161.X.

[27] E. A. Makris, P. Hadidi, and K. A. Athanasiou, "The knee meniscus: structure-function, pathophysiology, current repair techniques, and prospects for regeneration," *Biomaterials*, vol. 32, no. 30, pp. 7411–7431, Oct. 2011, doi: 10.1016/J.BIOMATERIALS.2011.06.037.

[28] "Treatment with Dr. Farr | OrthoIndy Surgeon." https://www.orthoindy.com/JackFarr/treatment (accessed Dec. 04, 2022).

[29] K. F. Bowman and J. K. Sekiya, "Anatomy and biomechanics of the posterior cruciate ligament, medial and lateral sides of the knee," *Sports Med. Arthrosc.*, vol. 18, no. 4, pp. 222–229, Dec. 2010, doi: 10.1097/JSA.0B013E3181F917E2.

[30] K. Muckenhirn, • J Chahla, R. F. Laprade, K. Muckenhirn, J. Chahla, and R. F. Laprade, "Anatomy and Biomechanics of the Native Knee and Its Relevance for Total Knee Replacement," 2017, doi: 10.1007/978-3-662-54082-4_1.

[31] J. R. Robinson, A. M. J. Bull, R. R. D. W. Thomas, and A. A. Amis, "The role of the medial collateral ligament and posteromedial capsule in controlling knee laxity," *Am. J. Sports Med.*, vol. 34, no. 11, pp. 1815–1823, Nov. 2006, doi: 10.1177/0363546506289433.

[32] G. F. Solitro, R. Fattori, K. Smidt, C. Nguyen, M. M. Morandi, and R. S. Barton, "Role of the transverse ligament of the ulnar collateral ligament of the elbow: a biomechanical study," *JSES Int.*, vol. 5, no. 3, p. 549, May 2021, doi: 10.1016/J.JSEINT.2021.01.009.

[33] L. Stijak *et al.*, "Anatomic description of the anterolateral ligament of the knee," *Knee Surgery, Sport. Traumatol. Arthrosc.*, vol. 24, no. 7, pp. 2083–2088, Jul. 2016, doi: 10.1007/S00167-014-3422-6.

[34] C. Biz *et al.*, "Are Patellofemoral Ligaments and Retinacula Distinct Structures of the

Knee Joint? An Anatomic, Histological and Magnetic Resonance Imaging Study," *Int. J. Environ. Res. Public Health*, vol. 19, no. 3, 2022, doi: 10.3390/ijerph19031110.

[35] H. H. Rachmat, D. Janssen, W. J. Zevenbergen, G. J. Verkerke, R. L. Diercks, and N. Verdonschot, "Generating finite element models of the knee: How accurately can we determine ligament attachment sites from MRI scans?," *Med. Eng. Phys.*, vol. 36, no. 6, pp. 701–707, 2014, doi: 10.1016/J.MEDENGPHY.2014.02.016.

[36] M. Bodor, "Quadriceps protects the anterior cruciate ligament," *J. Orthop. Res.*, vol. 19, no. 4, pp. 629–633, 2001, doi: 10.1016/S0736-0266(01)00050-X.

[37] G. A. Ramos, G. G. Arliani, D. C. Astur, A. de C. Pochini, B. Ejnisman, and M. Cohen, "Rehabilitation of hamstring muscle injuries: a literature review," *Rev. Bras. Ortop. (English Ed.*, vol. 52, no. 1, pp. 11–16, Jan. 2017, doi: 10.1016/J.RBOE.2016.12.002.

[38] "Quad Muscles: Function and Anatomy." https://my.clevelandclinic.org/health/body/22816-quad-muscles (accessed Dec. 04, 2022).

[39] J. McEvoy, K. O'Sullivan, and C. Bron, "Therapeutic Exercises for the Shoulder Region," *Neck Arm Pain Syndr. Evidence-informed Screening, Diagnosis Manag.*, pp. 296–311, May 2011, doi: 10.1016/B978-0-7020-3528-9.00022-4.

[40] M. Z. Bendjaballah, A. Shirazi-Adl, and D. J. Zukor, "Biomechanics of the human knee joint in compression: reconstruction, mesh generation and finite element analysis," *Knee*, vol. 2, no. 2, pp. 69–79, Jun. 1995, doi: 10.1016/0968-0160(95)00018-K.

[41] L. A. Whiteside, "Soft tissue balancing: the knee," *J. Arthroplasty*, vol. 17, no. 4 Suppl 1, pp. 23–27, 2002, doi: 10.1054/ARTH.2002.33264.

[42] X. Gasparutto, F. Moissenet, Y. Lafon, L. Chèze, and R. Dumas, "Kinematics of the Normal Knee during Dynamic Activities: A Synthesis of Data from Intracortical Pins and Biplane Imaging," *Appl. bionics Biomech.*, vol. 2017, 2017, doi: 10.1155/2017/1908618.

[43] P. Komdeur, F. E. Pollo, and R. W. Jackson, "Dynamic Knee Motion in Anterior Cruciate Impairment: A Report and Case Study," *Baylor Univ. Med. Cent. Proc.*, vol. 15, no. 3, pp. 257–259, 2002, doi: 10.1080/08998280.2002.11927850.

[44] N. M. Luís and R. Varatojo, "Radiological assessment of lower limb alignment," *EFORT Open Rev.*, vol. 6, no. 6, pp. 487–494, 2021, doi: 10.1302/2058-5241.6.210015.

[45] M. H. Gonzalez and A. O. Mekhail, "The failed total knee arthroplasty: evaluation and etiology," *J. Am. Acad. Orthop. Surg.*, vol. 12, no. 6, pp. 436–446, 2004, doi:

10.5435/00124635-200411000-00008.

[46] D. Roylance, “Finite Element Analysis,” 2001.

[47] Y. S. Choi, T. W. Kim, S. C. Song, S. Y. Kim, M. J. Chang, and S. B. Kang, “Asymmetric transepicondylar axis between varus and valgus osteoarthritic knees in windswept deformity can be predicted by hip-knee-ankle angle difference,” *Knee Surg. Sports Traumatol. Arthrosc.*, vol. 30, no. 9, pp. 3024–3031, Sep. 2022, doi: 10.1007/S00167-021-06661-1.

[48] A. Manuscript, “Knee joint forces : prediction , measurement , and significance,” vol. 226, no. 2, pp. 95–102, 2013.

[49] “Assessment of Gait | Musculoskeletal Key.” https://musculoskeletalkey.com/assessment-of-gait/ (accessed Dec. 04, 2022).

[50] R. F. Loeser, S. R. Goldring, C. R. Scanzello, and M. B. Goldring, “Osteoarthritis: A Disease of the Joint as an Organ,” *Arthritis Rheum.*, vol. 64, no. 6, p. 1697, Jun. 2012, doi: 10.1002/ART.34453.

[51] R. Sen and J. A. Hurley, “Osteoarthritis,” *StatPearls*, May 2022, Accessed: Dec. 03, 2022. [Online]. Available: https://www.ncbi.nlm.nih.gov/books/NBK482326/.

[52] S. M. Bindawas, V. Vennu, S. Alfhadel, A. D. Al-Otaibi, and A. S. Binnasser, “Knee pain and health-related quality of life among older patients with different knee osteoarthritis severity in Saudi Arabia,” *PLoS One*, vol. 13, no. 5, May 2018, doi: 10.1371/JOURNAL.PONE.0196150.

[53] J. Li, H. Yang, and T. Hu, “Comparison of Warming Needle Moxibustion and Drug Therapy for Treating Knee Osteoarthritis: A Systematic Review and Meta-analysis,” *Comput. Math. Methods Med.*, vol. 2022, 2022, doi: 10.1155/2022/3056109.

[54] “Knee Osteoarthritis – Jason H. Tam, M.D.” http://jhtammd.com/knee-osteoarthritis/ (accessed Dec. 04, 2022).

[55] A. J. Sophia Fox, A. Bedi, and S. A. Rodeo, “The basic science of articular cartilage: structure, composition, and function,” *Sports Health*, vol. 1, no. 6, pp. 461–468, Nov. 2009, doi: 10.1177/1941738109350438.

[56] A. Mittal, P. Meshram, W. H. Kim, and T. K. Kim, “Unicompartmental knee arthroplasty, an enigma, and the ten enigmas of medial UKA,” *J. Orthop. Traumatol.*, vol. 21, no. 1, pp. 1–23, Dec. 2020, doi: 10.1186/S10195-020-00551-X/FIGURES/5.

[57] D. C. Now, “The Seventh Annual Report of the AJRR on Hip and Knee Arthroplasty

PEEK INSIDE FOR A PREVIEW OF THE 2020 AJRR ANNUAL REPORT," 2020.

[58] B. D. Springer, B. R. Levine, and G. J. Golladay, "Highlights of the 2020 American Joint Replacement Registry Annual Report," *Arthroplast. Today*, vol. 9, p. 141, Jun. 2021, doi: 10.1016/J.ARTD.2021.06.004.

[59] "Medical devices; reclassification of the shoulder joint metal/polymer/metal nonconstrained or semi-constrained porous-coated uncemented prosthesis. Food and Drug Administration, HHS. Final rule.," *Fed. Regist.*, vol. 66, no. 40, pp. 12734–12737, Feb. 2001.

[60] V. Ucan, A. Pulatkan, and I. Tuncay, "Unicompartmental knee arthroplasty combined with high tibial osteotomy in anteromedial osteoarthritis: A case report," *Int. J. Surg. Case Rep.*, vol. 81, Apr. 2021, doi: 10.1016/J.IJSCR.2021.105746.

[61] M. Guénot *et al.*, "Surgical technique," *Neurophysiol. Clin.*, vol. 48, no. 1, pp. 39–46, 2018, doi: 10.1016/j.neucli.2017.11.008.

[62] D. W. Murray, J. W. Goodfellow, and J. J. O'Connor, "The Oxford medial unicompartmental arthroplasty: a ten-year survival study," *J. Bone Joint Surg. Br.*, vol. 80, no. 6, pp. 983–989, 1998, doi: 10.1302/0301-620X.80B6.8177.

[63] "Unicompartmental Knee Arthroplasty | Dr. K. Patel's Hip & Knee Pain Clinic." https://www.jointreplacementcare.com/Unicompartmental-Knee-Arthroplasty.html (accessed Dec. 04, 2022).

[64] B. Innocenti, Ö. F. Bilgen, L. Labey, G. H. Van Lenthe, J. Vander Sloten, and F. Catani, "Load sharing and ligament strains in balanced, overstuffed and understuffed UKA. A validated finite element analysis," *J. Arthroplasty*, vol. 29, no. 7, pp. 1491–1498, 2014, doi: 10.1016/j.arth.2014.01.020.

[65] J. F. Suggs, G. Li, S. E. Park, P. G. Sultan, H. E. Rubash, and A. A. Freiburg, "Knee biomechanics after UKA and its relation to the ACL—a robotic investigation," *J. Orthop. Res.*, vol. 24, no. 4, pp. 588–594, Apr. 2006, doi: 10.1002/JOR.20082.

[66] R. A. Berger *et al.*, "Unicompartmental knee arthroplasty. Clinical experience at 6- to 10-year followup.," *Clin. Orthop. Relat. Res.*, no. 367, pp. 50–60, Oct. 1999.

[67] P. Cartier, J. L. Sanouiller, and R. P. Grelsamer, "Unicompartmental knee arthroplasty surgery: 10-Year minimum follow-up period," *J. Arthroplasty*, vol. 11, no. 7, pp. 782–788, Oct. 1996, doi: 10.1016/S0883-5403(96)80177-X.

[68] M. W. Squire, J. J. Callaghan, D. D. Goetz, P. M. Sullivan, and R. C. Johnston, "Unicompartmental knee replacement. A minimum 15 year followup study.," *Clin.*

Orthop. Relat. Res., no. 367, pp. 61–72, Oct. 1999.

[69] G. D. Riebel, F. W. Werner, D. C. Ayers, J. Bromka, and D. G. Murray, "Early failure of the femoral component in unicompartmental knee arthroplasty," *J. Arthroplasty*, vol. 10, no. 5, pp. 615–621, Oct. 1995, doi: 10.1016/S0883-5403(05)80205-0.

[70] T. J. Aleto, M. E. Berend, M. A. Ritter, P. M. Faris, and R. M. Meneghini, "Early Failure of Unicompartmental Knee Arthroplasty Leading to Revision," *J. Arthroplasty*, vol. 23, no. 2, pp. 159–163, Feb. 2008, doi: 10.1016/J.ARTH.2007.03.020.

[71] S. Parratte, V. Pauly, J. M. Aubaniac, and J. N. A. Argenson, "No long-term difference between fixed and mobile medial unicompartmental arthroplasty," *Clin. Orthop. Relat. Res.*, vol. 470, no. 1, pp. 61–68, Jan. 2012, doi: 10.1007/S11999-011-1961-4.

[72] A. J. Price *et al.*, "Ten-year in vivo wear measurement of a fully congruent mobile bearing unicompartmental knee arthroplasty," *J. Bone Joint Surg. Br.*, vol. 87, no. 11, pp. 1493–1497, Nov. 2005, doi: 10.1302/0301-620X.87B11.16325.

[73] T. J. Heyse *et al.*, "Balancing UKA: overstuffing leads to high medial collateral ligament strains," *Knee Surg. Sports Traumatol. Arthrosc.*, vol. 24, no. 10, pp. 3218–3228, Oct. 2016, doi: 10.1007/S00167-015-3848-5.

[74] R. A. Berger *et al.*, "Results of unicompartmental knee arthroplasty at a minimum of ten years of follow-up," *J. Bone Jt. Surg.*, vol. 87, no. 5, pp. 999–1006, 2005, doi: 10.2106/JBJS.C.00568.

[75] S. H. L. Lygre, B. Espehaug, L. I. Havelin, O. Furnes, and S. E. Vollset, "Pain and function in patients after primary unicompartmental and total knee arthroplasty," *J. Bone Joint Surg. Am.*, vol. 92, no. 18, pp. 2890–2897, Dec. 2010, doi: 10.2106/JBJS.I.00917.

[76] P. J. S. Jeer, G. C. R. Keene, and P. Gill, "Unicompartmental knee arthroplasty: an intermediate report of survivorship after the introduction of a new system with analysis of failures," *Knee*, vol. 11, no. 5, pp. 369–374, Oct. 2004, doi: 10.1016/J.KNEE.2004.06.001.

[77] S. C. Kozinn and R. Scott, "Unicondylar knee arthroplasty.," *JBJS*, vol. 71, no. 1, 1989, [Online]. Available: https://journals.lww.com/jbjsjournal/Fulltext/1989/71010/Unicondylar_knee_arthroplasty_.23.aspx.

[78] S. Preston, M. Petrera, C. Kim, M. G. Zywiel, and R. Gandhi, "Towards an understanding of the painful total knee: what is the role of patient biology?," *Curr. Rev. Musculoskelet. Med.*, vol. 9, no. 4, pp. 388–395, Dec. 2016, doi: 10.1007/S12178-016-

9363-6.

[79] “Vision Research Reports - Market Research Reports & Consulting Firm.” https://www.visionresearchreports.com/ (accessed Dec. 03, 2022).

[80] “Knee Replacement Market Size, Growth Report, Trends, 2022-2030.” https://www.precedenceresearch.com/knee-replacement-market (accessed Dec. 03, 2022).

[81] “Knee Implants Market Analysis By Procedure Type (Total, Partial, Revision Knee Replacement), By Component Type (Fixed-Bearing, Mobile-Bearing Implants), And Segment Forecasts To 2024.” https://www.prnewswire.com/news-releases/knee-implants-market-analysis-by-procedure-type-total-partial-revision-knee-replacement-by-component-type-fixed-bearing-mobile-bearing-implants-and-segment-forecasts-to-2024-300373326.html (accessed Dec. 03, 2022).

[82] “Orthopedic Design & Technology | Orthopedic Design Technology.” https://www.odtmag.com/ (accessed Dec. 03, 2022).

[83] E. Burn *et al.*, “Choosing Between Unicompartmental and Total Knee Replacement: What Can Economic Evaluations Tell Us? A Systematic Review,” *PharmacoEconomics - Open*, vol. 1, no. 4, pp. 241–253, 2017, doi: 10.1007/s41669-017-0017-4.

[84] A. Fiocchi, V. Condello, V. Madonna, M. Bonomo, and C. Zorzi, “Medial vs lateral unicompartmental knee arthroplasty: Clinical results,” *Acta Biomed.*, vol. 88, pp. 38–44, 2017, doi: 10.23750/abm.v88i2-S.6510.

[85] A. J. Johnson, S. M. Howell, C. R. Costa, and M. A. Mont, “The ACL in the arthritic knee: How often is it present and can preoperative tests predict its presence? Knee,” *Clin. Orthop. Relat. Res.*, vol. 471, no. 1, pp. 181–188, 2013, doi: 10.1007/s11999-012-2505-2.

[86] Zimmer Biomet, “O xford Partial Knee ®,” [Online]. Available: https://www.zimmerbiomet.com/content/dam/zb-corporate/en/education-resources/surgical-techniques/specialties/knee/oxford-partial-knee/oxford-partial-knee-microplasty-instrumentation-surgical-technique1.pdf.

[87] H. A. Zuiderbaan *et al.*, “Modern Indications, Results, and Global Trends in the Use of Unicompartmental Knee Arthroplasty and High Tibial Osteotomy in the Treatment of Isolated Medial Compartment Osteoarthritis,” *Am. J. Orthop. (Belle Mead. NJ).*, vol. 45,

no. 6, pp. E355–E361, 2016.

[88] P. A. / Italy *et al.*, "Unicompartmental Knee Consensus on Patient Selection."

[89] F. Migliorini *et al.*, "Mobile Bearing versus Fixed Bearing for Unicompartmental Arthroplasty in Monocompartmental Osteoarthritis of the Knee: A Meta-Analysis," *J. Clin. Med.*, vol. 11, no. 10, 2022, doi: 10.3390/jcm11102837.

[90] A. Kannan, P. L. Lewis, C. Dyer, W. A. Jiranek, and S. McMahon, "Do Fixed or Mobile Bearing Implants Have Better Survivorship in Medial Unicompartmental Knee Arthroplasty? A Study from the Australian Orthopaedic Association National Joint Replacement Registry," *Clin. Orthop. Relat. Res.*, vol. 479, no. 7, pp. 1548–1558, 2021, doi: 10.1097/CORR.0000000000001698.

[91] "Cemented vs. Cementless Alternatives in Joint Replacement | Arthritis-health." https://www.arthritis-health.com/surgery/shoulder-surgery/cemented-vs-cementless-alternatives-joint-replacement (accessed Dec. 03, 2022).

[92] T. Ashraf, J. H. Newman, V. V. Desai, D. Beard, and J. E. Nevelos, "Polyethylene wear in a non-congruous unicompartmental knee replacement: A retrieval analysis," *Knee*, vol. 11, no. 3, pp. 177–181, Jun. 2004, doi: 10.1016/j.knee.2004.03.004.

[93] B. J. L. Kendrick *et al.*, "Polyethylene wear in Oxford unicompartmental knee replacement: a retrieval study of 47 bearings," *J. Bone Joint Surg. Br.*, vol. 92, no. 3, pp. 367–373, Mar. 2010, doi: 10.1302/0301-620X.92B3.22491.

[94] S. Lewold, S. Goodman, K. Knutson, O. Robertson, and L. Lidgren, "Oxford meniscal bearing knee versus the Marmor knee in unicompartmental arthroplasty for arthrosis. A Swedish multicenter survival study," *J. Arthroplasty*, vol. 10, no. 6, pp. 722–731, 1995, doi: 10.1016/S0883-5403(05)80066-X.

[95] M. G. Li, F. Yao, B. Joss, J. Ioppolo, B. Nivbrant, and D. Wood, "Mobile vs. fixed bearing unicondylar knee arthroplasty: A randomized study on short term clinical outcomes and knee kinematics," *Knee*, vol. 13, no. 5, pp. 365–370, Oct. 2006, doi: 10.1016/J.KNEE.2006.05.003.

[96] Z. W. Cao, C. L. Niu, C. Z. Gong, Y. Sun, J. H. Xie, and Y. L. Song, "Comparison of Fixed-Bearing and Mobile-Bearing Unicompartmental Knee Arthroplasty: A Systematic Review and Meta-Analysis," *J. Arthroplasty*, vol. 34, no. 12, pp. 3114-3123.e3, Dec. 2019, doi: 10.1016/J.ARTH.2019.07.005.

[97] "Lima Corporate Acquires Unicompartmental And Total Knee For European Markets." https://www.meddeviceonline.com/doc/lima-corporate-acquires-

unicompartmental-european-markets-0001 (accessed Dec. 03, 2022).

[98] "Zimmer Launches First High Flexion Unicompartmental Knee – Zimmer Biomet." https://investor.zimmerbiomet.com/news-and-events/news/archive/29-09-2004-192529559 (accessed Dec. 03, 2022).

[99] M. C. Sobieraj and C. M. Rimnac, "Ultra high molecular weight polyethylene: Mechanics, morphology, and clinical behavior," *J. Mech. Behav. Biomed. Mater.*, vol. 2, no. 5, pp. 433–443, 2009, doi: 10.1016/j.jmbbm.2008.12.006.

[100] A. J. Price, J. J. O'Connor, D. W. Murray, C. A. F. Dodd, and J. W. Goodfellow, "A history of Oxford unicompartmental knee arthroplasty.," *Orthopedics*, vol. 30, no. 5 Suppl, pp. 7–10, May 2007.

[101] S. J. Janssen, I. van Oost, S. J. M. Breugem, and R. C. I. van Geenen, "A structured evaluation of the symptomatic medial Oxford unicompartmental knee arthroplasty (UKA)," *EFORT Open Rev.*, vol. 6, no. 10, pp. 850–860, 2021, doi: 10.1302/2058-5241.6.200105.

[102] L. Marmor, "The modular knee," *Clin. Orthop. Relat. Res.*, vol. no.94, no. 94, pp. 242–248, 1973, doi: 10.1097/00003086-197307000-00029.

[103] R. S. Laskin, "Unicompartmental tibiofemoral resurfacing arthroplasty.," *J. Bone Joint Surg. Am.*, vol. 60, no. 2, pp. 182–185, Mar. 1978.

[104] J. Insall and P. Walker, "Unicondylar knee replacement.," *Clin. Orthop. Relat. Res.*, no. 120, pp. 83–85, Oct. 1976.

[105] L. Marmor, "Unicompartmental knee arthroplasty. Ten- to 13-year follow-up study.," *Clin. Orthop. Relat. Res.*, no. 226, pp. 14–20, Jan. 1988.

[106] A. Lindstrand, A. Stenström, and S. Lewold, "Multicenter study of unicompartmental knee revision. PCA, Marmor, and St Georg compared in 3,777 cases of arthrosis.," *Acta Orthop. Scand.*, vol. 63, no. 3, pp. 256–259, Jun. 1992, doi: 10.3109/17453679209154777.

[107] L. J. Kleeblad, H. A. Zuiderbaan, G. J. Hooper, and A. D. Pearle, "Unicompartmental knee arthroplasty: state of the art," *J. ISAKOS*, vol. 2, no. 2, pp. 97–107, 2017, doi: 10.1136/jisakos-2016-000102.

[108] B. C. Fuller, J. H. Lonner, K. R. Berend, R. A. Berger, and T. L. Gerlinger, "Partial Knee Arthroplasty: The State of the Art.," *Instr. Course Lect.*, vol. 70, pp. 235–246, 2021.

[109] F. Mancuso, C. A. Dodd, D. W. Murray, and H. Pandit, "Medial unicompartmental knee arthroplasty in the ACL-deficient knee," *J. Orthop. Traumatol.*, vol. 17, no. 3, pp.

267–275, Sep. 2016, doi: 10.1007/S10195-016-0402-2.

[110] M. J. Kraeutler, R. M. Wolsky, A. F. Vidal, and J. T. Bravman, "Anatomy and Biomechanics of the Native and Reconstructed Anterior Cruciate Ligament: Surgical Implications," *J. Bone Joint Surg. Am.*, vol. 99, no. 5, pp. 438–445, 2017, doi: 10.2106/JBJS.16.00754.

[111] J. M. Bert, "10-year survivorship of metal-backed, unicompartmental arthroplasty.," *J. Arthroplasty*, vol. 13, no. 8, pp. 901–905, Dec. 1998, doi: 10.1016/s0883-5403(98)90197-8.

[112] A. D. Liddle *et al.*, "Cementless fixation in Oxford unicompartmental knee replacement: a multicentre study of 1000 knees," *Bone Joint J.*, vol. 95-B, no. 2, pp. 181–187, Feb. 2013, doi: 10.1302/0301-620X.95B2.30411.

[113] S. Campi, H. G. Pandit, C. A. F. Dodd, and D. W. Murray, "Cementless fixation in medial unicompartmental knee arthroplasty: a systematic review.," *Knee Surg. Sports Traumatol. Arthrosc.*, vol. 25, no. 3, pp. 736–745, Mar. 2017, doi: 10.1007/s00167-016-4244-5.

[114] T. M. Wright, "Polyethylene in knee arthroplasty: what is the future?," *Clin. Orthop. Relat. Res.*, vol. 440, pp. 141–148, 2005, doi: 10.1097/01.BLO.0000187811.48717.9D.

[115] J. W. Goodfellow and J. O'Connor, "Clinical results of the Oxford knee. Surface arthroplasty of the tibiofemoral joint with a meniscal bearing prosthesis.," *Clin. Orthop. Relat. Res.*, no. 205, pp. 21–42, Apr. 1986.

[116] J. P. Whittaker, D. D. R. Naudie, J. P. McAuley, R. W. McCalden, S. J. MacDonald, and R. B. Bourne, "Does bearing design influence midterm survivorship of unicompartmental arthroplasty?," *Clin. Orthop. Relat. Res.*, vol. 468, no. 1, pp. 73–81, 2010, doi: 10.1007/S11999-009-0975-7.

[117] S. Parratte, V. Pauly, J. M. Aubaniac, and J. N. A. Argenson, "No long-term difference between fixed and mobile medial unicompartmental arthroplasty," *Clin. Orthop. Relat. Res.*, vol. 470, no. 1, pp. 61–68, Jan. 2012, doi: 10.1007/S11999-011-1961-4.

[118] M. Vasso, C. Del Regno, A. D'Amelio, D. Viggiano, K. Corona, and A. Schiavone Panni, "Minor varus alignment provides better results than neutral alignment in medial UKA.," *Knee*, vol. 22, no. 2, pp. 117–121, Mar. 2015, doi: 10.1016/j.knee.2014.12.004.

[119] J. F. Plate *et al.*, "Achieving accurate ligament balancing using robotic-assisted unicompartmental knee arthroplasty," *Adv. Orthop.*, vol. 2013, pp. 1–6, 2013, doi:

10.1155/2013/837167.

[120] M. B. Collier, T. H. Eickmann, F. Sukezaki, J. P. McAuley, and G. A. Engh, "Patient, implant, and alignment factors associated with revision of medial compartment unicondylar arthroplasty.," *J. Arthroplasty*, vol. 21, no. 6 Suppl 2, pp. 108–115, Sep. 2006, doi: 10.1016/j.arth.2006.04.012.

[121] P. Weber *et al.*, "Improved accuracy in computer-assisted unicondylar knee arthroplasty: a meta-analysis," *Knee Surg. Sports Traumatol. Arthrosc.*, vol. 21, no. 11, pp. 2453–2461, Nov. 2013, doi: 10.1007/S00167-013-2370-X.

[122] J. H. Lonner, T. K. John, and M. A. Conditt, "Robotic arm-assisted UKA improves tibial component alignment: a pilot study.," *Clin. Orthop. Relat. Res.*, vol. 468, no. 1, pp. 141–146, Jan. 2010, doi: 10.1007/s11999-009-0977-5.

[123] A. D. Pearle, P. F. O'Loughlin, and D. O. Kendoff, "Robot-assisted unicompartmental knee arthroplasty.," *J. Arthroplasty*, vol. 25, no. 2, pp. 230–237, Feb. 2010, doi: 10.1016/j.arth.2008.09.024.

[124] W. E. Moschetti, J. F. Konopka, H. E. Rubash, and J. W. Genuario, "Can Robot-Assisted Unicompartmental Knee Arthroplasty Be Cost-Effective? A Markov Decision Analysis.," *J. Arthroplasty*, vol. 31, no. 4, pp. 759–765, Apr. 2016, doi: 10.1016/j.arth.2015.10.018.

[125] D. Kluess, "Finite Element Analysis in Orthopaedic Biomechanics," 2010.

[126] K. Iesaka, H. Tsumura, H. Sonoda, T. Sawatari, M. Takasita, and T. Torisu, "The effects of tibial component inclination on bone stress after unicompartmental knee arthroplasty.," *J. Biomech.*, vol. 35, no. 7, pp. 969–974, Jul. 2002, doi: 10.1016/s0021-9290(01)00244-5.

[127] T. Sawatari, H. Tsumura, K. Iesaka, Y. Furushiro, and T. Torisu, "Three-dimensional finite element analysis of unicompartmental knee arthroplasty--the influence of tibial component inclination," *J. Orthop. Res.*, vol. 23, no. 3, pp. 549–554, May 2005, doi: 10.1016/J.ORTHRES.2004.06.007.

[128] D. J. Simpson, A. J. Price, A. Gulati, D. W. Murray, and H. S. Gill, "Elevated proximal tibial strains following unicompartmental knee replacement--a possible cause of pain.," *Med. Eng. Phys.*, vol. 31, no. 7, pp. 752–757, Sep. 2009, doi: 10.1016/j.medengphy.2009.02.004.

[129] B. Innocenti, S. Pianigiani, G. Ramundo, and E. Thienpont, "Biomechanical Effects of Different Varus and Valgus Alignments in Medial Unicompartmental Knee

Arthroplasty," *J. Arthroplasty*, vol. 31, no. 12, pp. 2685–2691, 2016, doi: 10.1016/j.arth.2016.07.006.

[130] A. R. Hopkins, A. M. New, F. Rodriguez-y-Baena, and M. Taylor, "Finite element analysis of unicompartmental knee arthroplasty," *Med. Eng. Phys.*, vol. 32, no. 1, pp. 14–21, 2010, doi: 10.1016/j.medengphy.2009.10.002.

[131] R. H. Emerson, O. Alnachoukati, J. Barrington, and K. Ennin, "The results of Oxford unicompartmental knee arthroplasty in the United States: a mean ten-year survival analysis," *Bone Joint J.*, vol. 98-B, no. 10 Supple B, pp. 34–40, 2016, doi: 10.1302/0301-620X.98B10.BJJ-2016-0480.R1.

[132] O. R. Kwon *et al.*, "Biomechanical comparison of fixed- and mobile-bearing for unicomparmental knee arthroplasty using finite element analysis," *J. Orthop. Res.*, vol. 32, no. 2, pp. 338–345, 2014, doi: 10.1002/jor.22499.

[133] Altamore Virginia, "Sensitivity analysis of design parameters in a Fixed Bearing Unicompartimental Knee Arthroplasty," 2022.

[134] Sara Fiore, "Sensitivity Analysis of a Mobile-Bearing Unicompartmental Knee Prosthesis," 2021.

[135] "Abaqus Unified FEA - SIMULIA™ di Dassault Systèmes®." https://www.3ds.com/it/prodotti-e-servizi/simulia/prodotti/abaqus/ (accessed Dec. 03, 2022).

[136] "SIMULIA > Products." https://web.archive.org/web/20100502080747/http://www.simulia.com/products/abaqus_fea.html (accessed Dec. 03, 2022).

[137] K. Zhang, W. Li, Y. Zheng, W. Yao, and C. Zhao, "Dynamic Constitutive Model of Ultra-High Molecular Weight Polyethylene (UHMWPE): Considering the Temperature and Strain Rate Effects," *Polymers (Basel).*, vol. 12, no. 7, pp. 1–15, Jul. 2020, doi: 10.3390/POLYM12071561.

[138] R. S. J. Burnett, R. Nair, C. A. Hall, D. A. Jacks, L. Pugh, and M. M. McAllister, "Results of the Oxford Phase 3 Mobile Bearing Medial Unicompartmental Knee Arthroplasty From an Independent Center: 467 Knees at a Mean 6-Year Follow-Up: Analysis of Predictors of Failure," *J. Arthroplasty*, vol. 29, no. 9, pp. 193–200, Sep. 2014, doi: 10.1016/J.ARTH.2014.01.035.

[139] "Prof. dr. Thomas Luyckx MD, PhD | AZ Delta Roeselare-Menen-Torhout."

https://www.azdelta.be/nl/arts/luyckx-md-phd (accessed Dec. 03, 2022).

[140] M. Sobociński, "Analysis of friction and lubrication of human joint's surfaces," *J. Appl. Math. Comput. Mech.*, vol. 15, no. 1, pp. 161–167, Mar. 2016, doi: 10.17512/JAMCM.2016.1.16.

[141] J. Brihault *et al.*, "All-polyethylene tibial components generate higher stress and micromotions than metal-backed tibial components in total knee arthroplasty," *Knee Surg. Sports Traumatol. Arthrosc.*, vol. 24, no. 8, pp. 2550–2559, Aug. 2016, doi: 10.1007/S00167-015-3630-8.

[142] "Finite element analysis—theory and application with ANSYS," *Minerals Engineering*, vol. 12, no. 8. pp. 992–993, 1999, doi: 10.1016/s0892-6875(99)90030-4.

[143] W. T. Thomson, "Introduction to the Finite Element Method," *Theory Vib. with Appl.*, pp. 301–344, 2018, doi: 10.1201/9780203718841-11.

[144] "Introduction to Finite Element Analysis 1 Introduction to." https://slidetodoc.com/introduction-to-finite-element-analysis-1-introduction-to/ (accessed Dec. 03, 2022).

[145] T. Yoda, "The effect of collaborative relationship between medical doctors and engineers on the productivity of developing medical devices," *R D Manag.*, vol. 46, pp. 193–206, 2016, doi: 10.1111/radm.12131.

[146] J. Wolff, "The Law of Bone Remodelling," *Law Bone Remodel.*, 1986, doi: 10.1007/978-3-642-71031-5.

[147] R. Popescu, E. G. Haritinian, and S. Cristea, "Relevance of finite element in total knee arthroplasty - Literature review," *Chir.*, vol. 114, no. 4, pp. 437–442, 2019, doi: 10.21614/chirurgia.114.4.437.

[148] "BEAMS." https://beams.polytech.ulb.be/ (accessed Dec. 03, 2022).

[149] "Bernardo INNOCENTI | Professor | PhD | Université Libre de Bruxelles, Brussels | ULB." https://www.researchgate.net/profile/Bernardo-Innocenti-2 (accessed Dec. 04, 2022).

[150] G. M. Treece and A. H. Gee, "Independent measurement of femoral cortical thickness and cortical bone density using clinical CT," *Med. Image Anal.*, vol. 20, no. 1, pp. 249–264, Feb. 2015, doi: 10.1016/J.MEDIA.2014.11.012.

[151] M. Sadat-Ali, E. Elshaboury, A. S. Al-Omran, M. Q. Azam, A. Syed, and A. H. Gullenpet, "Tibial cortical thickness: A dependable tool for assessing osteoporosis in the absence of dual energy X-ray absorptiopmetry," *Int. J. Appl. Basic Med. Res.*, vol. 5,

no. 1, p. 21, 2015, doi: 10.4103/2229-516X.149228.

[152] G. Castellarin, S. Pianigiani, and B. Innocenti, "Asymmetric polyethylene inserts promote favorable kinematics and better clinical outcome compared to symmetric inserts in a mobile bearing total knee arthroplasty," *Knee Surg. Sports Traumatol. Arthrosc.*, vol. 27, no. 4, pp. 1096–1105, Apr. 2019, doi: 10.1007/S00167-018-5207-9.

[153] B. Innocenti, E. Bori, and S. Pianigiani, "Biomechanical Analysis of the Use of Stems in Revision Total Knee Arthroplasty," *Bioengineering*, vol. 9, no. 6, 2022, doi: 10.3390/bioengineering9060259.

[154] L. Blankevoort and R. Huiskes, "Ligament-bone interaction in a three-dimensional model of the knee," *J. Biomech. Eng.*, vol. 113, no. 3, pp. 263–269, 1991, doi: 10.1115/1.2894883.

[155] F. Galbusera *et al.*, "Material models and properties in the finite element analysis of knee ligaments: A literature review," *Front. Bioeng. Biotechnol.*, vol. 2, no. NOV, p. 54, Nov. 2014, doi: 10.3389/FBIOE.2014.00054/BIBTEX.

[156] M. G. Pandy, K. Sasaki, and S. Kim, "A Three-Dimensional Musculoskeletal Model of the Human Knee Joint. Part 1: Theoretical Construct," *Comput. Methods Biomech. Biomed. Engin.*, vol. 1, no. 2, pp. 87–108, 1998, doi: 10.1080/01495739708936697.